A

THESIS

SUBMITTED IN PARTIAL FULFILLMENT OF THE REQUIREMENTS

FOR THE HONORS DEGREE OF

BACHELOR OF SCIENCE IN PHYSICS

Urban Surface Characteristics for Turbulent Source Areas: Calculation of Roughness Length under Neutral Conditions

Reiko Toriumi

DEPARTMENT OF PHYSICS

INDIANA UNIVERSITY

June, 2003

Supervisor: Prof. Sue Grimmond
Indiana University, Bloomington
Atmospheric Science Program, Geography Department

Signature 

Co-signer: Prof. Rick Van Kooten
Indiana University, Bloomington
Physics Department

Signature 

Undergraduate Research and Creative Activity Partnership

Urban Surface Characteristics for Turbulent Source Areas: Calculation of Roughness Length under Neutral Conditions

Reiko Toriumi
Indiana University, Bloomington
Physics Department.

Advisor: Prof. Sue Grimmond
Indiana University, Bloomington
Atmospheric Science Program, Geography Department

June, 2003

Abstract

In this paper, the focus was placed on determining the stability conditions at a suburban site over a range of seasons. For neutral condition, under different restrictions on micrometeorological parameters, roughness length (z_0) was determined. Eddy correlation stress method is used for the calculation of roughness length. The Obukhov length is used for stability variability. Roughness lengths under different conditions (e.g., by wind directions and by seasons) are calculated and their histograms were created. Under the actual measurement height (z_m) to be 40.5 m and the zero plane displacement length (z_d) to be 7.4 m (summer), 3.5 m (winter), and 5.5 m (fall & spring), mean roughness length was 2.0 m for summer and 1.7 m for winter which gave z_0 in winter to be about 95 % of that in summer.

Contents

Introduction

Urban areas have a large and increasing number of people living in them and hence lead to an unbalanced demand of natural resources, such as fossil fuels. This is why the role of urban areas on global carbon budget is gathering much attention, being followed by many studies of CO_2 concentrations in those urban environments (ref. [5]).

Roughness length (z_0) is a function of the surface characteristics. Methods to determine roughness lengths can be categorized into those that require observations of wind (called anemometric), and those that are based on the morphology and spatial arrangement of surface roughness elements (ref. [1]). In this study one of the former methods is used. The roughness length (z_0) is a key issue to understand the behavior of urban winds and turbulence.

In urban areas we observe a wider range of surface characteristics than forests, agricultural areas, or wetlands, some complications and difficulties occur in urban studies, sequentially, a much closer attention needs to be paid to determination of z_0. As determination of z_0 in cities is not straightforward, there are needs for more studies which provide sufficient information on the measurement sites and their vicinities.

The stability parameter, z'/L (z' is the difference of measurement height and the zero plane displacement length and L is the Obukhov length) is also important to for this parameter to be varying with the stability conditions, in other words, z'/L determines neutral conditions.

The objective of this research, therefore, is to calculate roughness lengths under the neutral conditions with different constraints on parameters; friction velocity (u*) and dimensionless stability parameter (z'/L).

One of the advantages of this study compared to past studies is that there is a large amount of good quality eddy covariance data. This type of data set is rarely available in urban areas.

Meteorological Theory

Since the fast response three-dimensional anemometry is available for this Baltimore study (i.e., 10 Hz sonic anemometer is considered to be fast response), it is possible to determine friction velocity (u*) directly using rotated longitudinal and vertical components of wind velocity. Then by using u*, roughness length will be calculated. The method used to determine the roughness length is the eddy correlation stress method, referred to as Es. (ref. [1])

$$z_o = (z_m - z_d) e^{-\frac{u_z \kappa}{u^*}} \quad (1)$$

where u* : = friction velocity (m s^{-1}), u_z: = vertical wind velocity (m s^{-1}), z_m : = measurement height (m), z_d : = displacement length (m) and κ : = von Karman constant (0.4).

Stress can be interpreted as a friction caused by both objects that are sliding against each other. Hence where boundaries of different layers lie in the atmosphere, this stress occurs ceaselessly. Friction velocity is related to (or u^{*2} is given by) the (kinematic) air stress against the earth's surface, where kinematic stress is the stress per unit density of air. Notice if this u* is low in value, then there tend to cause measurements with large errors (ref. [6]).

For this method to estimate roughness length (z_0), some applications of criteria need to be assessed: site characteristics (ideally horizontal terrain and extensive fetch with no anomalous structures nearby); tower exposure (slender and open structure to avoid wake effects); measurement height (above roughness sublayer but low enough to be in an adjusted boundary layer); instrumentation (response characteristics, spacing if profiles are used, and sampling period);

atmospheric stability (neutral, or stability corrected); and inclusion of zero-plane displacement. (ref. [1])

To calculate the atmospheric stability, the Obukhov length (L) (ref. [1]):

$$L = -\frac{\overline{\theta}}{\kappa g}\frac{u^{*3}}{\overline{\omega'\theta'}} \quad : \text{Obukhov length} \tag{2}$$

with g : = gravitational acceleration, θ : = potential temperature (K), and ωθ : = kinematic heat flux (K m s^{-1}).

The Obukhov length represents the height in the stable surface layer below which shear production of turbulence exceeds buoyant consumption. Further interpretation can be made by dividing L into two clear categories: stable and unstable conditions. If L < 0, then it means that the temperature gradient is directing upward (the ground is warmer than the adjacent air with vigorous turbulence and light winds), implying that the condition tend to happen rather daytime: unstable conditions. On the other hand, if L > 0, then the temperature gradient is now downward (the adjacent air is warmer than the ground with weak turbulence and moderate to strong winds), which tends to happen at night: stable conditions. The third condition is called neutral conditions, in which there is little heating or cooling at the boundary of the ground and the surrounding air, usually being resulted from windy conditions. Therefore the logarithmic wind profile occurs under neutral conditions which estimate the roughness length. The characteristics of stability conditions depending on L signs was beautifully observed when number of data as a function of z'/L (= (z_m - z_d) / L) which is inversely proportional to L was plotted (Fig.5). The details of this discussion will be reviewed later in the section *Stability Calculations (with z_m = 30 m and z_d = 27 m) in Data Analyses*.

Therefore, since under neutral conditions, there is a relationship between some coefficient (which is called drag coefficient that is linearly related to u^{*2} (kinematic stress)) and aerodynamic roughness length, i.e., u*:friction velocity and z_0, consequently extraction of the data under neutral condition needs to be done.

Measurements

Site:

The measurements for this study have been taken at the Cub Hill site, Baltimore, Maryland, USA. This Baltimore site is a part of the Baltimore Ecosystem Study (BES), which is an Urban Long Term Ecological Research (LTER) site. The tower is operated by Prof. Sue Grimmond (Indiana University).

In this urban area, further increase in housing density is expected. Trees within the neighbor of the tower are ~20-25 m tall and are more than 120 years old. Their kinds are mixture of yellow poplar and oak hickory. This site has an eddy covariance tower where CO_2, heat, water, and radiative fluxes have been measured almost continuously since May 2001. The data measured at the site are very similar to whose of Morgan-Monroe State Forest project, which I had been involve for a year, except that Baltimore site has only one measurement height. (ref. [4])

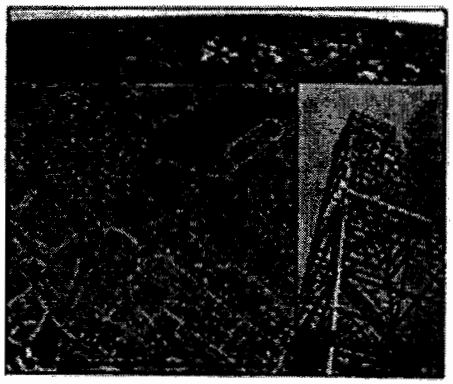

Fig. 1: Baltimore, Maryland, Cub Hill Site. The tower and its vicinity. Source: ref. [4]

Instrumentation:

The turbulent flux instrumentation is mounted at a height of 40.5 m. An RM Young (RMY) 81000 sonic anemometer is used with a Licor 7500 open path infrared gas analyzer (IRGA) to calculate the turbulent fluxes using the eddy covariance technique. The components of net all wave radiation are measured using Kipp and Zonen CNR 1 net radiometer, mounted on a boom which extends 2.7 m from the tower at a height of 38.2 m. At this level, a Campbell Scientific (CSI) 500 temperature and relative humidity sensor is housed in an aspirated shield that is located 1.6 m from the tower face (ref. [4]).

Data Acquisition and Processing:

Data from the sonic are archived at 10 Hz which are logged directly to a PC housed at the bottom of the tower via a serial port using inhouse software (Tower). The fluxes are computed using in-house (IUFlux) software. These generated data are for an interval of 30 minutes. Via the program (see Appendix I) which was created for this study, the 30 minute interval data were processed to calculate neutral conditions in accordance with roughness lengths. Hence there will be 48 data points per one day at maximum.

The data started to be taken on DOY 134, year of 2001, and those until DOY 57, year of 2002 have been analyzed in this paper. Parameters (symbols) and notations that are used are explained in Appendix II.

Data Analyses

Bad Data (Q* = -999. values)

In the data file, data that are considered to be bad are specified as –999. All of these data were excluded from the calculations for this study. When filtering for these bad data takes place for stability conditions analyses, as opposed to initial 22173 of available data, -999 data for Q*s are counted as 1299 excluding the data which also have either / both bad temperature, u*, or /and wT values (Table 1). (wT = 0 values are also considered not to be preferable because it would give us an infinite value for L (eq. (2))). (For the reference, the number of data with a –999 for temperature, u*, or wT, and null for wT, is 2034.) The investigation to see what kind of conditions when we have bad

Q* values was conducted (Fig. 2). There is no specific time range which causes bad Q*s, as well as specific seasonality or a year, rather, they tend to appear on the same day, in other words, one day tends to have all its data points with bad Q*s.

	number of data
initial data	22173
data with only bad Q* (all T, u*, and wT are good)	1299
data with bad T, u*, and / or wT	2034
data with bad Q*, T, u*, and / or wT	3333

Table 1. Number of data (30 minutes period) associated with bad values for relevant parameters.

Stability Calculations (with $z_m = 30$ m and $z_d = 27$ m):

* From this section, a reader has to pay attention to the values of measurement height (z_m) and zero-plane displacement length (z_d) with which the data have been processed and analyzed. The first analyses are with $z_m = 30$ m and $z_d = 27$ m as indicated.

For the stability condition analyses, the time ranges are defined as follows;
day time: $50\ W\ m^{-2} \leq Q^*$
transitional time: $-10\ W\ m^{-2} < Q^* < 50\ W\ m^{-2}$
night time: $Q^* \leq -10\ W\ m^{-2}$

When u* values are low, the other measurements are affected by having comparably big errors (ref. [6]). Fig. 3 was plotted to see what kind of u* values are influencing the data which determines stability conditions. With these plots, $u^* \geq 0.5\ m\ s^{-1}$, and $\geq 0.2\ m\ s^{-1}$ are chosen to be the thresholds for reliable data. From Fig. 4, the number of data points in relation to the time of the day (which was determined by Q* values given by definition above) can be seen for both $u^* \geq 0.5\ m\ s^{-1}$, and $\geq 0.2\ m\ s^{-1}$. However, in further detail, according to these plots in Fig.4, with $u^* \geq 0.2\ m\ s^{-1}$, we would still have good division of data with three different time ranges, but with surely larger number of data. Since it gives us better statistical analyses by providing a larger number of data, $u^* \geq 0.2\ m\ s^{-1}$ has chosen to be a better value for the threshold.

Histograms with the data sorted according to Q* values with different u* thresholds were given in Fig. 5. If we come back to the Obukhov length theory, we will be convinced that there surely exists the dependence of frequency of conditions on the time range of the day. Especially the distribution for $u^* \geq 0.2\ m\ s^{-1}$ beautifully shows the unstable, neutral, and stable conditions in correlation with the time of the day range.

Now then what kind of data with u* are taken out? (Fig. 6) For both $u^* < 0.2\ m\ s^{-1}$ and $u^* < 0.5\ m\ s^{-1}$, the data in night range are observed in significantly large number as compared to those in day time range, while no significant difference was observed in months of the year.

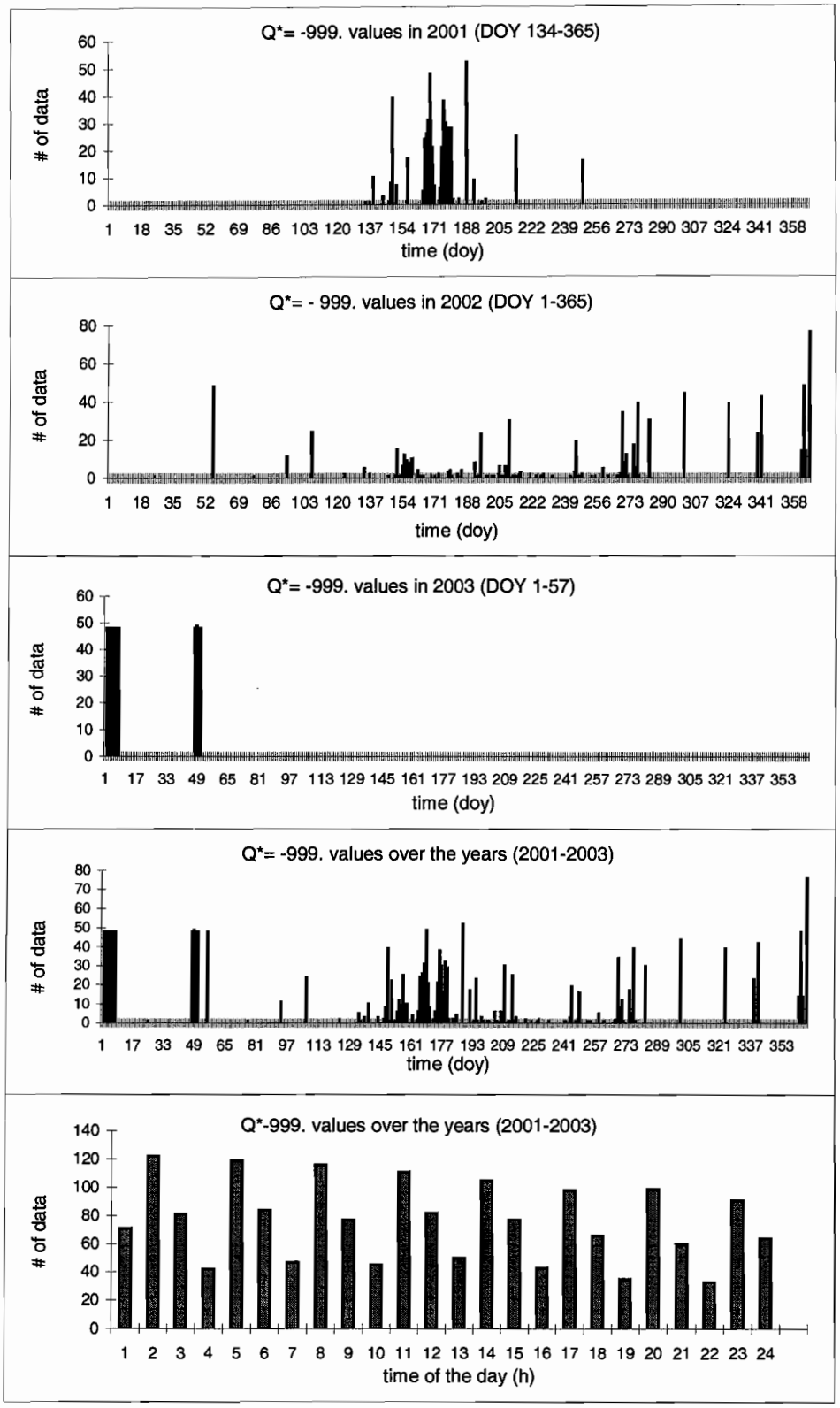

Fig.2 : Distribution of data with Q* = -999. DOY stands for day of the year.
Data are uniformly spread out through the time of the day and no significant characteristics in time of the day is observed. Rather, one particular day seem to posses many bad Q* data.

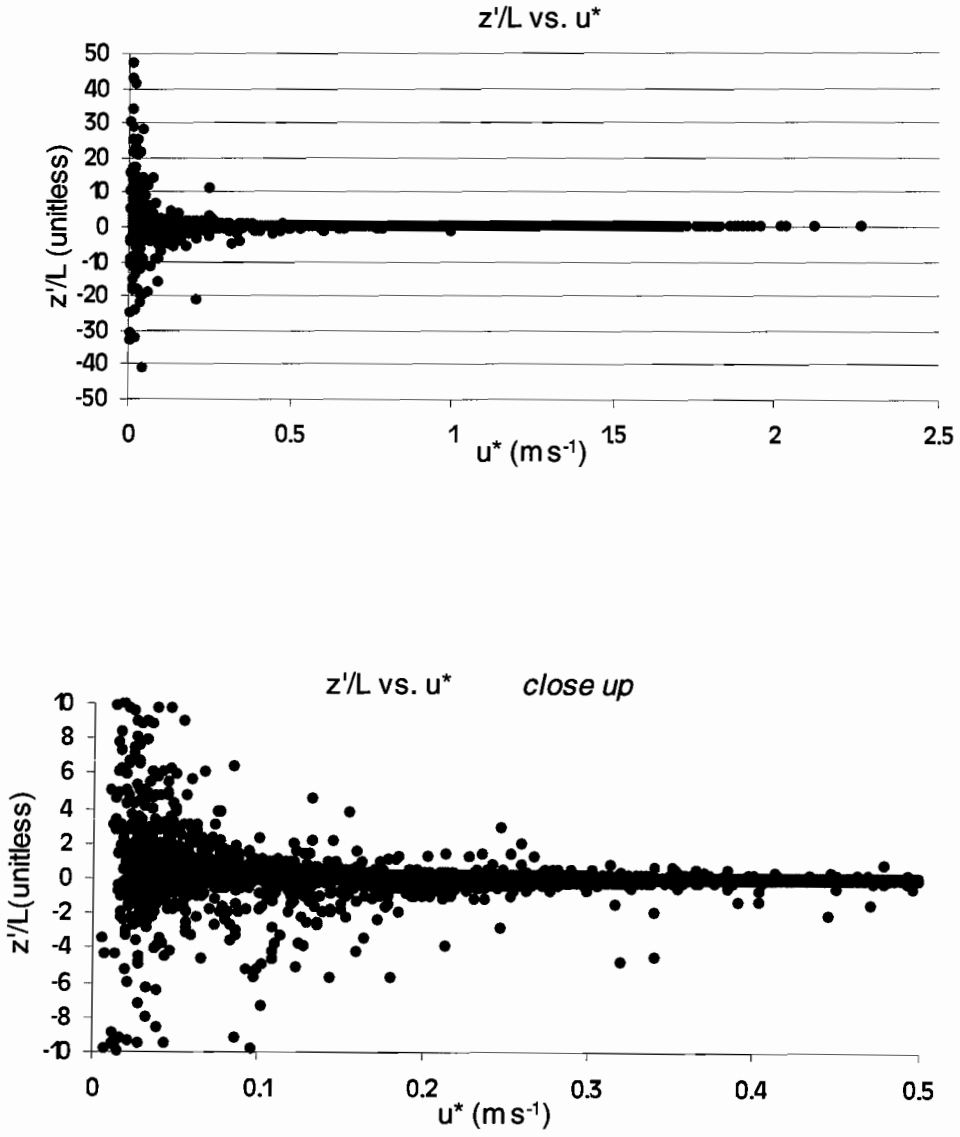

Fig. 3: u* threshold determination. u* = 0.2 m s^{-1} and 0.1 m s^{-1} are picked to be better candidates. z_m = 30 m, z_d = 27 m, and hence z' = $z_m - z_d$ = 3 m.

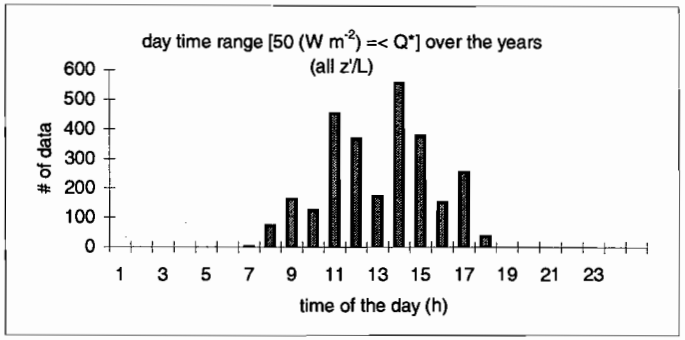

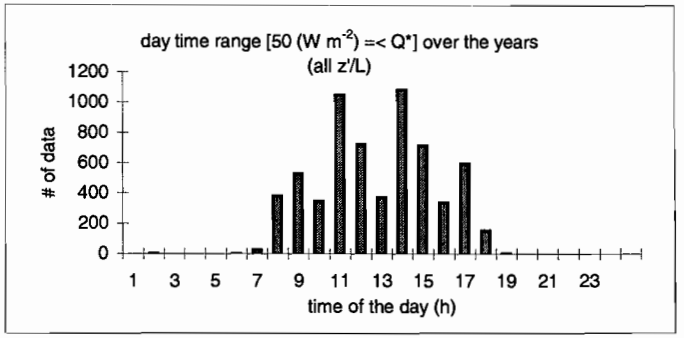

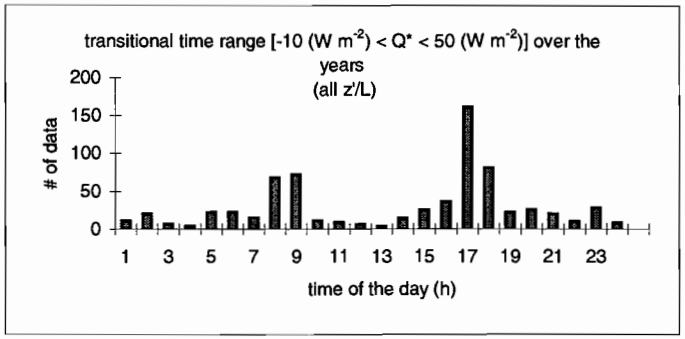

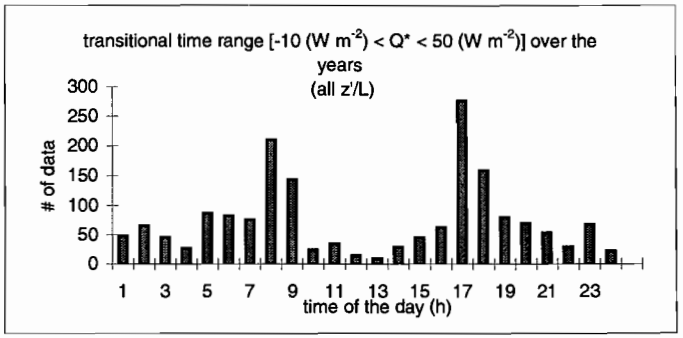

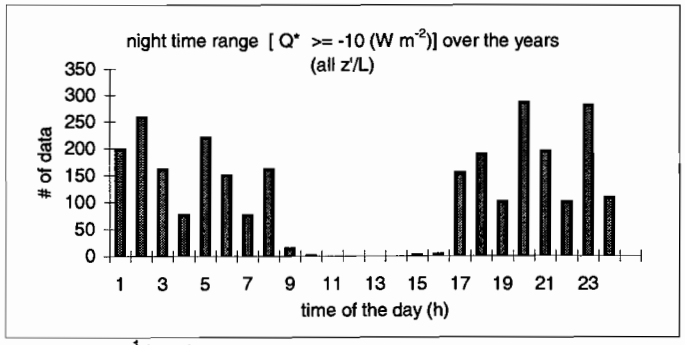

u* < 0.5 m s^{-1} has been cut.

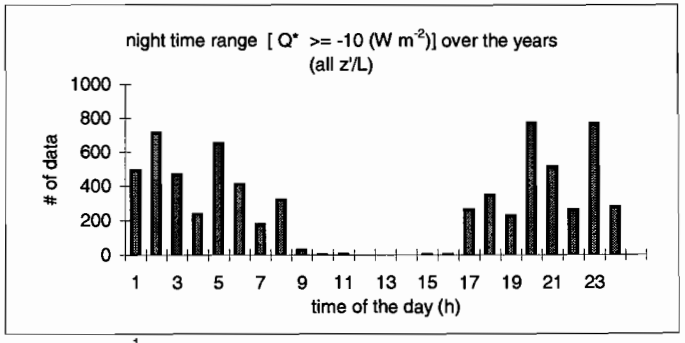

u* < 0.2 m s^{-1} has been cut.

Fig. 4: In order to sort the data out to day, night, and transitional time ranges, Q* values are used. With these figures, it is confirmed that by sorting by Q* values would divide the data into the group of day, night, and transitional time of the day with good approximation.

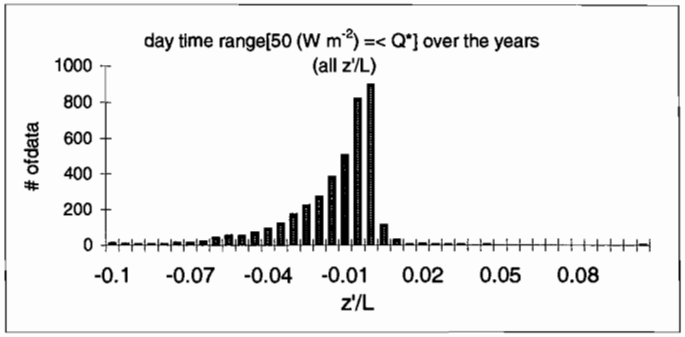

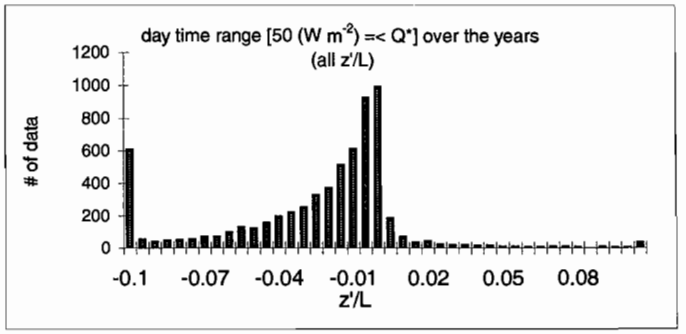

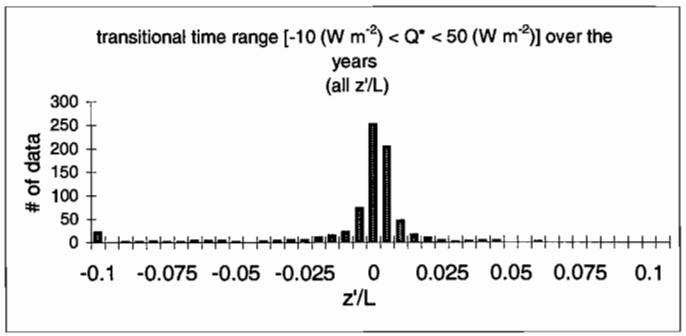

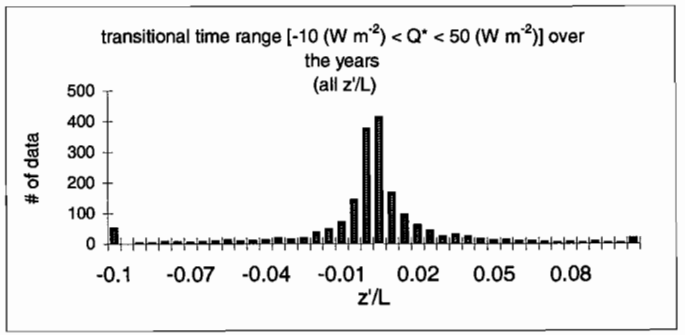

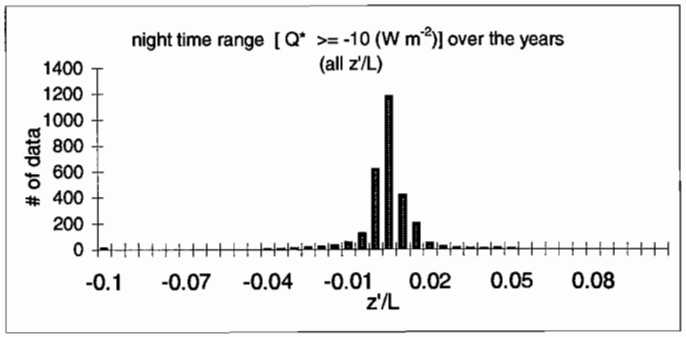

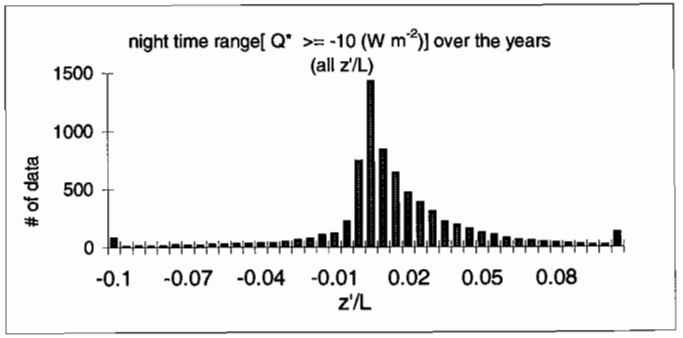

$u^* < 0.5$ m s^{-1} has been cut.

$u^* < 0.2$ m s^{-1} has been cut.

Fig. 5: Unstable, stable, and neutral conditions with different time range of the day are observed.

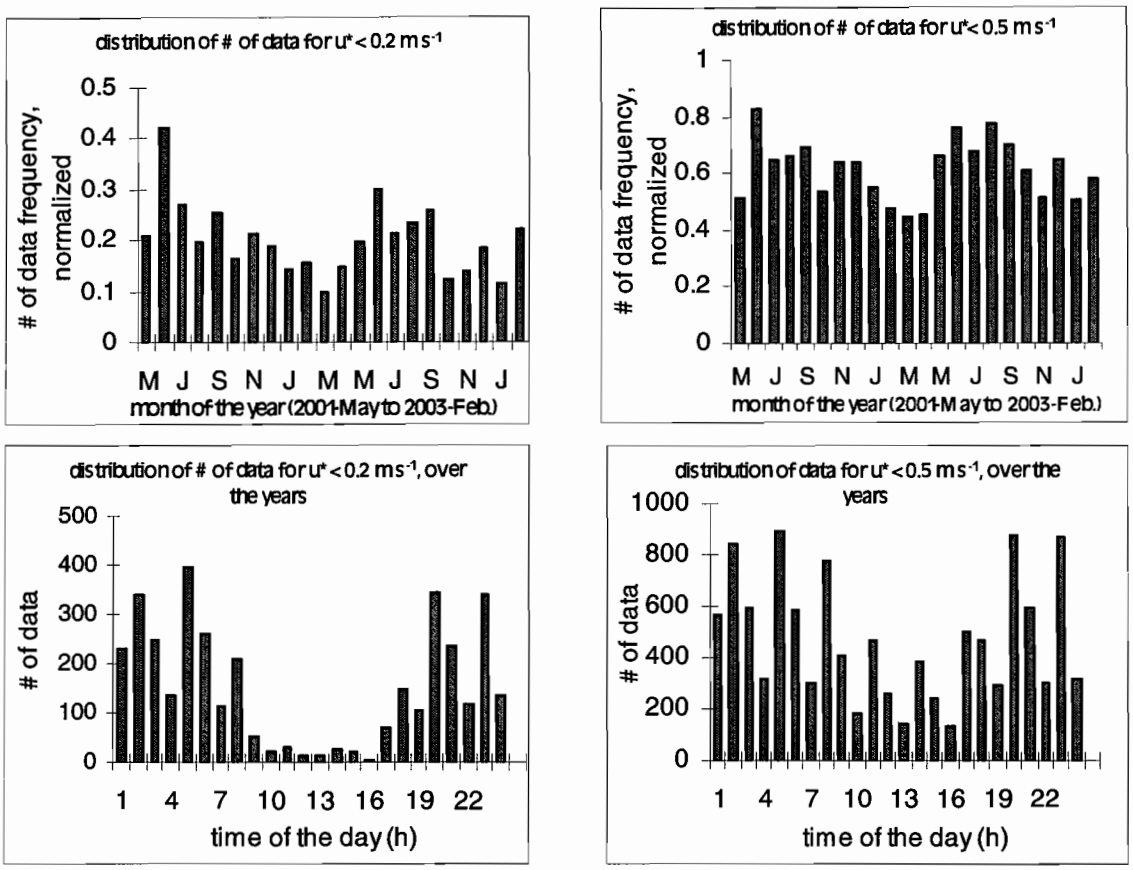

Fig. 6: Distribution of the data with below u* threshold. Normalization refers to (# of data with u* < 0.2 m s^{-1}) / (# of data with all u*).

Neutral Condition Analyses (with z_m = 30 m and z_d = 27 m):

1. Threshold Determinations

Firstly, threshold setting on roughness length parameter was considered and tested (with z_0 > 0.005 m) according to the Fig. 7 below. Theoretically the histograms should be showing us Gaussian function, however, when breaking down the increments smaller at less than 0.1 m roughness length, then spikes in number of data at 0.005 m are observed in Fig. 7. As a consequence, in order for us to deal only with good (or reliable) data, the conditions which generate data with z_0 < 0.005 m were investigated. Most of these data were associated with low u* values (i.e., usually less than 0.2 m s^{-1}).

However, after the comparison between the calculated mean and median roughness length between z_0 threshold and u* threshold, u* threshold was concluded to be better. In addition, according to the calculated indication of data reliability (Δ ($z_{0,mean}$ - $z_{0,\,median}$)/$z_{0,\,mean}$), u* threshold was also determined to be better. More precisely speaking, those with z_0 threshold, is about 25%, whereas those with u* threshold is about 15 % (Fig.8), i.e., there is a greater departure from the mean to the median values if z_0 threshold is used instead of u* threshold.

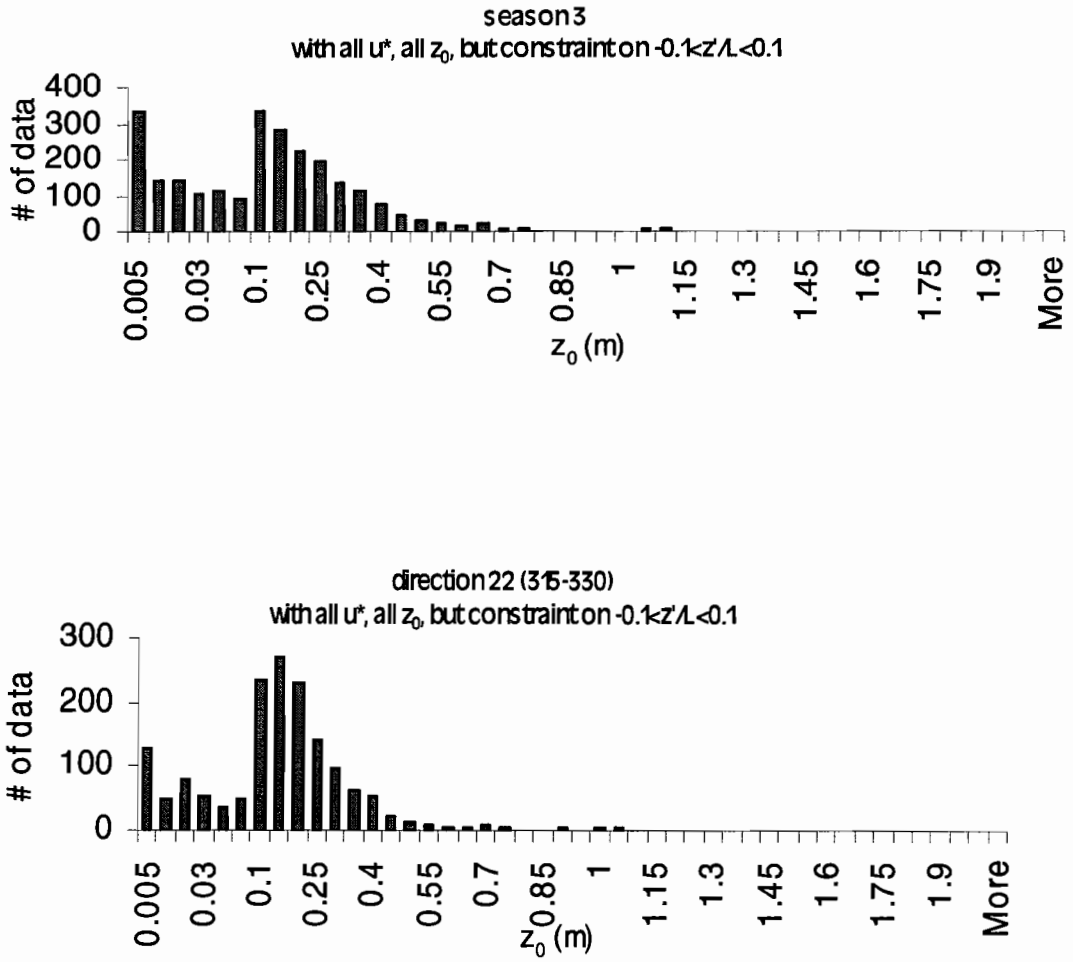

Fig. 7: Examples of histograms for a direction and a season for z_0 threshold determination.
Note that for horizontal axis, z_0 increment when bigger than 0.1 m is 0.05 m, while smaller than 0.1 m is 0.005 m.
$z' = z_m - z_d = 30\text{ m} - 27\text{ m} = 3\text{ m}$.

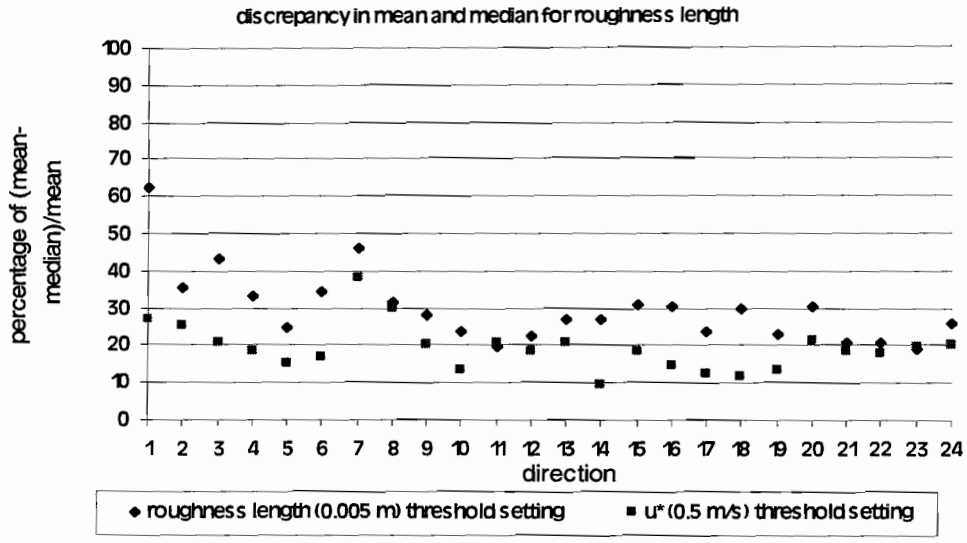

Fig. 8: Difference in $(z_{0,mean} - z_{0,median}) / z_{0,mean}$ values which occur being followed by u* and z_0 thresholds.

a.) $u^* \geq 0.5\ m\ s^{-1}$, $-0.1 < z'/L < 0.1$.

Neutral conditions can be defined more than one way (ref. [7]). First, we will use ref. [1], neutral conditions of $-0.1 < z'/L < 0.1$. With this suggestion, after generating the data with roughness lengths under neutral conditions, however, both too small and too large values of roughness lengths were found to be calculated. Consequently, some refinement for the data filtering was needed. The complication is that the small roughness lengths are not necessarily related to the small u* values, although we expected small u* to be related to small z_0 (ref. [6]). After plotting the roughness length and u* relation (Fig. 9), when u* is smaller than $0.5\ m\ s^{-1}$, there found most of the data points with too large and too small roughness lengths in this range. Therefore, u* threshold ($0.5\ m\ s^{-1}$) has determined to be set in addition to the neutral condition $-0.1 < z'/L < 0.1$.

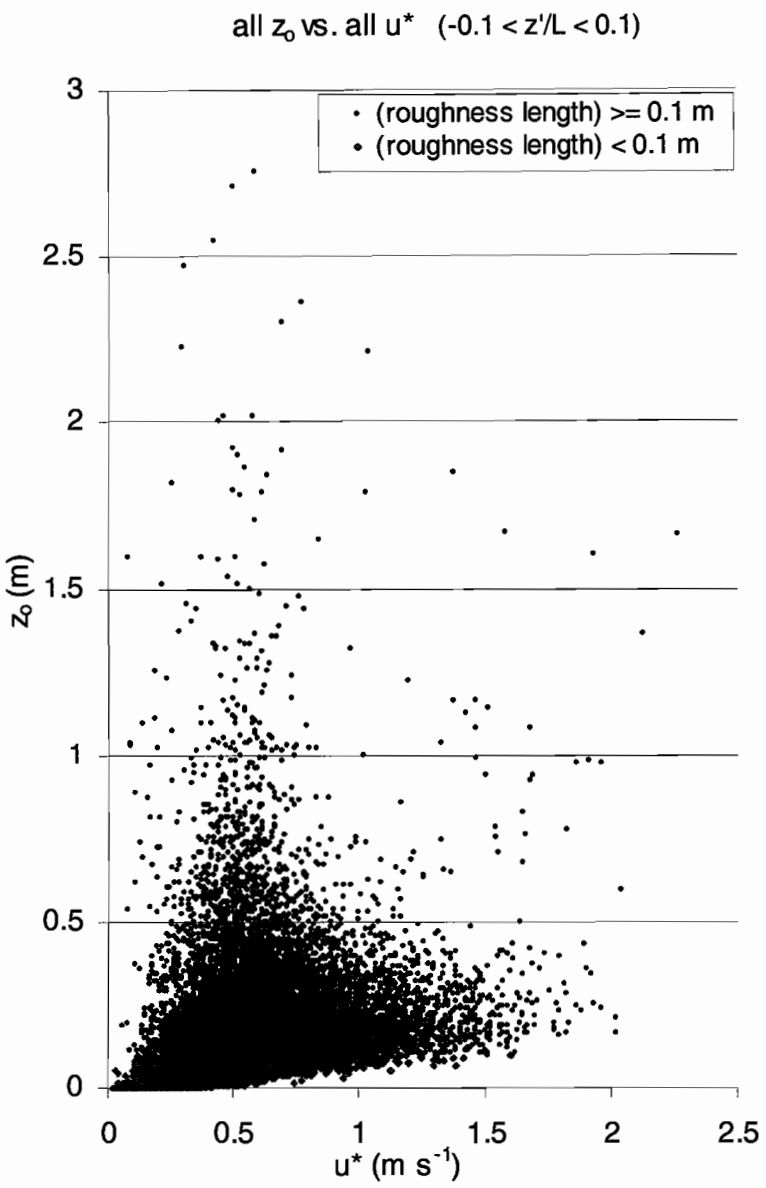

Fig. 9: u* threshold determination. There are relatively large number of data whose roughness length values are either too small (~0 m) or too big (greater than 0.5 m), if u* is less than 0.5 m s^{-1}. z_m = 30 m and z_d = 27 m are used.

b) u* ≥ 0.2 m s^{-1}, -0.01 < z'/L < 0.01

Without restricting z'/L values, z'/L vs. u* has been plotted as in Fig. 3. In order to have less variability in z'/L values to deduce neutral conditions, a better u* threshold value seems to be 0.2 m s^{-1}. The histograms for u* ≥ 0.1 m s^{-1} were also tested to check the variability of z'/L (Fig. 10) to confirm the existence of stable and unstable conditions (which can be determined by z'/L) not only of neutral conditions. For u* ≥ 0.2 m s-1, z'/L has determined to be -0.01 < z'/L < 0.01 to deduce neutral conditions, given the observation of data distribution in Fig. 11, that depicts most of the data with a large frequency seem to be confined in the range of -0.01 < z'/L < 0.01.

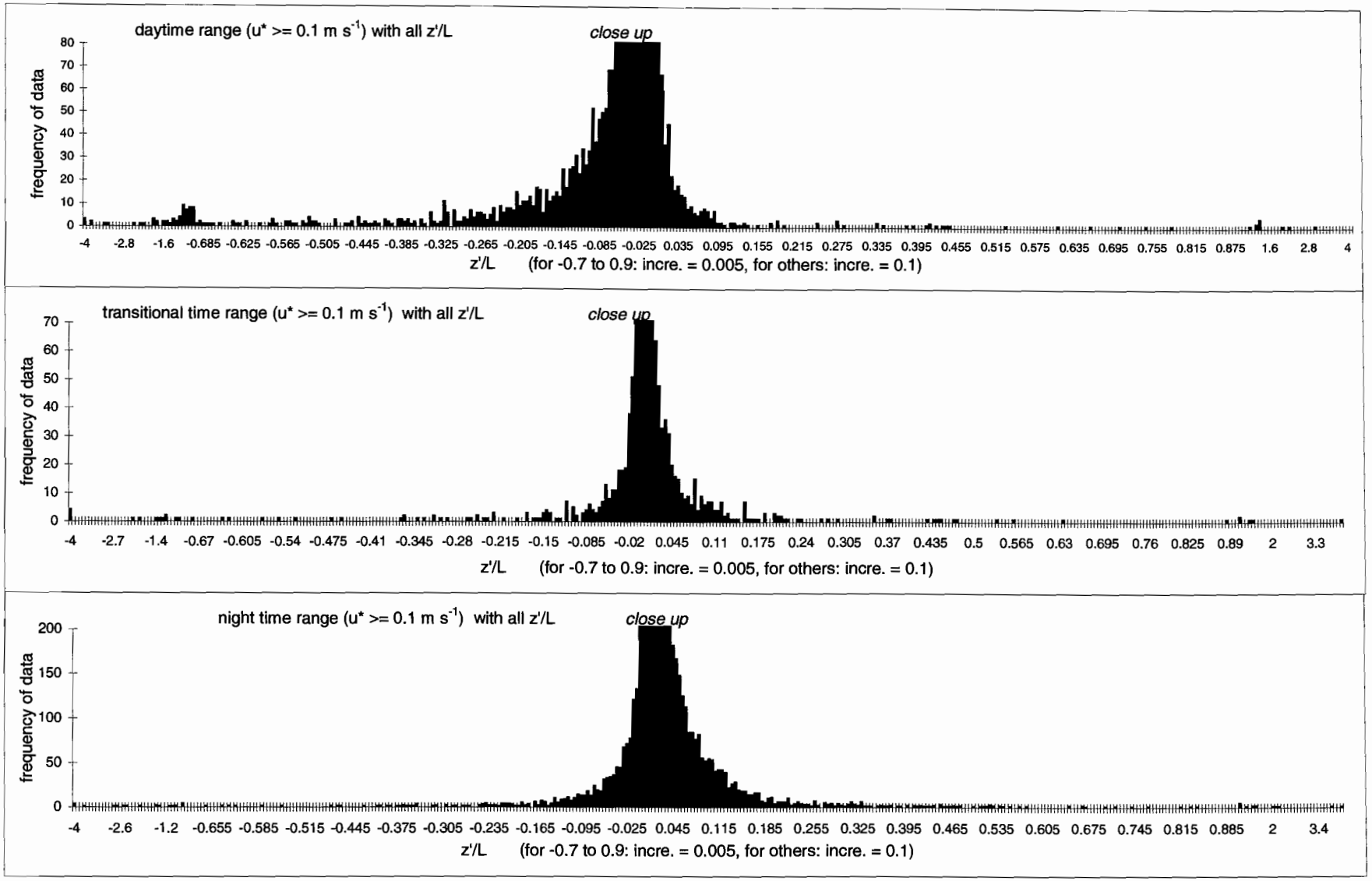

Fig. 10: One can observe the presence of unstable conditions ($z'/L < 0$), as well as stable conditions ($z'/L > 0$). Neutral consitions exist in the vicinity of $z'/L = 0$. Vertical axis has cut off low in order to observe the variability of z'/L, i.e., the existence of variability of conditions: unstable, neutral, and stable. $z' = z_m - z_d = 3$ m, with $z_m = 30$ m and $z_d = 27$ m.

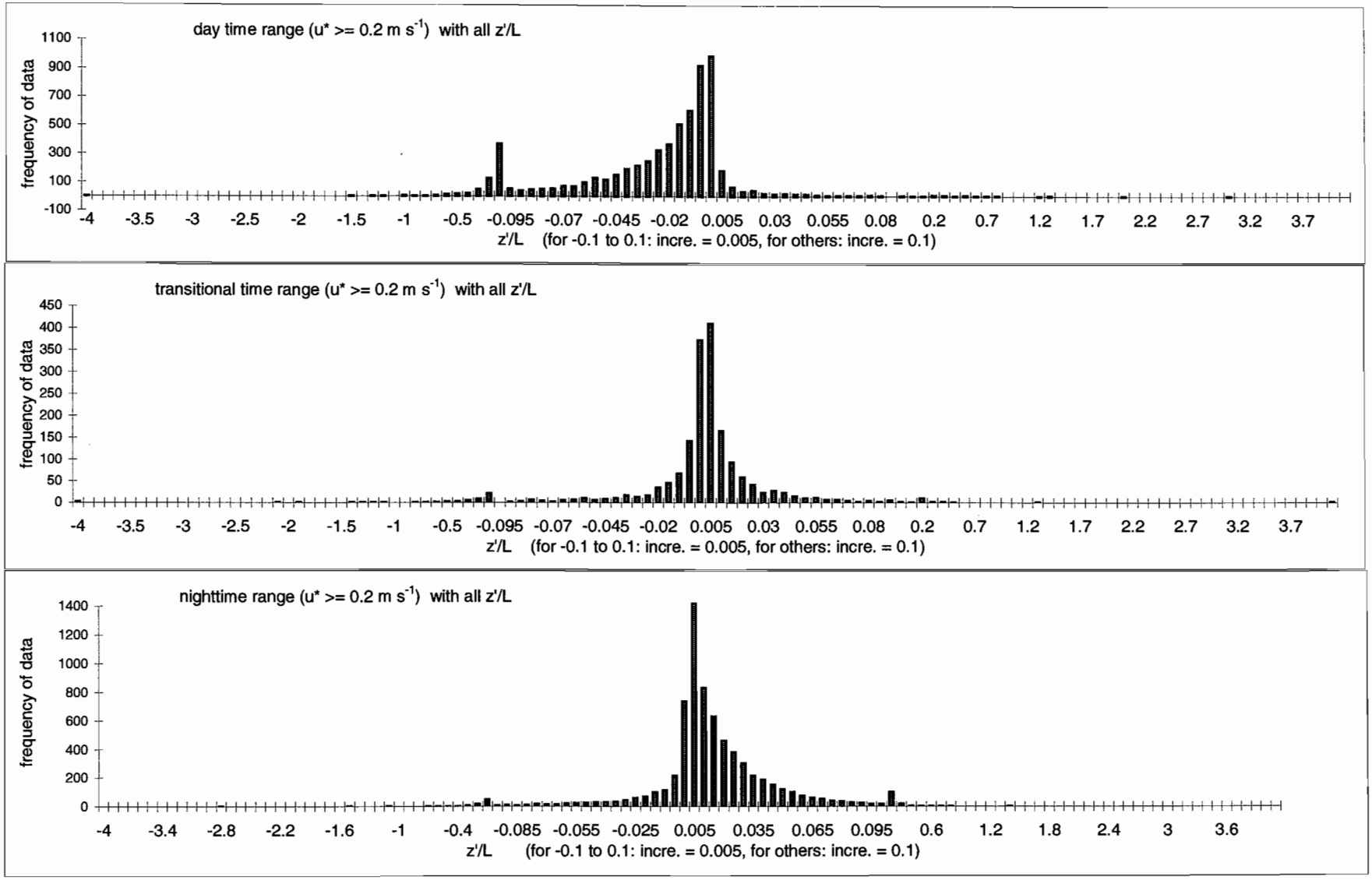

Fig. 11: Threshold determination for z'/L. Spikes of frequency at either side of the skirt of the histograms happened because of the change of the size of the increments along the horizontal axis. $z' = z_m - z_d = 3$ m, with $z_m = 30$ m and $z_d = 27$ m.

c) $u^* \geq 0.5$ m s^{-1}, $-0.05 < z'/L < 0.05$

Observation of Fig. 11 also gives another possibility for z'/L threshold to be determined as 0.05, if we decide to have neutral conditions to be in broader span. The threshold, $-0.05 < z'/L < 0.05$, will allow us to have statistically better calculations. For this, $u^* \geq 0.5$ m s^{-1}, which has deduced from Fig. 10 was used.

2. Preference in Direction

There are preferred wind directions and therefore variable number of data points (Fig. 12). Preference in direction under neutral conditions indicates that there is a certain direction of wind that tends to occur with comparably high frequency. Regardless of different u* and z'/L restrictions for neutral conditions, direction of 285-360 degree seems to be preferred throughout the seasons with the exception of summer. This is a function of synoptic conditions, as the site is located in Midwest region in the United States.

3. Roughness Length Calculations

Under different constraints on z'/L with different u*s for neutral conditions, roughness lengths are calculated and mean and median values for the distribution of z_0 have also deduced and given in Appendix IV. In Fig. 13-a & b, z_0 are also plotted with respect to the directions sorted by seasons. If the data points are less than 20 (which is considered to be not enough to generate a good statistical values for mean and median), then the hollow dots are used instead of solid. In ref. [1], it is stated that the roughness length in winter is 80-90 % of the roughness length in summer. The mean for summer gives 0.26 m $\pm$ 0.06 m, while that for winter is 0.19 m $\pm$ 0.06 m (Table 2). In fact, this yields the ratio of summer and winter to be about 74 % (with median, it is about 69 %), which resulted in slightly smaller value as indicated in ref. [1]. This would make sense given the very large amount of vegetation at this site. The reliability of data can be interpreted in ratio of median roughness length to mean. If one is close to unity, then the data is more likely reliable. For the transitional seasons, i.e., fall and spring, roughness lengths are hard to be determined accurately, since availability of number of data is not enough.

		summer		fall		winter		spring	
	u*, z'/L	$\langle z_0 \rangle$ (m)	$\sigma \langle z_0 \rangle$ (m)	$\langle z_0 \rangle$ (m)	$\sigma \langle z_0 \rangle$ (m)	$\langle z_0 \rangle$ (m)	$\sigma \langle z_0 \rangle$ (m)	$\langle z_0 \rangle$ (m)	$\sigma \langle z_0 \rangle$ (m)
z_0, mean	$u^* >= 0.5$ m s^{-1}, $-0.1 < z'/L < 0.1$	0.31	0.07	0.24	0.08	0.22	0.06	0.26	0.09
	$u^* >= 0.2$ m s^{-1}, $-0.01 < z'/L < 0.01$	0.19	0.04	0.16	0.08	0.15	0.04	0.16	0.07
	$u^* >= 0.5$ m s^{-1}, $-0.05 < z'/L < 0.05$	0.29	0.06	0.23	0.07	0.21	0.06	0.24	0.08
	all	**0.26**	0.06	**0.21**	0.08	**0.19**	0.06	**0.22**	0.08
z_0, median	$u^* >= 0.5$ m s^{-1}, $-0.1 < z'/L < 0.1$	0.25	0.06	0.20	0.08	0.17	0.04	0.22	0.08
	$u^* >= 0.2$ m s^{-1}, $-0.01 < z'/L < 0.01$	0.17	0.04	0.14	0.07	0.11	0.03	0.14	0.07
	$u^* >= 0.5$ m s^{-1}, $-0.05 < z'/L < 0.05$	0.24	0.06	0.19	0.07	0.16	0.04	0.21	0.08
	all	**0.22**	0.05	**0.18**	0.07	**0.15**	0.04	**0.19**	0.08

Table 2: Average z_0 ($\langle z_0 \rangle$) values in connection with different u* and z'/L values. For deviation calculation, $s = \sqrt{\frac{1}{n}\sum_{i=1}^{n}(x_i - \bar{x})^2}$, for small n, was used. z_d= 27 m and z_m = 30 m were used for displacement height and measurement height for calculation of roughness lengths. For fall, in averaging process, the data point with direction of 90 – 105 (degree) was excluded for it to have a large departure from the other data points (see Fig. 13-a).

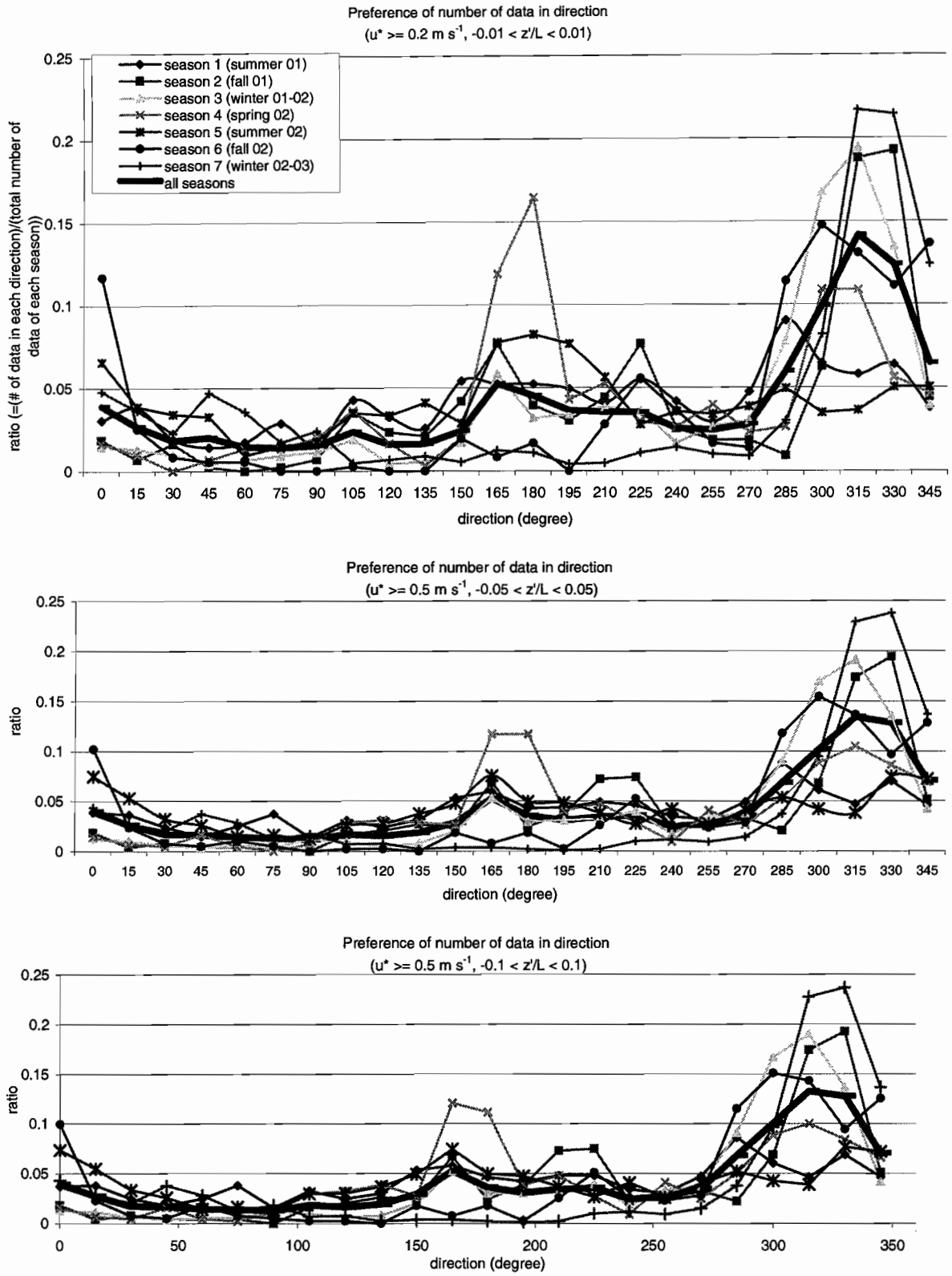

Fig. 12: Preference in direction, indicating the tendency of occurrence of strong winds in 270 to 360 degree (i.e., west to north). North as 0 degree, east as 90 degree and so forth. z_m = 30 m and z_d = 27 m.

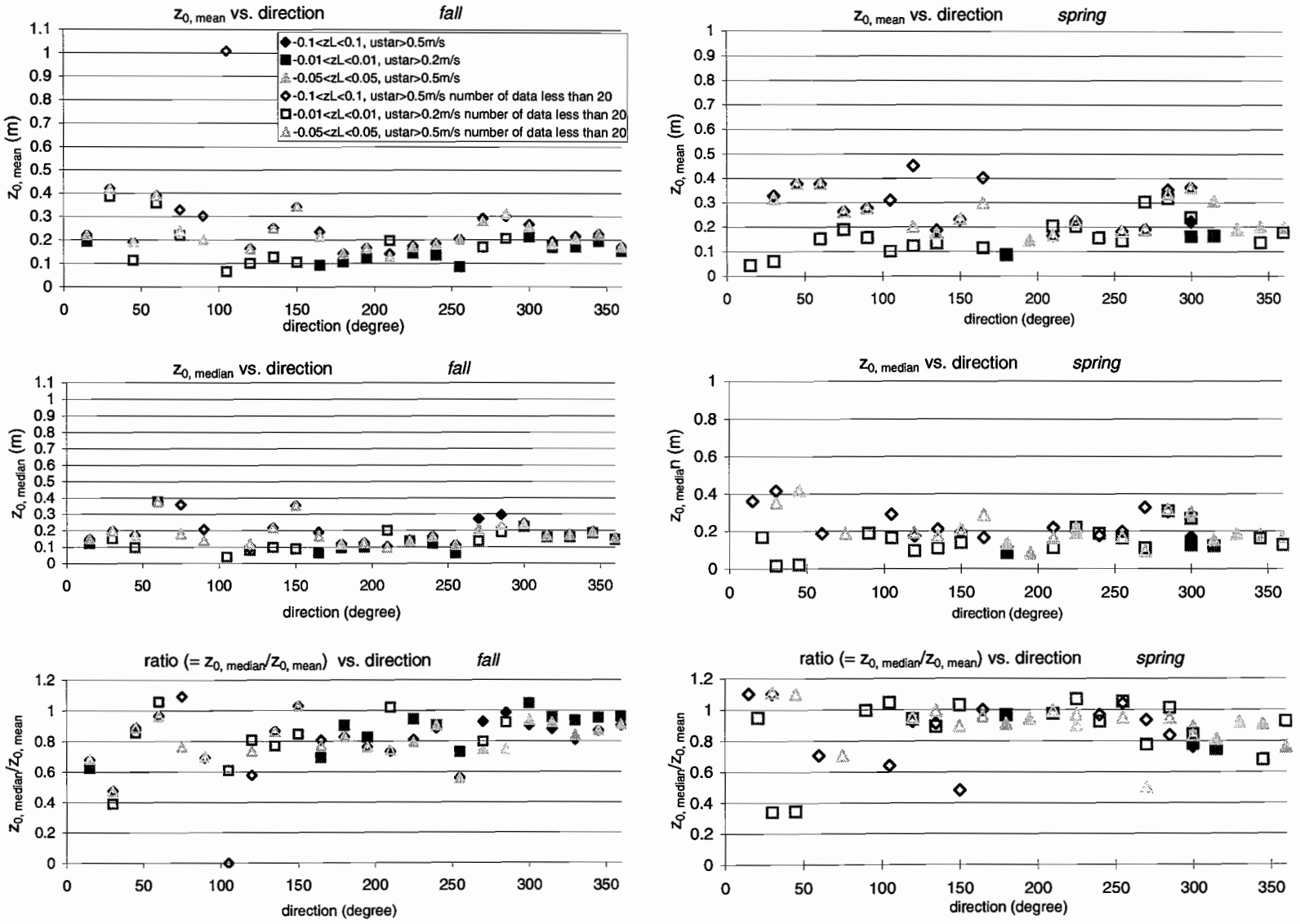

Fig. 13-a: Roughness lengths showing seasonal dependence. Fall and spring. z_m = 30 m and z_d = 27m are used.

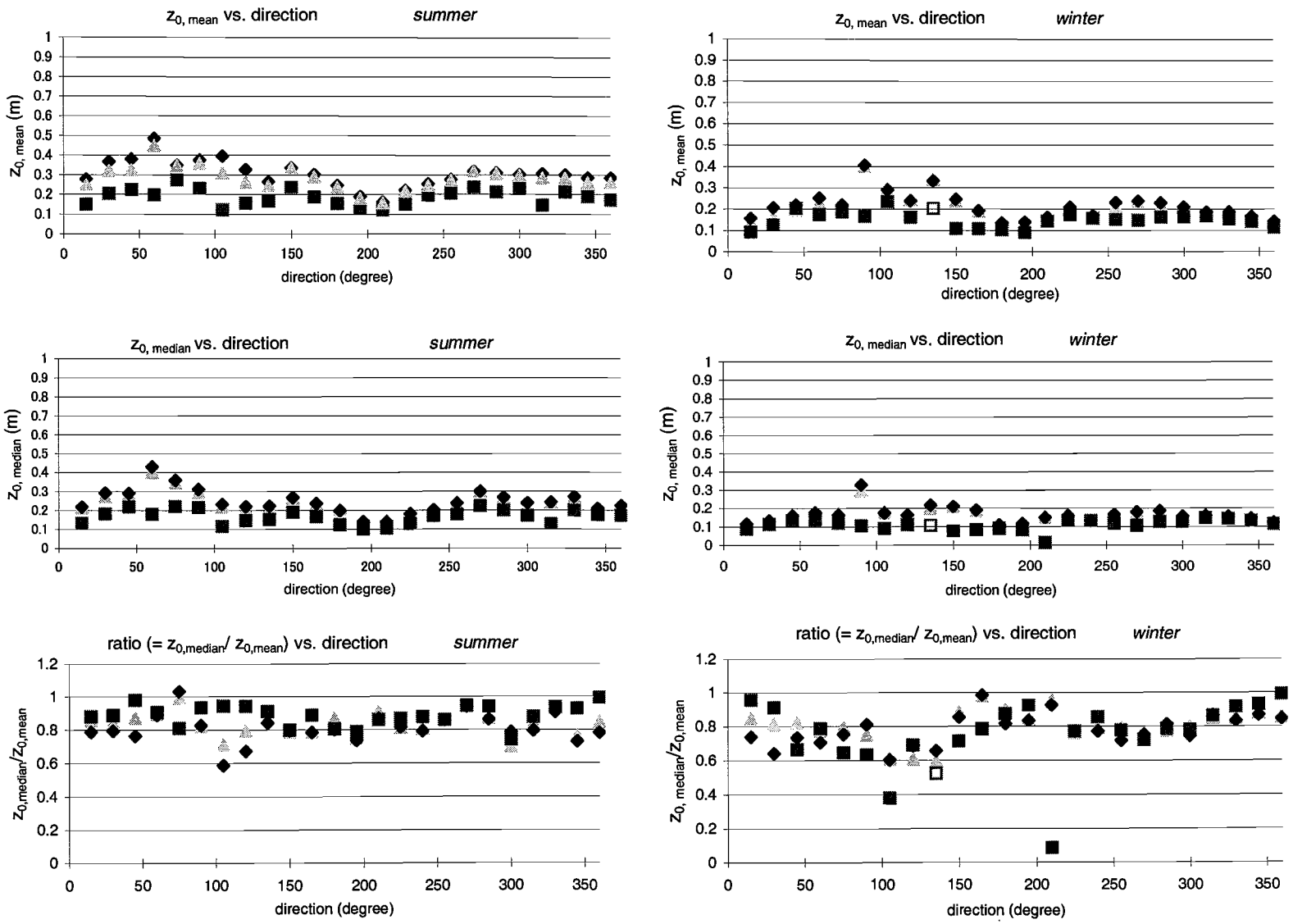

Fig. 13-b: Roughness lengths showing seasonal dependence. Summer and winter. z_m = 30 m and z_d = 27m are used.

Impacts: Change in z_m and z_d values:

Throughout the study described up until now, z_m and z_d values were set to be not the right values for the study site, hence the calculated roughness lengths are not in reality usable for future study at this Baltimore site. The actual z_m for this site was 40.5 m, and the seasonal z_d values are given in the following table.

	Heights			
	Trees (height of trees) x (porosity)	Buildings	z_H: height of roughness element	z_d: displacement length $z_d = 0.7\ z_H$
fraction	0.8	0.2		
summer	15 m x 0.8 = 12 m	5 m	12 m x 0.8 + 5 m x 0.2 = 10.6 m	**7.4** m
winter	15 m x 0.33 = 5 m	5 m	5 m x 0.8 + 5 m x 0.8 = 5 m	**3.5** m
spring				(7.4 m + 3.5 m) / 2 = **5.5** m
fall				(7.4 m + 3.5 m) / 2 = **5.5** m

Table 3: Calculation of displacement length. Porosities of the trees for summer and winter are estimated to be 0.8 and 0.33 respectively. Ref. [2].

1. Stability Calculations

(z_m = 40.5 m, z_d = 7.4 m (summer), 3.5 m (winter), and 5.5 m (fall & spring))

a) u* threshold determination

The stability calculation analyses can be conveyed as in the same way as discussed in earlier sections with z_m = 30 m and z_d = 27 m.

The data were generated using the program based on that in Appendix I with z_m and z_d given in Table 3, and again z'/L was plotted as a function of u* to see how data points were scattered for low u*. $u^* \geq 0.2\ m\ s^{-1}$ is determined to be set since we still observe many data points that are clearly with large errors for u* to be less than $0.2\ m\ s^{-1}$ (Fig. 14).

b) σ_v/u^* vs. z'/L

Also, the σ_v/u^* vs. z'/L relation was plotted in (Fig. 15) for the restriction of $u^* \geq 0.2\ m\ s^{-1}$. Most of the data points are fitting in the range of σ_v/u^* to be 0 to 6. The data is used to model the turbulent source area (ref. [3]).

2. Neutral Conditions

(z_m = 40.5 m, z_d = 7.4 m (summer), 3.5 m (winter), and 5.5 m (fall & spring))

a) z'/L threshold determination

In order to determine the neutral conditions with z'/L values, frequency of data with respect to z'/L were taken a look at (Fig. 16). Especially for transitional time range and night time range, one

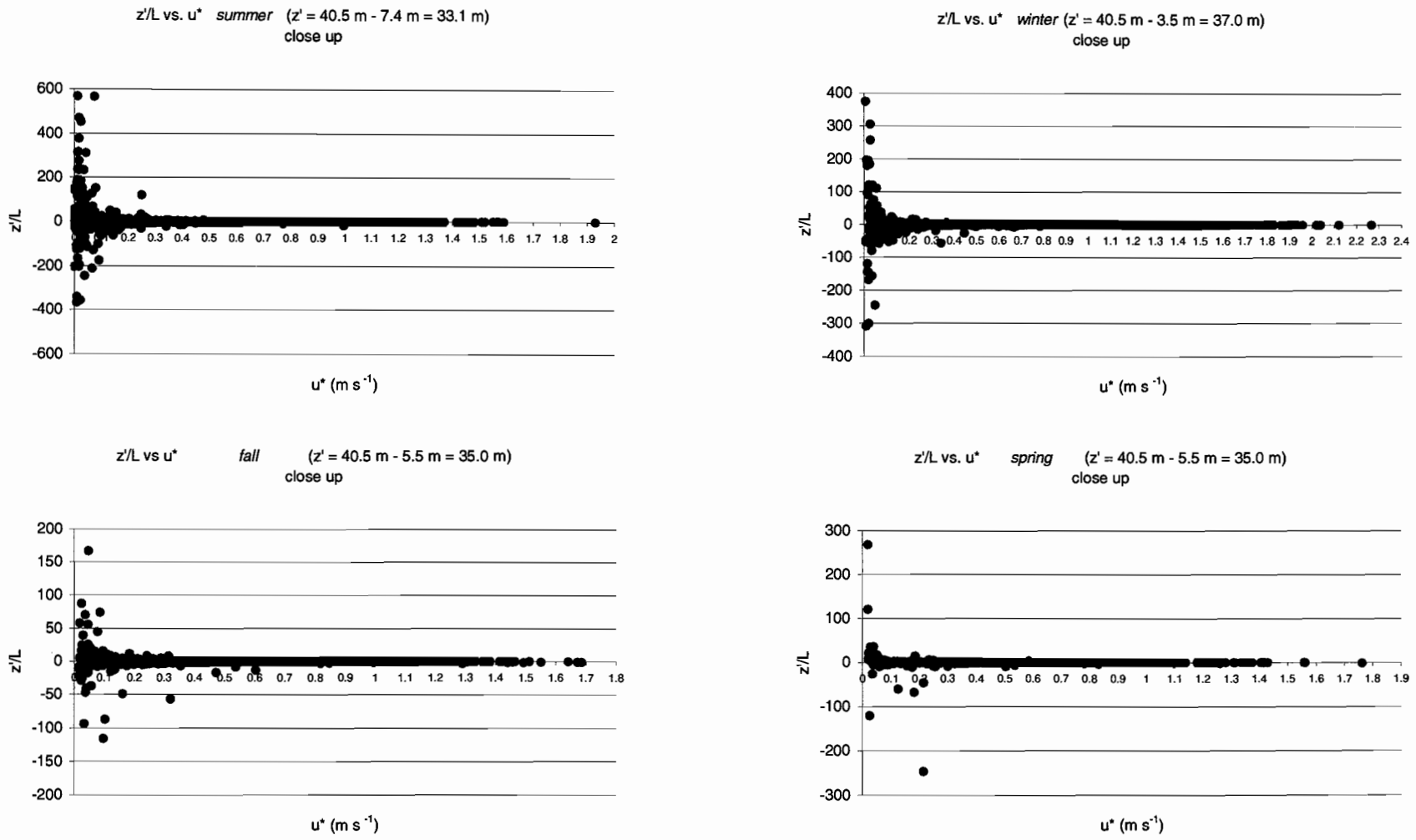

Fig.14: Threshold determination for u*. There observed a scatter of data in small u*, which, in fact, as stated in ref. [6], implies that a low u* value associates with measurements with large errors.

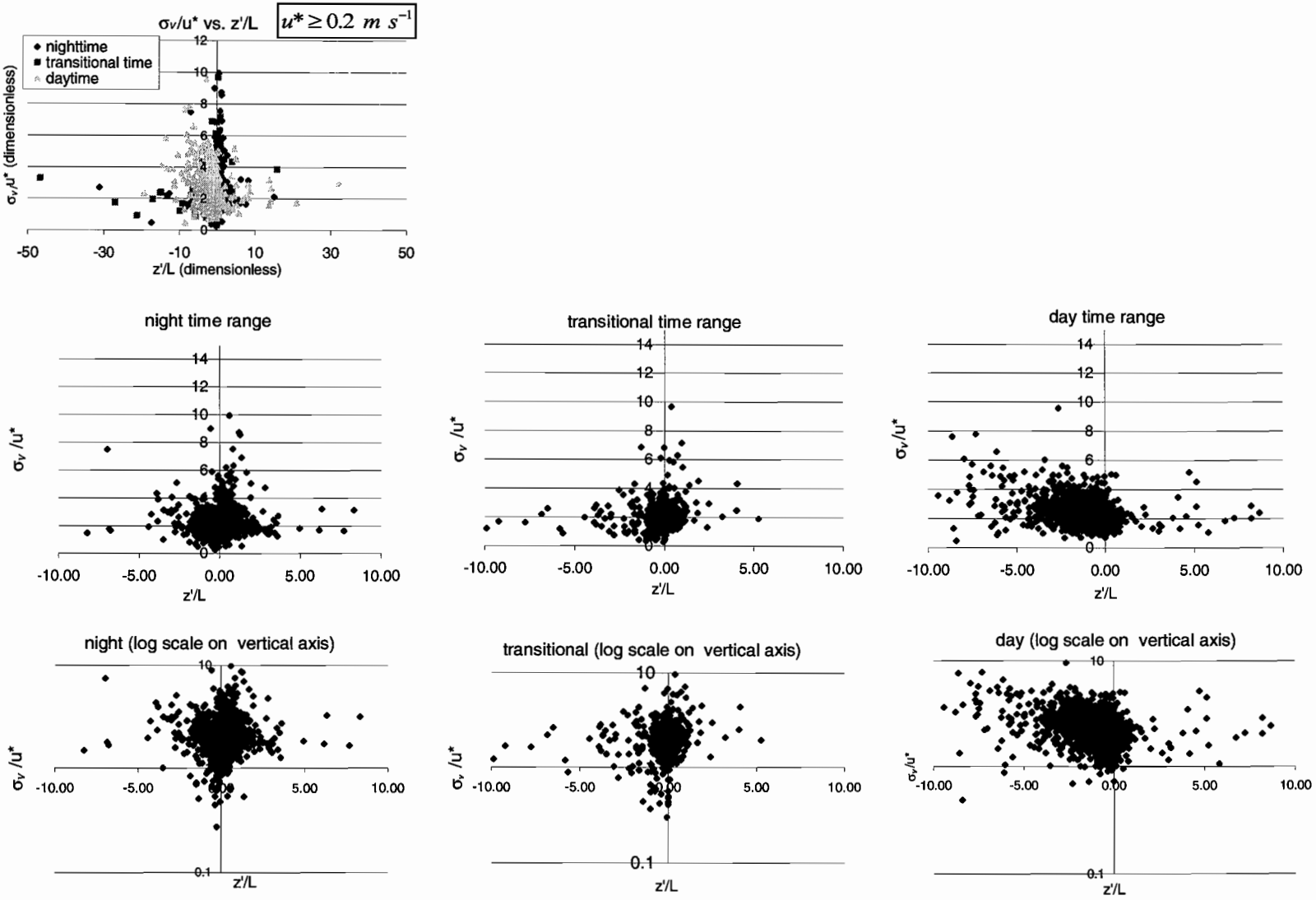

Fig. 15: Relation between σ_v/u^* and z'/L in urban areas. z_m = 40.5 m. z_d as indicated in Table 3. Both linear scale (up) and logarithmic scale (down) are shown. Note that there is some characteristics for each time range in shape of the data distribution, i.e., for night time, it is shifted toward positive z'/L and for daytime, it is shifted toward negative z'/L.

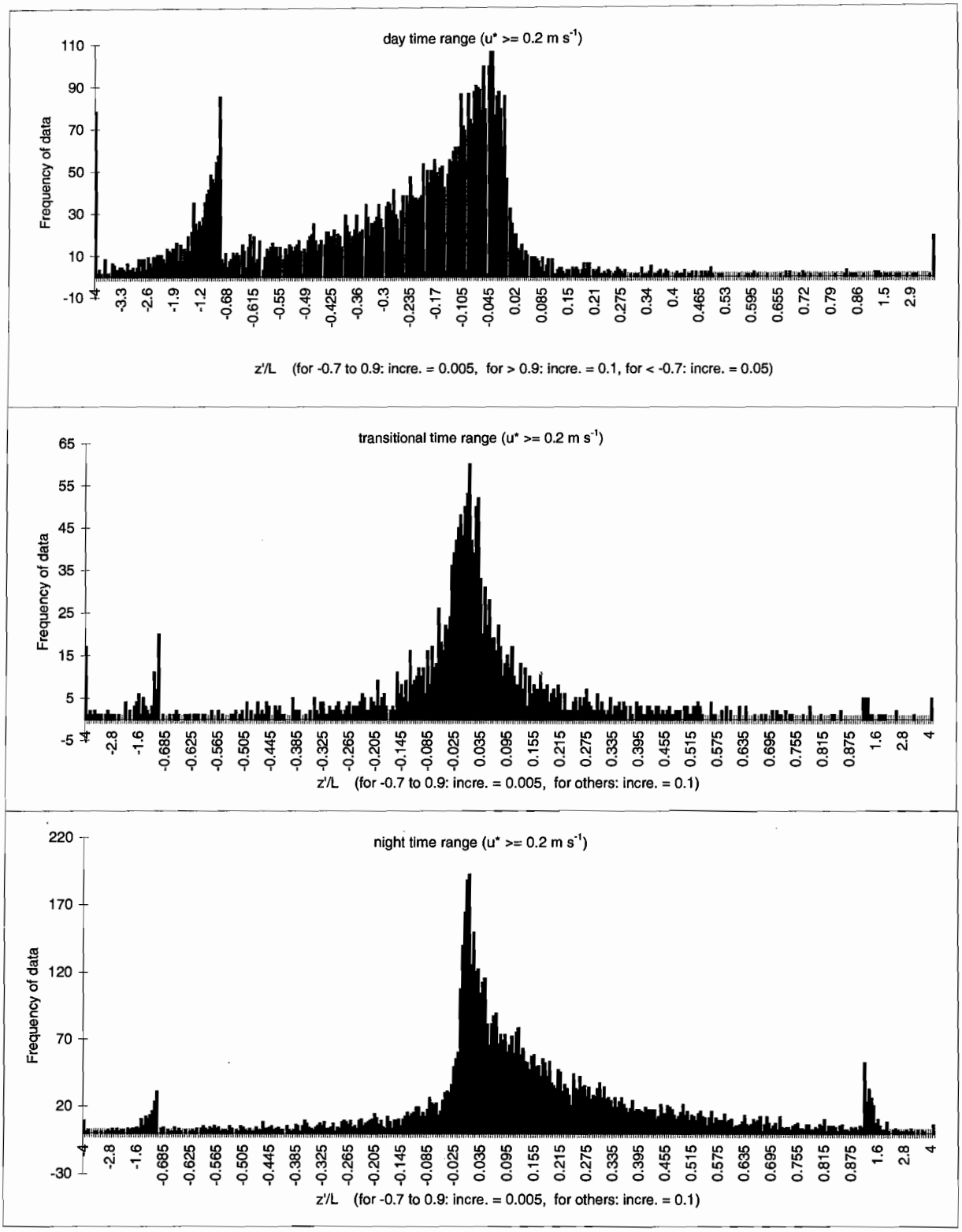

Fig 16:Threshold determination for z'/L to limit the data points for neutral conditions. Since neutral conditions exist in the vicinity of z'/L = 0, and especially the observation of the plot in transitional time range will allow one to see the great concentration of data points in the range of -0.05 < z'/L < 0.05. Spikes of frequency at either side of the skirt of the histograms happened because of the change of the size of the increments along the horizontal axis. z_m = 40.5m, z_d s are given in Table 3.

can see the prominently higher frequency in the vicinity of $-0.05 < z'/L < 0.05$, which implies those data to be under neutral conditions.

b) Roughness length calculations

The z_0 and u* relations were again seasonally investigated (Fig. 17). If compared with Fig. 9 which was with $z_m = 30$ m, and $z_d = 27$ m, the shapes of the data points are clearly shown to be different. In Fig. 17 ($z_m = 40.5$ m), it seems that relatively large z_0 values are less related to small u* in comparison with Fig. 9. However, it is also noticeable that there is a smaller number of outliers (those data with $z_0 > 6$ m) in Fig. 17.

Fig. 18 was given using the data under the conditions of $-0.05 < z'/L < 0.05$ and $u^* \geq 0.2$ m s^{-1}. These plots in Fig. 18 by seasons show the distribution of data points along with z_0 values so that they also give an idea of how many outliers there are in each season. Fig. 18 tells that the occurrence of these outliers does not necessarily depend on wind directions. Noting the variables in eq. 1 to see what is causing the z_0 to be too high given as outliers, one sees that it must depend on vertical wind velocity (u_z). In fact, outliers are caused when the ratio of u_z/u^* is smaller than about 4 (4.5 for winter, 4.3 for summer with $z_m = 40.5$ m and 4.0 for $z_m = 30$ m and $z_d = 27$ m). Clearly from eq. 1, the values for z_m and z_d have a great impact on z_0 values, since z_0 is linearly dependent of the value of the difference between z_m and z_d.

The mean and median values for z_0 are also investigated (Fig. 19-a & b). The averaged z_0 lengths in Table 4 were calculated using the data appeared in Fig. 19-a & b. Note that in the averaging process, three data points in the fall; direction of 15 – 30 (degree), 270 – 285 (degree) and 285 – 300 (degree), were excluded based on the investigation of reliability of data given by the ratio of $z_{0,\,median}/z_{0,\,mean}$ in addition to the clear fact that those data located relatively very far from the other data values. As Table 4 provides, under the conditions of $z_m = 40.5$ m, and $z_d = 7.4$ m, averaged $z_{0,\,mean} = 2.0$ m $\pm$ 0.4 m, and averaged $z_{0,\,median} = 1.8$ m $\pm$ 0.4 m for summer as an example. As compared to those values in Table 2 (under $z_m = 30$ m and $z_d = 27$ m), which are average $z_{0,\,mean} = 0.26$ m $\pm$ 0.06 m, and average $z_{0,\,median} = 0.22$ m $\pm$ 0.05 m for summer, the roughness lengths are about 10 times bigger, it is solely depending on the difference in z_m and z_d. The ratio of the z_0 in winter and summer is 95 % for mean and 89 % for median, which resulted in bigger than the value (74% and 69 % for mean and median) calculated with Table 2 but is closer to the value (80 – 90 %) that is indicated in ref. [1].

		summer		fall		winter		spring	
	u*, z'/L	$\langle z_0 \rangle$ (m)	$\sigma \langle z_0 \rangle$ (m)	$\langle z_0 \rangle$ (m)	$\sigma \langle z_0 \rangle$ (m)	$\langle z_0 \rangle$ (m)	$\sigma \langle z_0 \rangle$ (m)	$\langle z_0 \rangle$ (m)	$\sigma \langle z_0 \rangle$ (m)
$z_{0,\,mean}$	$u^* >= 0.2$ m s^{-1}, $-0.05 < z'/L < 0.05$	2.0	0.4	1.7	0.6	1.9	0.7	1.7	0.5
$z_{0,\,median}$	$u^* >= 0.2$ m s^{-1}, $-0.05 < z'/L < 0.05$	1.8	0.4	1.5	0.5	1.6	0.2	1.7	0.4

Table 4: Summary of averaged roughness lengths for mean and median values. $z_m = 40.5$ m is used. $z_d = 7.4$ m, 3.5 m and 5.5 m for summer, winter, and fall & spring are used. Compare the values with those provided in Table 2. The same equation as Table 2 was used for the deviation calculations.

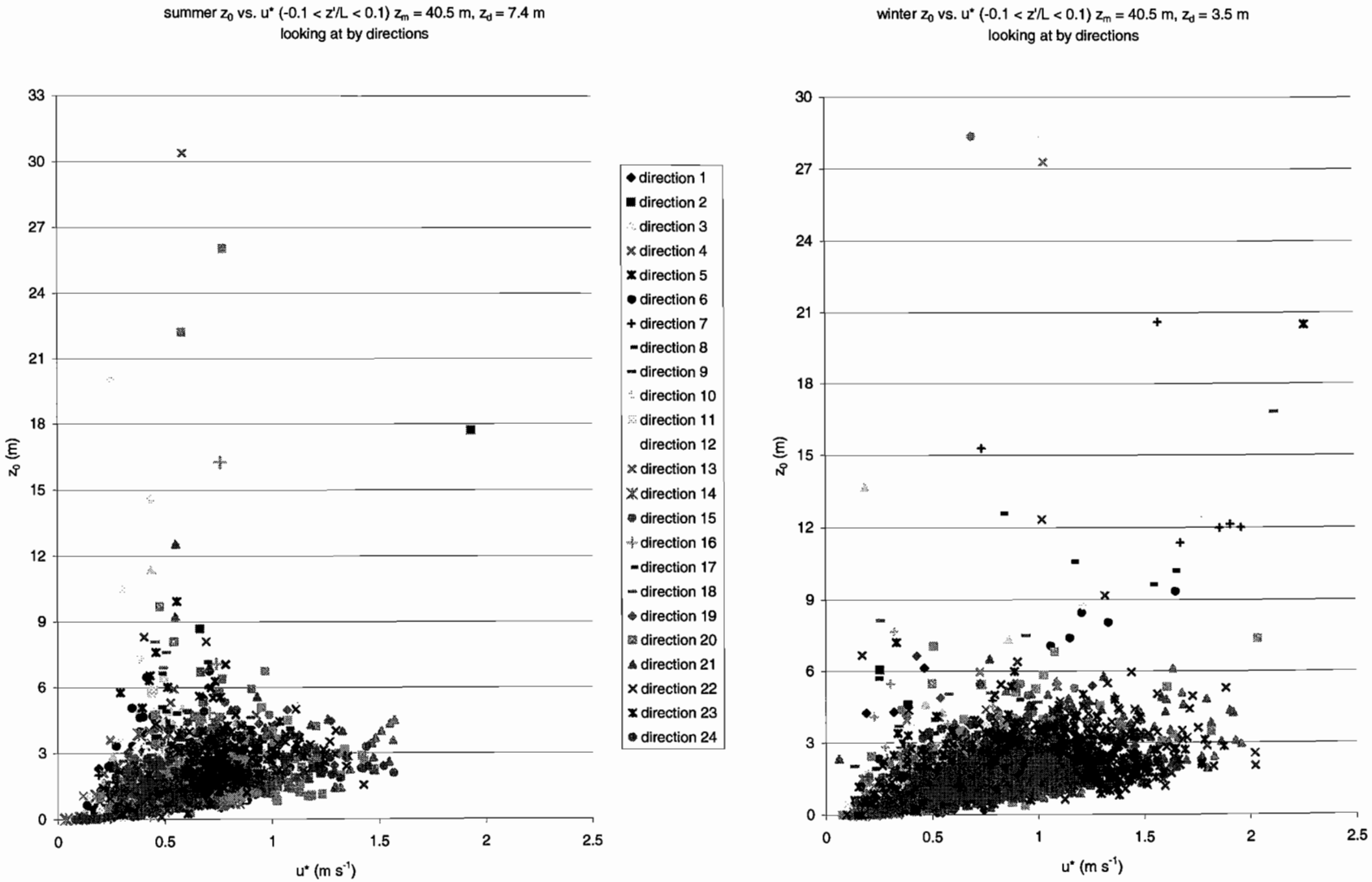

Fig. 17-a: z_0 distribution with respect to u* values for summer and winter. -0.1 < z'/L < 0.1, z_m = 40.5 m. z_d = 7.4 m for summer and 3.5 m for winter. Those data with z_0 larger than 6 m can be considered as outliers.

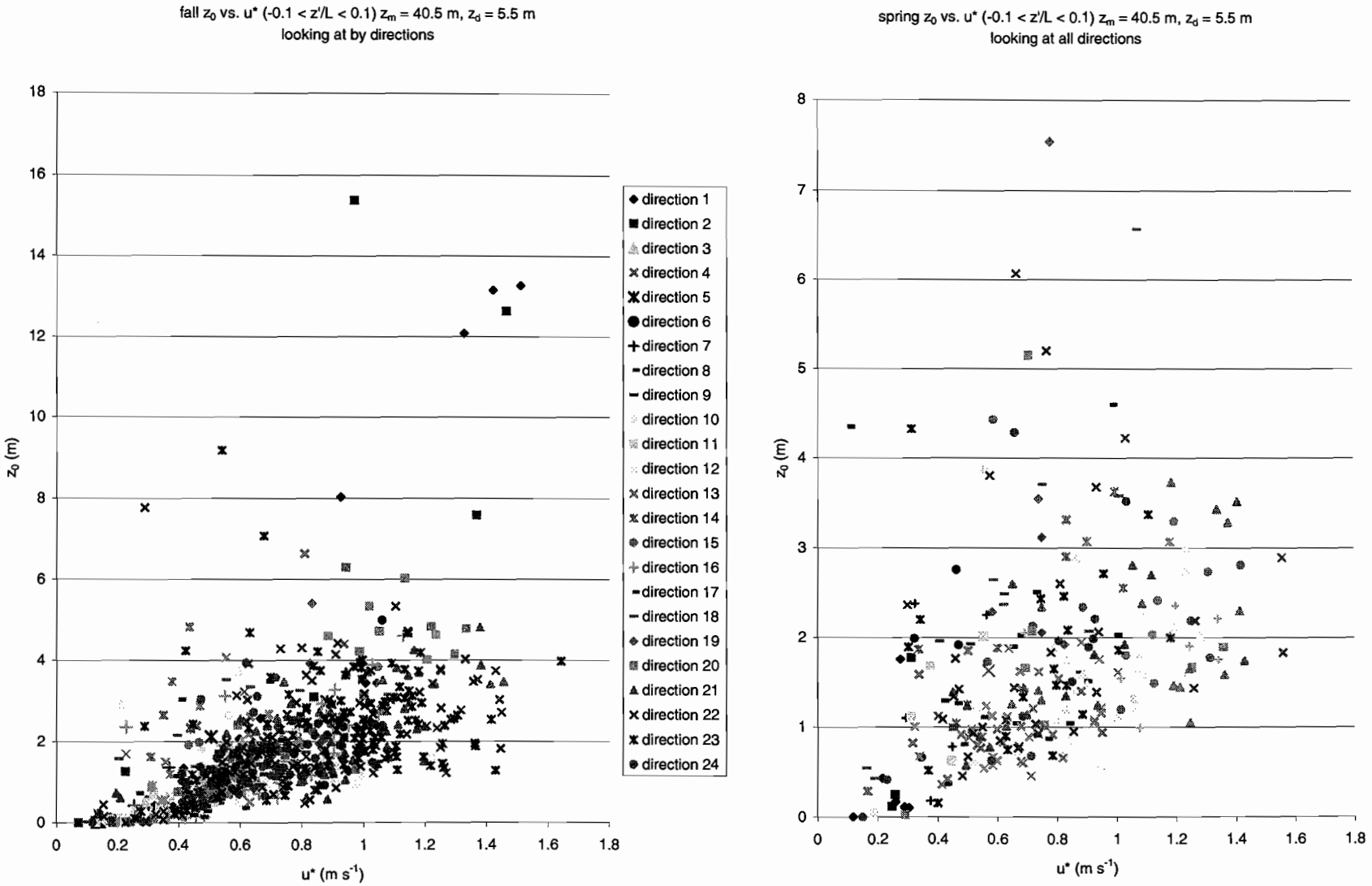

Fig. 17-b: z_0 distribution with respect to u* values for fall and spring. -0.1 < z'/L < 0.1, z_m = 40.5 m. z_d = 5.5 m for both fall and spring. Those data with z_0 larger than 6 m can be considered to be outliers.

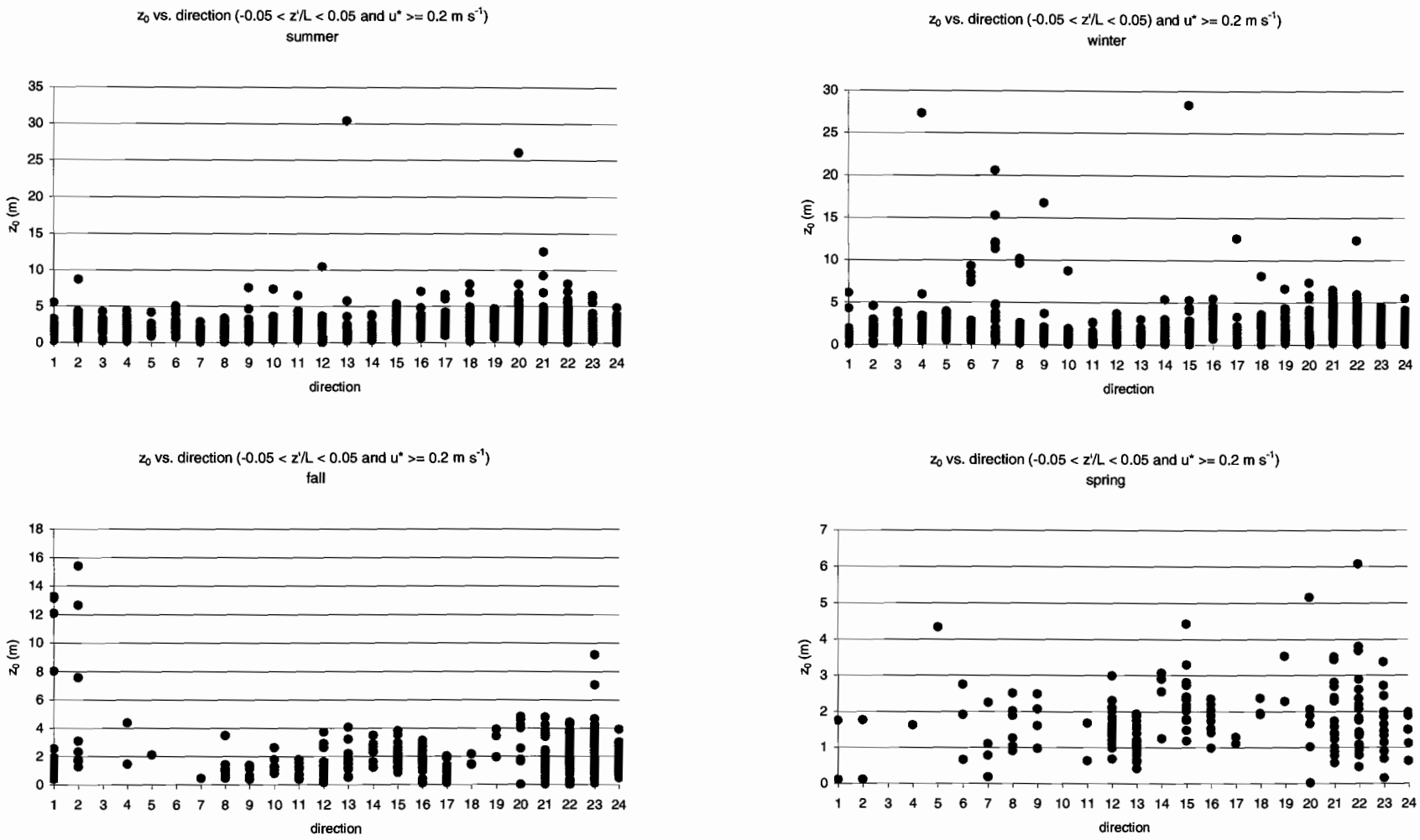

Fig. 18 : Observation of distribution of data in connection with z_0 values. z_m = 40.5 m is used. z_d = 7.4 m, 3.5 m, and 5.5 m are used for summer, winter, and fall & spring respectively.

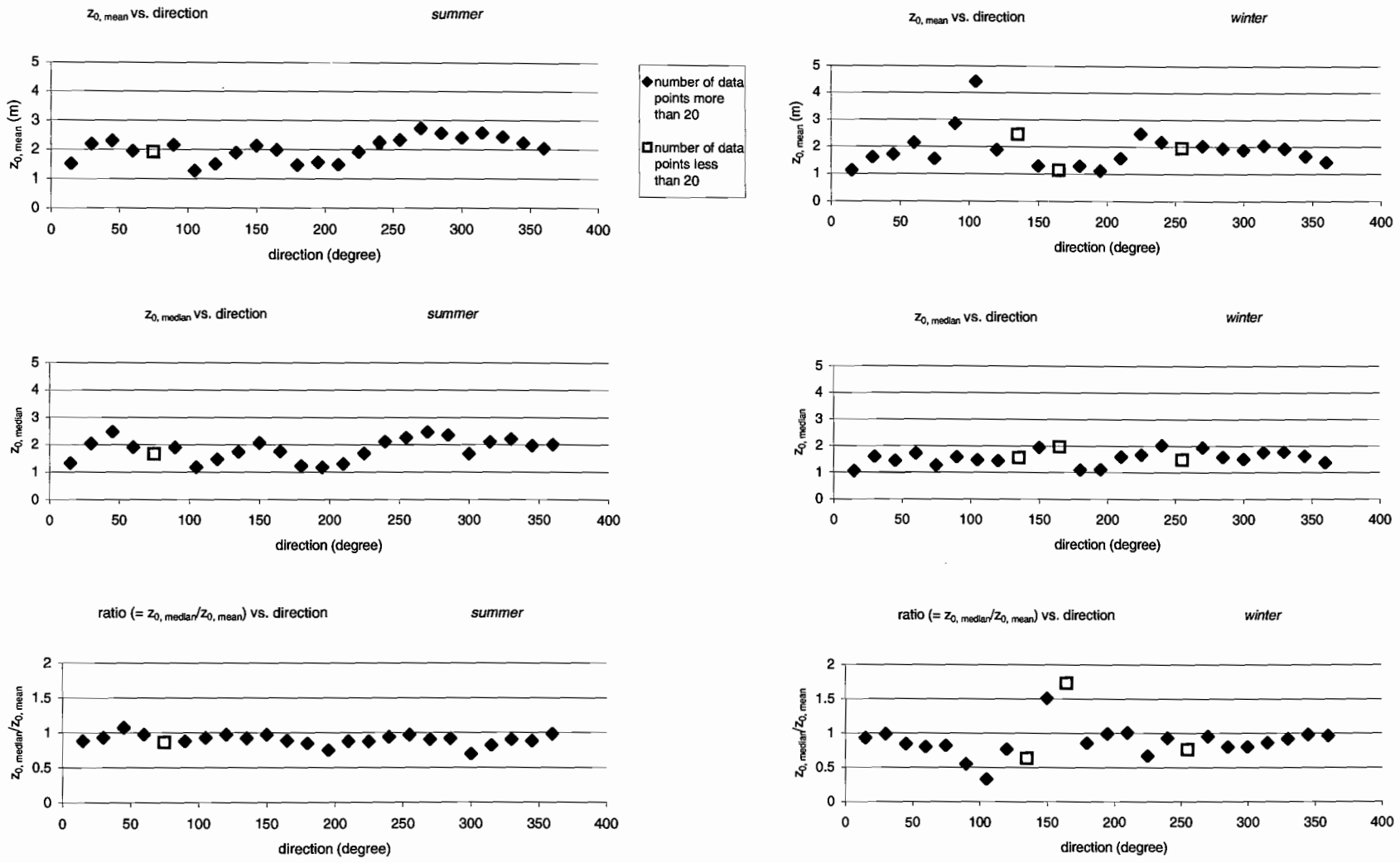

Fig. 19-a: Roughness lengths showing seasonal dependence. For neutral conditions, $-0.05 < z'/L < 0.05$ is used. $u^* >= 0.2$ m s^{-1}. $z_m = 40.5$ m and $z_d = 7.4$ m for summer and $z_d = 3.5$ m for winter. Departure of the ratio of $z_{0, median}/z_{0, mean}$ from unity also implies reliability of data.

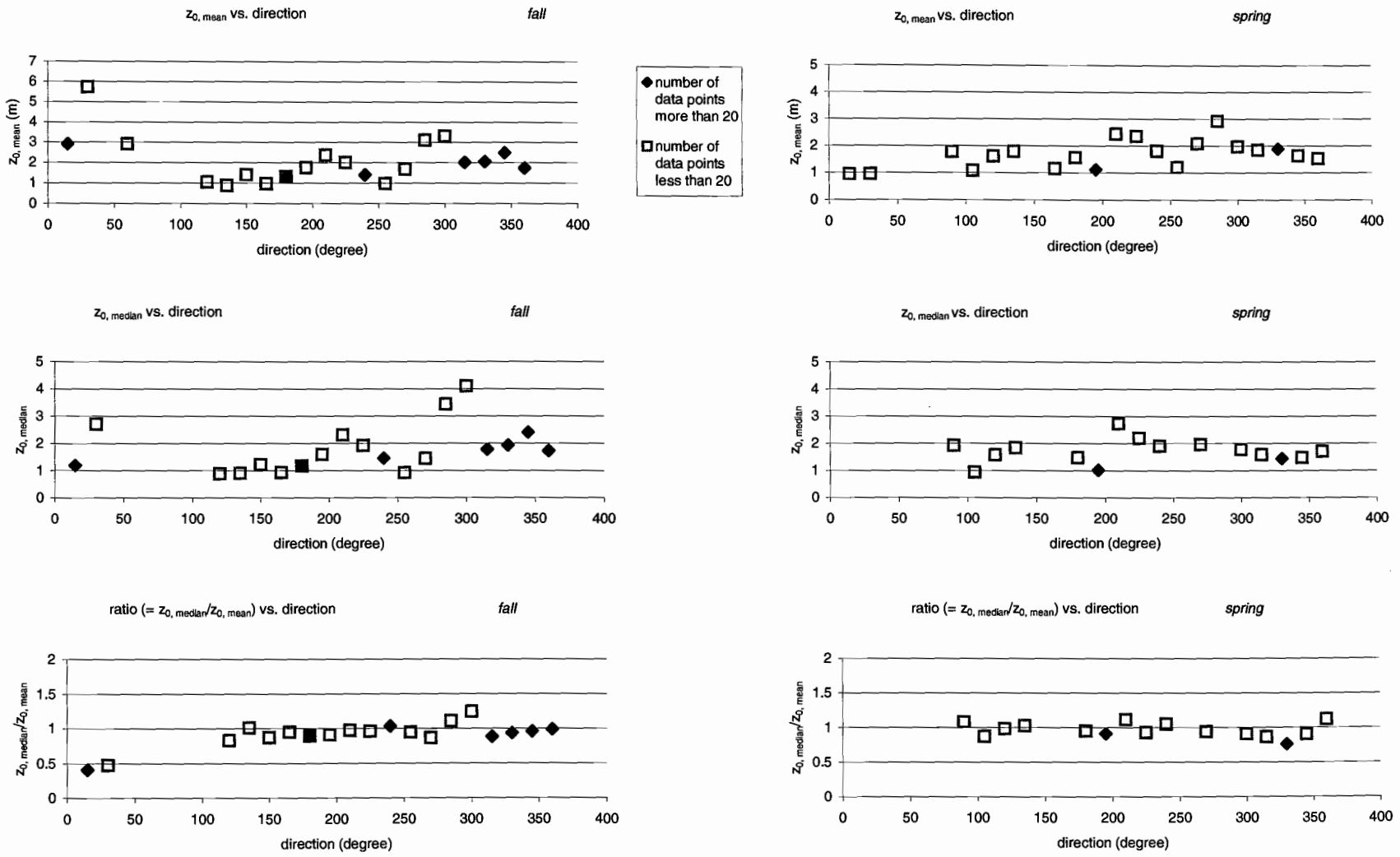

Fig. 19-b: Roughness lengths showing seasonal dependence. For neutral conditions, $-0.05 < z'/L < 0.05$ is used. $u^* >= 0.2$ m s^{-1}. $z_m = 40.5$ m and $z_d = 5.5$ m for both fall and spring. Departure of the ratio of $z_{0, median}/z_{0, mean}$ from unity also implies reliability of data.

Conclusions and Future Studies

The roughness length ($z_{0,\ mean}$ = 0.26 m for summer and 0.19 m for winter) was determined with the given z_m = 30 m and z_d = 27 m under neutral conditions at the Cub Hill Site, Baltimore, Maryland, USA. However, as discussed in section of *Impacts: Change in z_m and z_d values*, data were tested with the actual z_m = 40.5 m and z_d = 7.4 m (summer), 3.5 m (winter), and 5.5 m (fall & spring) later on and found to be $z_{0,\ mean}$ = 2.0 m for summer and 1.7 m for winter. Further analyses with these actual values for z_m and z_d need to be studied. Also as the measurements at the site runs in a longer span of time, the collected data will be accumulated further, then there will be less errors and more accuracy obtained in determination of parameters, giving us better knowledge on this urban area. This study can be carried out to be related to the dependence of CO_2 fluxes on surface characteristics which were just discussed here. Further, how the results for Baltimore can be applied to other cities and also related to the contribution of urban areas to global CO_2 concentration may be pursued.

Acknowledgement

The project was granted by Undergraduate Research and Creative Activity Partnership, Office of Research, Indiana University.

Special thanks to Prof. Sue Grimmond for her strongest support and instructions leading me to much further questions as I was working on my project.

I also would like to thank Brian Offerele (PhD student) for his patience and helps.

And also thanks for the senior thesis committee members in Physics Department representaed by Prof. Rick Van Kooten for their waiting for me to submit this report.

References

[1] Grimmond, C.S.B., King, T.S., Roth, M., and Oke, T.R., 1998: Aerodynamic Roughness of Urban Areas Derived From Wind Observations. *Bound.-Layer Meteor.*, **89**, 1-24.

[2] Grimmond, C.S.B. and Oke, T.R., 1998: Aerodynamic Properties of Urban Areas Derived from Analysis of Surface Form. *J. Appl. Meteor.*, **38**, 1262-1292.

[3] Schmid, H.P., 1994: Source Areas for Scalars and Scalar Fluxes. *Bound.-Layer Meteor.*, **67**, 293-318.

[4] Grimmond, C.S.B. and Offerle, B.D., Hom, J., Golub, D.: Observations of Local-Scale Heat, Water, Momentum and CO2 fluxes at Cub Hill, Baltimore, *American Meteorological Society*. **4** Urban Environment, 117-118.

[5] Grimmond, C.S.B., King, T.S., Cropley, F.D., Nowak, D.J., Souch, C., 2002: Local-scale fluxes of carbon dioxide in urban environments: methodological challenges and results from Chicago. *Environmental Pollution* **116**, S243-S254.

[6] Schmid, H.P., Grimmond C.S.B., Cropley F.D., Offerle, B., and Su H.B., 2000: Measurements of CO_2 and energy fluxes over a mixed hardwood forest in the Midwestern United States. *Agricultural and Forest Meteorology*, **103**, 355-373.

[7] Roth, M., 2000: Review of atmospheric turbulence over cities. *Quarterly Journal of the Royal Meteorological Society* **126**, 941-990.

[8] Stull, R. B.: *Meteorology for Scientists and Engineers*, 2nd ed., Brooks/Cole, 2000, Pacific Grove, CA, USA.

Appendix I: Program

```
!this is a program to calculate neutral stability condition. march, 2003
!Reiko Toriumi (rtoriumi@indiana.edu) under supervision of Prof. Sue Grimmond (grimmon@indiana.edu)

program stability
implicit none
real::dectime, temp, ustar, k, grav, wtheta, l, Qh, QhTc, Qe, FCo2, U,&
    V, W, TC, H20, C02, WS, DIR, UU, VV, WW, TT, TCTC, HH, CC, wTC, wq, wC,&
    rho_a, rho_v, cp, ea, es, T2, RH2, P, Vane, Kdn, Kup, Ldn, Lup, Tkz, &
    Qstar, QG, Tsoil, Moist, SW, Rain, zL, z0          !! define variables
integer::i, ios, HR, MN, IL, ii
real::zmeas, zd, zzd, bad=-999.


character (len=120)::filename
                                   ! set the limit of the number of columns (characters) to be 120
open(10, file=res.txt')
write(10,*)'dectime     l          zL          z0          dir          u*          T          wT          Uz'
                                   !write out dectime and l(obukhov length) and z0(roughness length)....
                                   !to the output file
write(10,*)'#units      m     dimensionless     m          degree      m/s      Celsius     cm*C/s      m/s'
                                        !write out the units for the header to the output file
open(12,file="list_all.txt")          !input file

k=0.4                              !von Karman's constant
grav=9.8                           !gravitational acceleration
zmeas=30.                          !measurement height in meters (this needs to be corrected later)
zd=zmeas*0.9                       !displacement length (right now, zd = 27)
zzd=zmeas-zd                       !right now zzd = 3.



!This loop will calculate a roughness length under neutral static stability.

do ii=1,1000000            !check if the number of execution is enough!!

read(12,*,iostat=ios)filename      !read filenames
if(ios<0) exit                     !if the number of files is less than the number that is defined,
                                   !then exit loop.
        print*,trim(filename)      !to know which data I am running

        open(11,file=trim(filename))

!loop to read different data files


read(11,*)                 !skip header (first line) in input file
read(11,*)                 !skip header (second line) in input file


  !This sub-loop will calculate the obukhov lengths
  do i = 1, 100
  read(11, *, iostat=ios)dectime, HR, MN, IL, ustar, Qh, QhTc, Qe, FCo2, &
              U, V, W, temp, TC, H20, C02, WS, DIR, UU, VV, WW, TT, TCTC, &
              HH, CC, wtheta, wTC, wq, wC, rho_a, rho_v, cp, ea, es, T2, &
              RH2, P, Vane, Kdn, Kup, Ldn, Lup, Tkz, Qstar, QG, Tsoil, Moist, SW, Rain

  If (ios.lt.0) exit                          ! if # of rows in the file is less than the # of defined loop,
                                              ! then exit the program
```

Appendix I: Program

```
  if (temp /=bad .and. ustar /= bad .and. wtheta /=bad .and. wtheta /= 0.000) then
                                        ! for Q* grouping, (or stability conditions study) , add " .and. Qstar /=bad ".
                                                                ! if data are not missing(=-999.0)
                                                                ! otherwise wtheta is not zero, then do calculation.

  L=-1*(temp+273.16)*ustar**3/(k*grav*wtheta/100)  ! calculate L.
                                      ! ref. C.S.B. Grimmond, T.R. Oke et al.:
                                      !Boundary-Layer Meteorology 89:
                                      !1-24, Netherlands, 1998
                                      !(Aerodynamic Roughness of Urban Areas
                                      !Derived From Wind Observations)- eq.(6)
                                      !wT/100 will be in SI unit.

                                                                !If L<0, then the condition is unstable.
                                                                !If L>0, then the condition is stable.



                                      !Since we can establish good empirical relation between u* (friction vel) and
                                      !z0 (roughness length) in neutral stability,
                                      !we limit the condition to be neutral in order to calculate z0.


 zL=zzd/L

                        ! use obukhov length to limit the condition for neutral.
                        ! abs(zL)< 0.1, or 0.05 or 0.01.
 if(abs(zL) < 0.01) then          ! condition for neutral static stability prior to roughness length calc.
                        ! see Grimmond et al.1998 :   eq.(7)  BLM 89,1-24
                        ! -C1(C2-zL)^(-1/3) approaches a const. in neutral stability.
                        ! -> C2 >> zL
                        ! the exact value needs to be determined

                                      ! z0:= roughness length -  Grimmond et al.1998 :   eq.(5)  BLM 89,1-24
 z0=zzd*exp(-1*(WS*k)/ustar)          ! WS = Uz.



 write(10,100)dectime, L, zL, z0, dir, ustar, temp, wtheta, WS
                                      ! write the calculated L, dectime, z0, and so forth
                                      !to the output file
 100 format(f9.4,8g14.4)              ! to modify the length of data, f<width>
                                      !i.e., representation of 10^
   end if

 end if



 enddo          !finish the sub-loop
 enddo            !finish the main loop

 write(10,*)"#meas:", zmeas,"          zd:",zd                                   !write out to the output file

 Stop"Finished" !write out finished

 end program stability
```

Appendix II: Symbols and Notations

Symbols:

u^*: friction velocity (ms^{-1})
u_z: vertical wind velocity (ms^{-1})
z_0: surface roughness length (m)
L: the Obukhov length (m)
σ_v: standard deviation of lateral wind speed fluctuations (ms^{-1})
z_m: reference height or measurement height (m)
z_d:displacement length (m)
z_H: height of roughness element (m)
$z' = z_m - z_d$ (m)
$z'/L = (z_m - z_d)/L$ (indicating the strength of buoyancy at the reference height) (dimensionless)
σ_v / u^*: magnitude of crosswind turbulence (indicating the strength of lateral wind fluctuations) (dimensionless)
Q^* : Net heat flux (Wm^{-2})
T: temperature (K)
wT : kinematic heat flux (Kms^{-1})
(In this study, T/ wT is used instead of $\bar{\theta} / \overline{\omega'\theta'}$.)
DOY: day of the year

Notations:

Seasons are determined by observation of the photos of the vicinity of the site that were taken from the tower during the site maintenances. They are defined as follows:

notation	season	period	
season1 (s1)	summer *(leaf on)*	DOY 134-304	(May, June, July, Aug., Sep., and Oct. –2001)
season2 (s2)	fall (*transition*)	DOY 305-334	(Nov. –2001)
season3 (s3)	winter *(leaf off)*	DOY 335-90	(Dec. –2001, Jan., Feb., Mar., and Apr. –2002)
season4 (s4)	spring (*transition*)	DOY 91-120	(Apr.—2002)
season5 (s5)	summer *(leaf on)*	DOY 121-304	(May, June, July, Aug., Sep., and Oct.—2002)
season6 (s6)	fall (*transition*)	DOY 305-334	(Nov. –2001)
season7 (s7)	winter *(leaf off)*	DOY 335-57	(Dec.—2002, Jan., and Feb.—2003)

For the stability condition analyses, the time ranges are defined as follows;
day time: $50\ W\ m^{-2} \leq Q^*$
transitional time: $-10\ W\ m^{-2} < Q^* < 50\ W\ m^{-2}$
night time: $Q^* \leq -10\ W\ m^{-2}$

The directions were divided into 24 groups and named direction 1, 2, 3, …, and 24 with 15 degree widths, i.e.:

notation	angle (degree)
direction1	0-15
direction2	15-30
direction3	30-45
direction4	45-60
direction5	60-75
direction6	75-90
direction7	90-105
direction8	105-120
direction9	120-135
direction10	135-150
direction11	150-165
direction12	165-180
direction13	180-195
direction14	195-210
direction15	210-225
direction17	225-240
direction18	240-255
direction19	255-270
direction20	270-285
direction21	285-300
direction22	300-315
direction23	315-330
direction24	330-360

Note that the north is on 0 degree, east on 90, hence south 180, west 270.

Appendix III: Histograms (z_m = 30 m, z_d = 27 m)

Data are sorted according to Q* values and by seasons with u* thresohold bigger than 0.5 m s^{-1}.

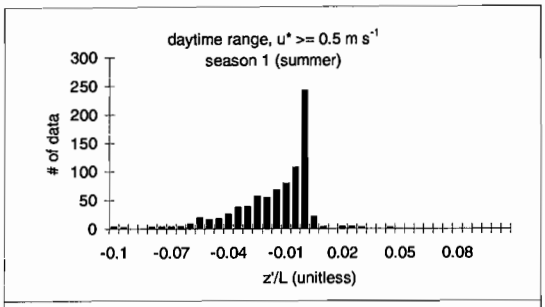

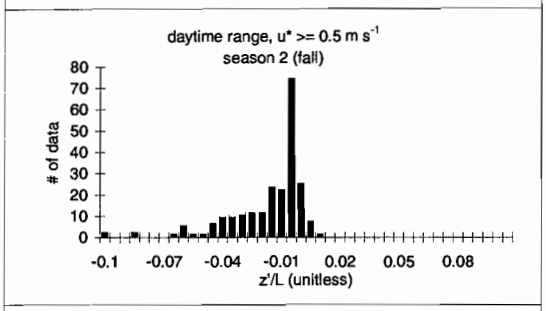

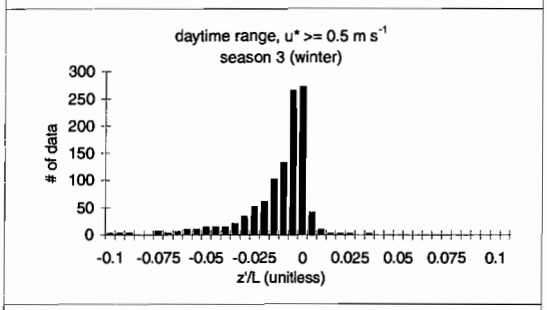

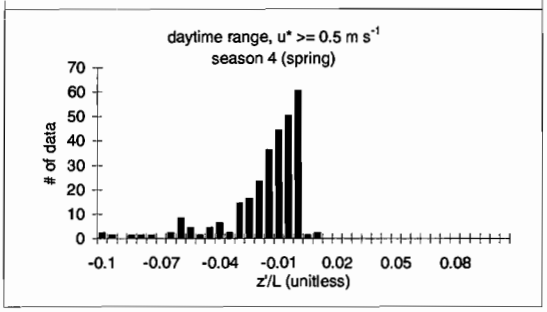

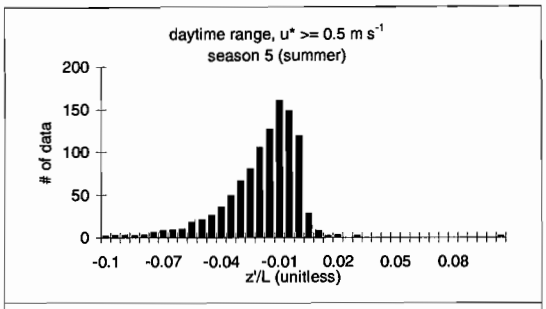

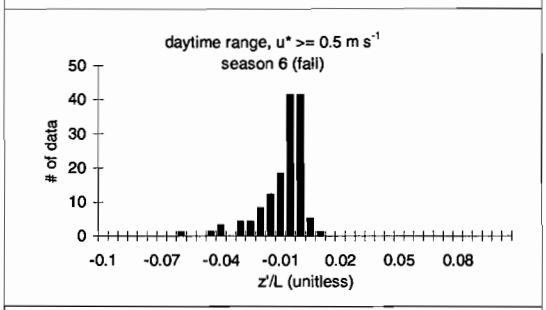

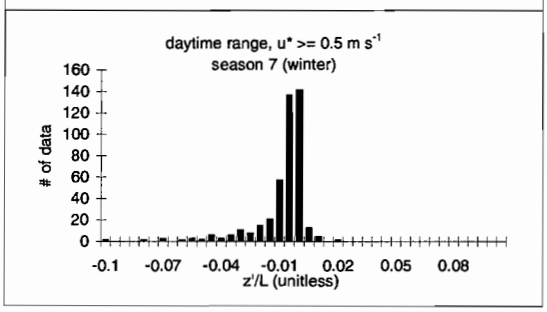

Appendix III: Histograms (z_m = 30 m, z_d = 27 m)

Data are sorted according to Q* values and by seasons with u* thresohold bigger than 0.5 m s^{-1}.

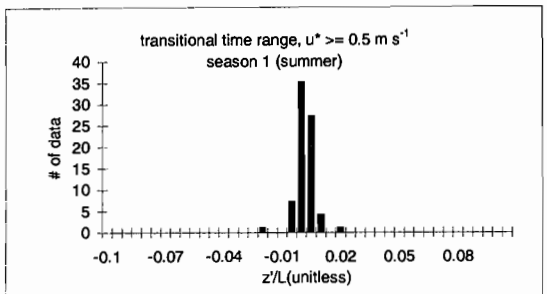

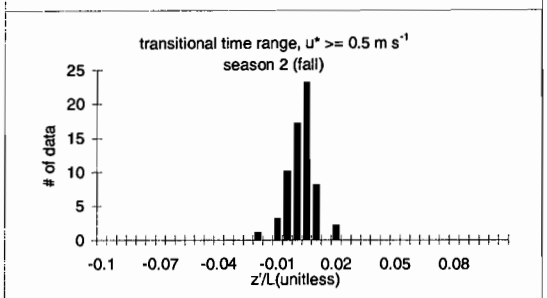

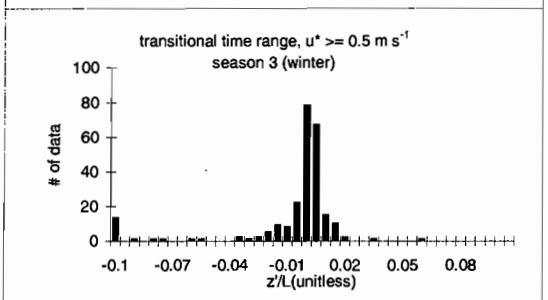

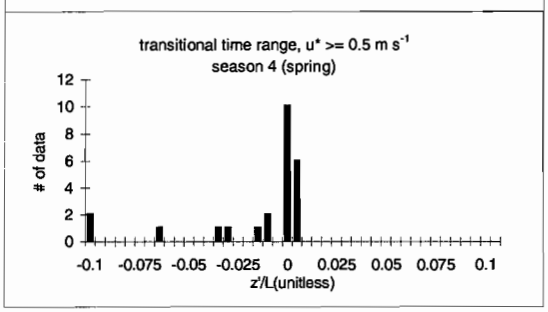

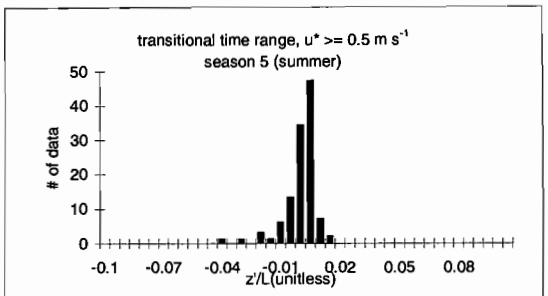

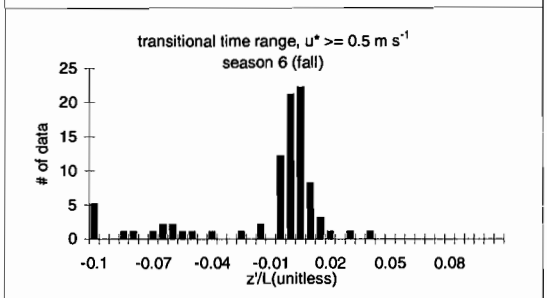

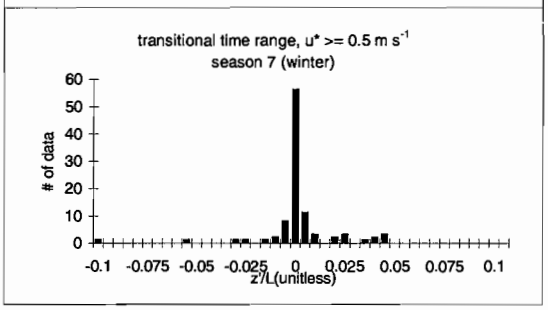

Appendix III: Histograms (z_m = 30 m, z_d = 27 m)

Data are sorted according to Q* values and by seasons with u* thresohold bigger than 0.5 m s^{-1}.

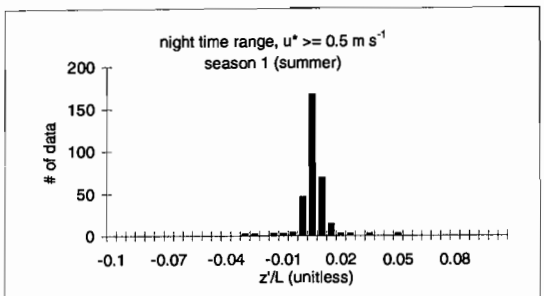

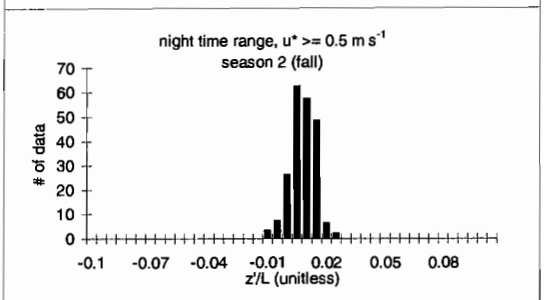

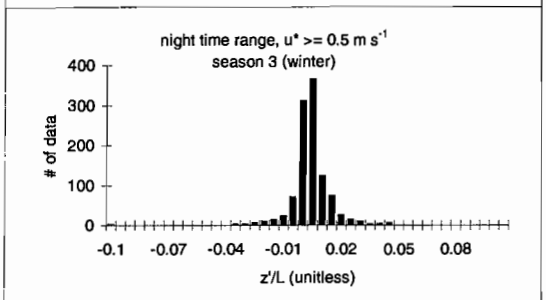

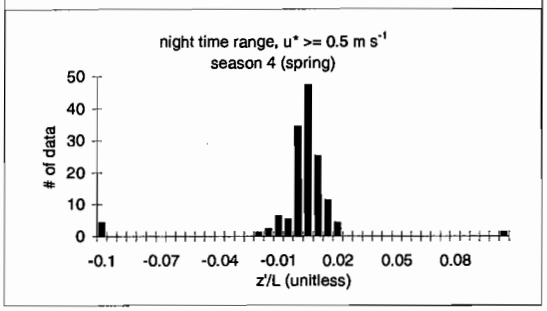

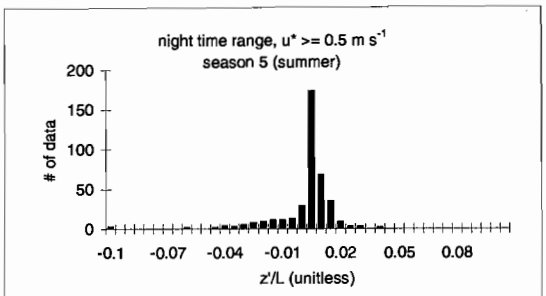

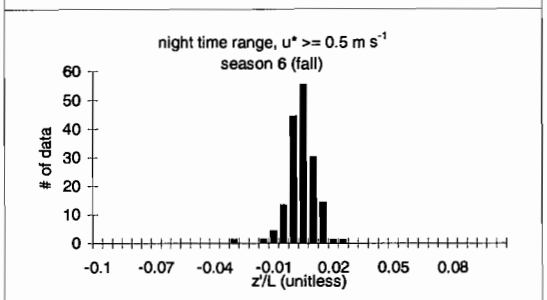

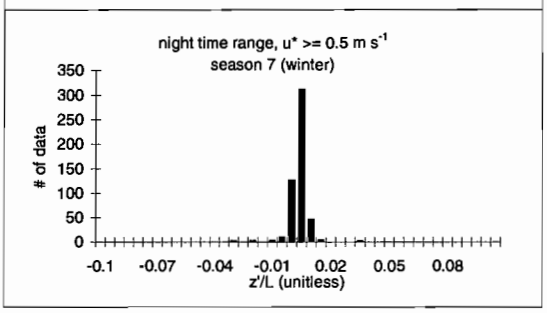

Appendix III: Histograms (z_m = 30 m, z_d = 27 m)

Data are sorted according to Q* values and by seasons with u* thresohold bigger than 0.2 m s^{-1}.

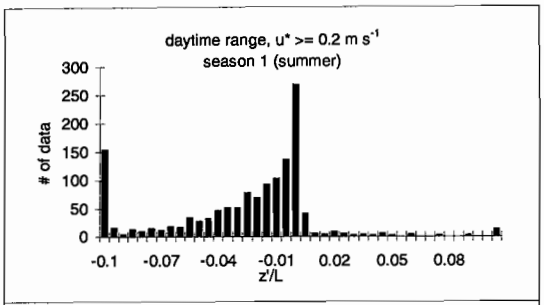

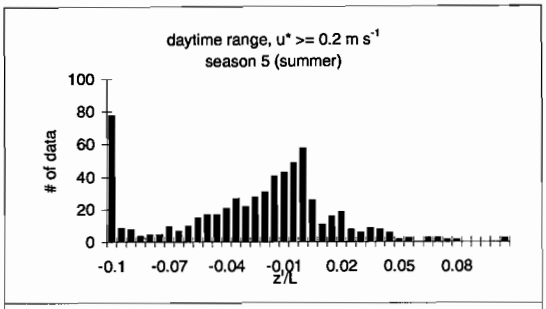

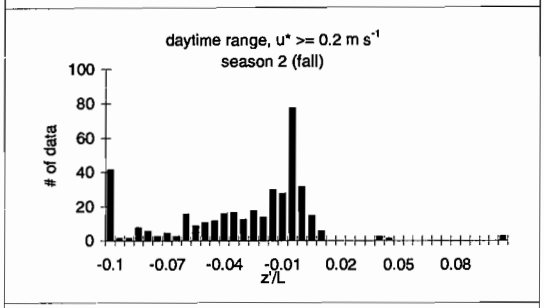

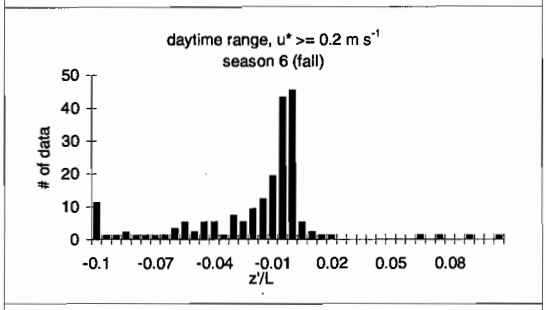

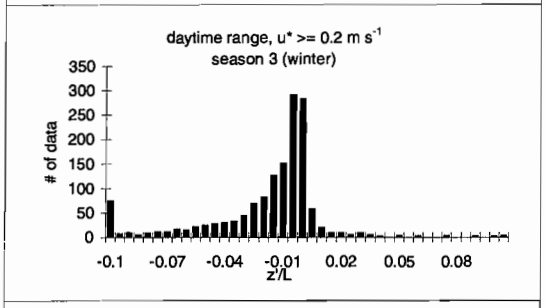

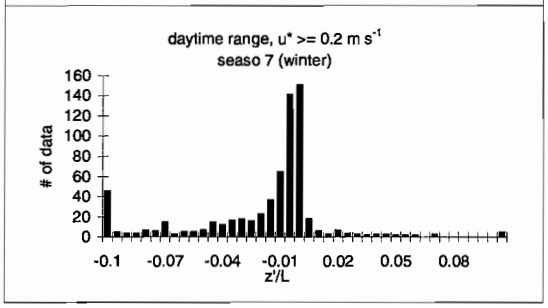

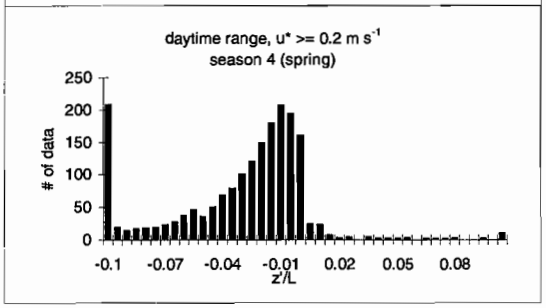

Appendix III: Histograms (z_m = 30 m, z_d = 27 m)

Data are sorted according to Q* values and by seasons with u* thresohold bigger than 0.2 m s^{-1}.

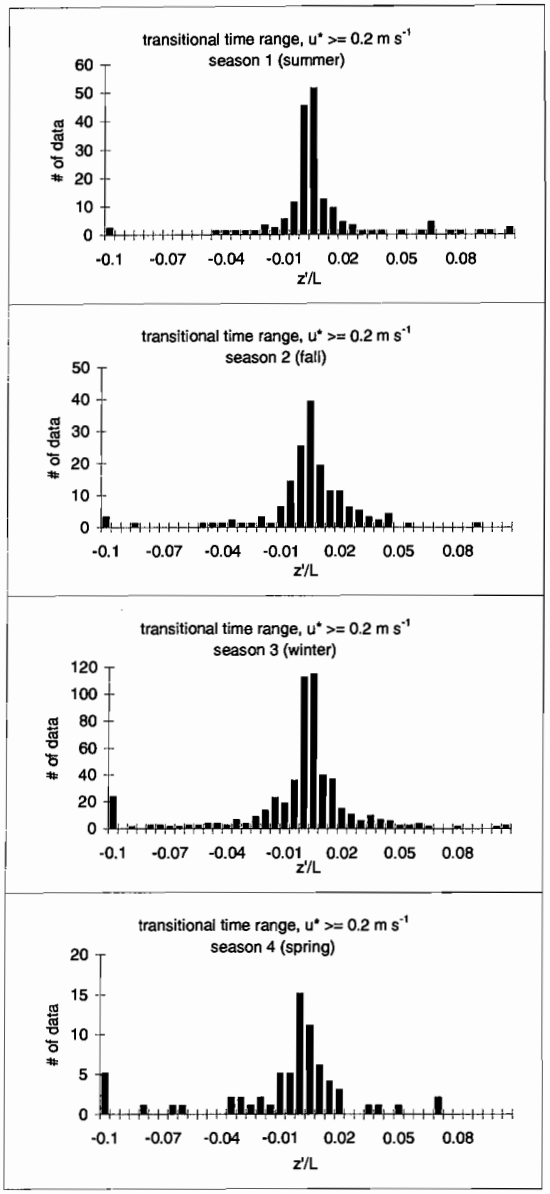

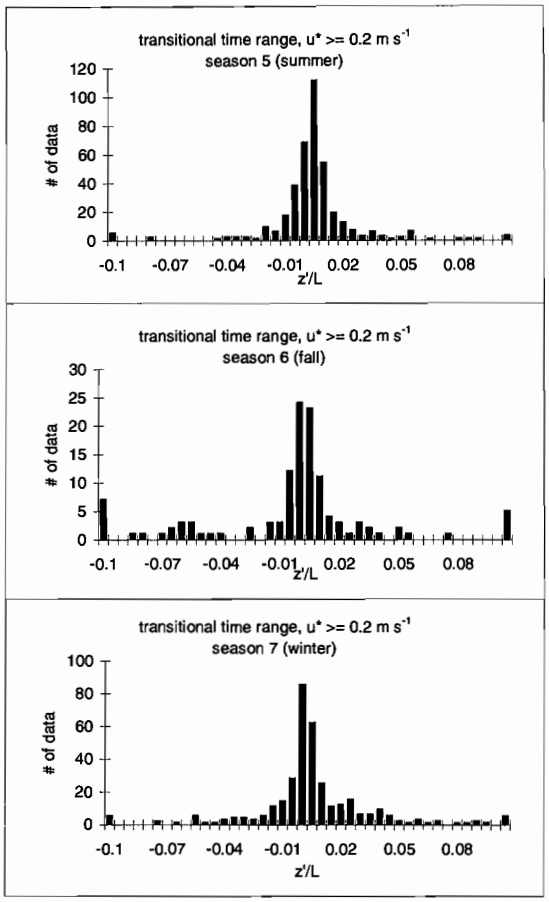

Appendix III: Histograms (z_m = 30 m, z_d = 27 m)

Data are sorted according to Q* values and by seasons with u* thresohold bigger than 0.2 m s^{-1}.

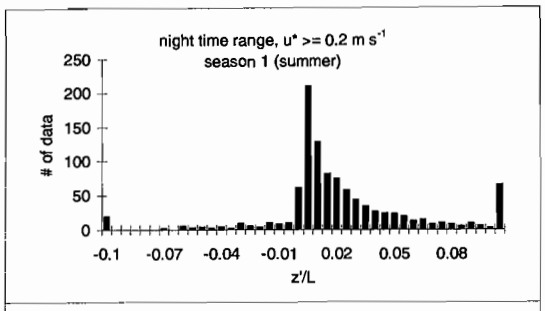

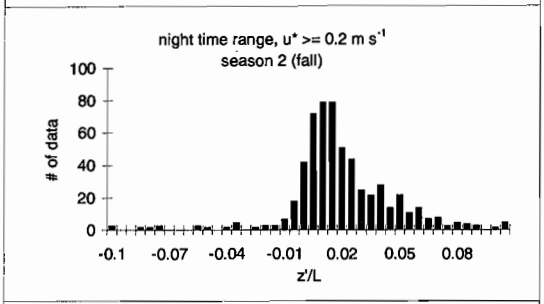

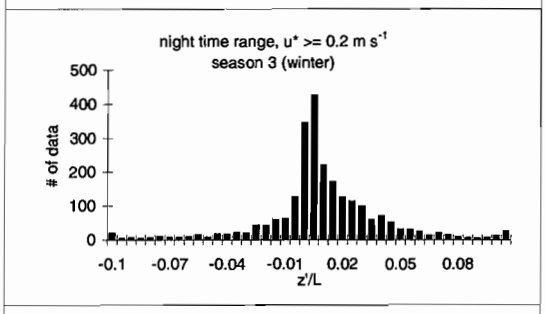

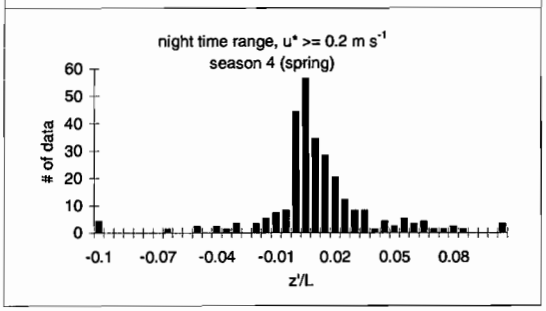

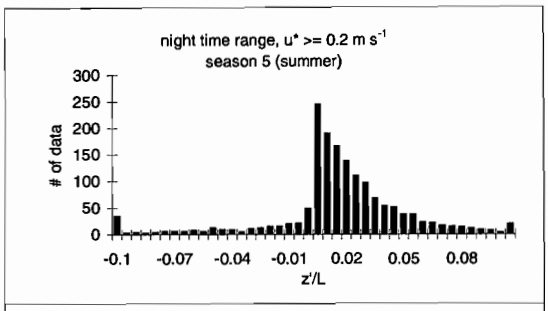

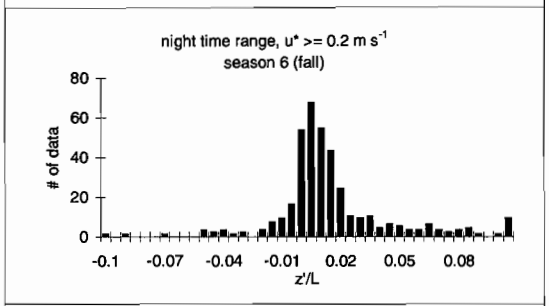

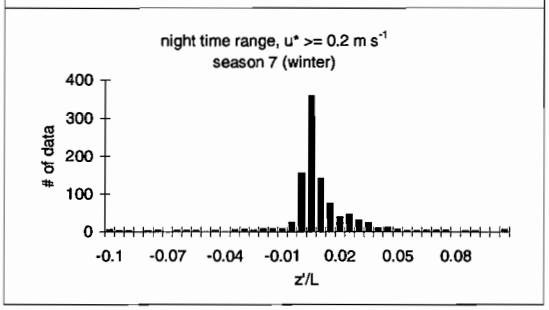

Appendix III: Histograms (z_m = 30 m, z_d = 27 m)

Data are sorted by season and by direction.

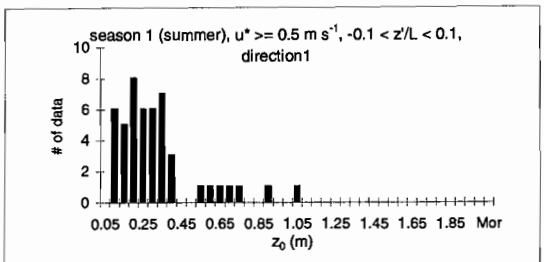

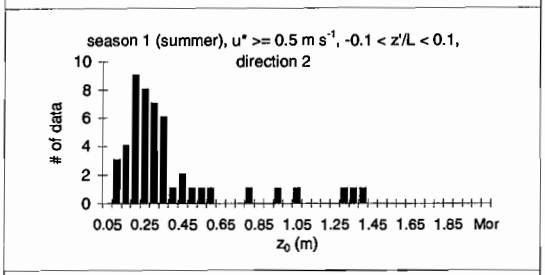

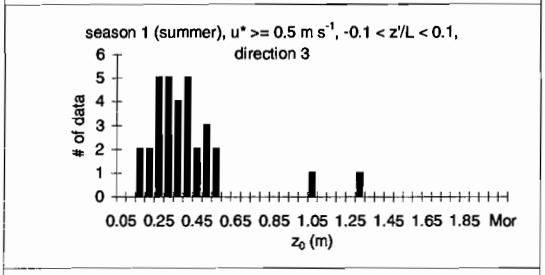

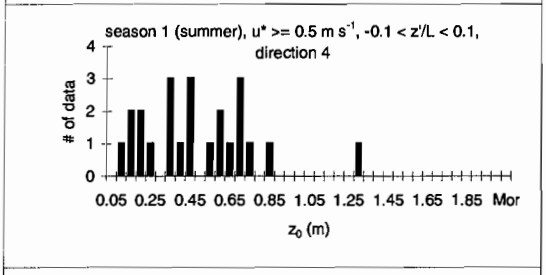

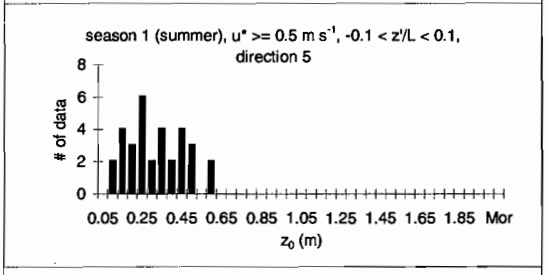

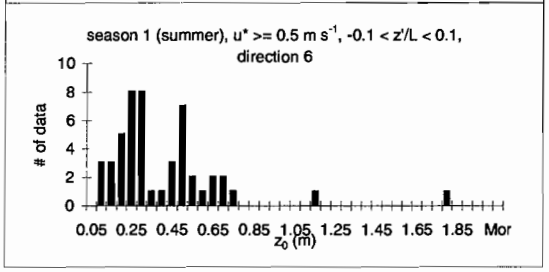

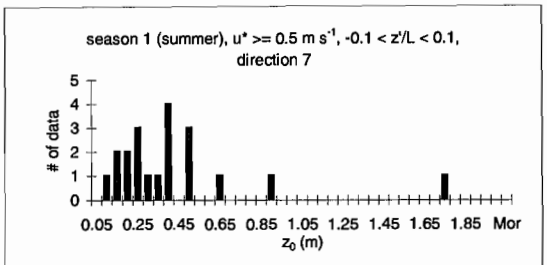

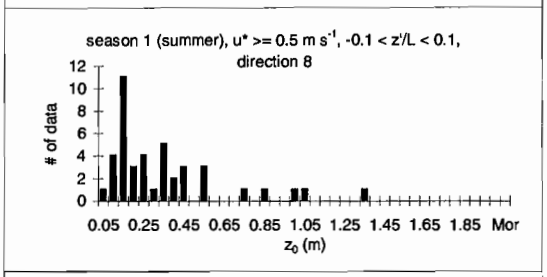

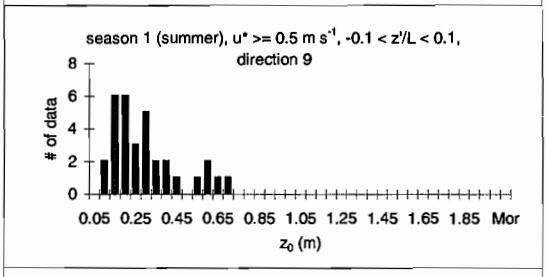

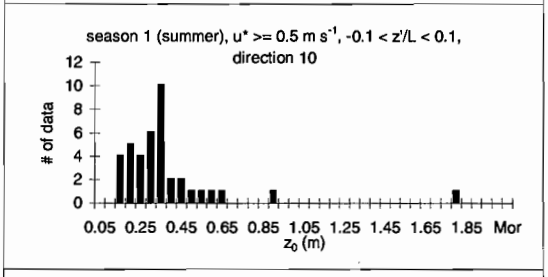

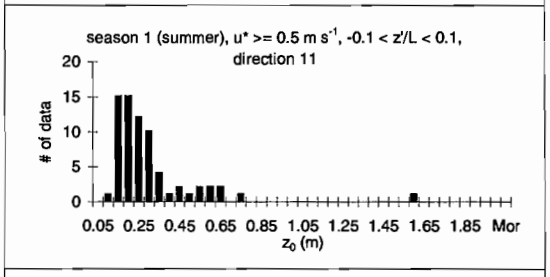

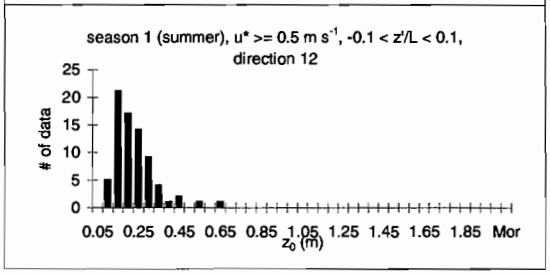

Appendix III: Histograms (z_m = 30 m, z_d = 27 m)

Data are sorted by season and by direction.

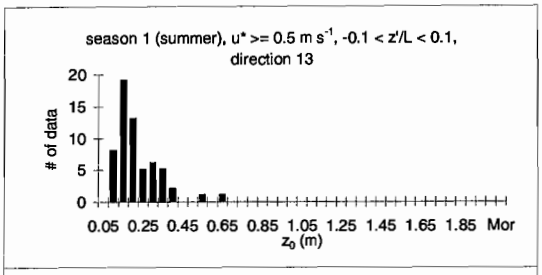

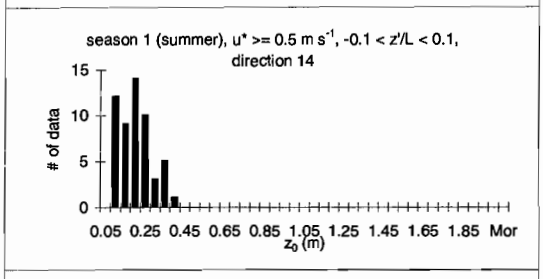

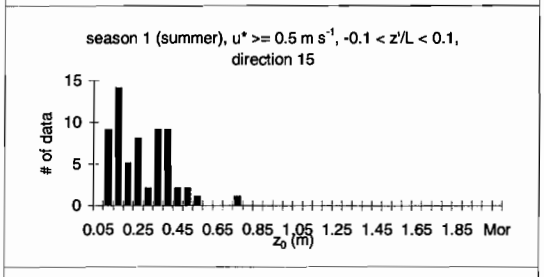

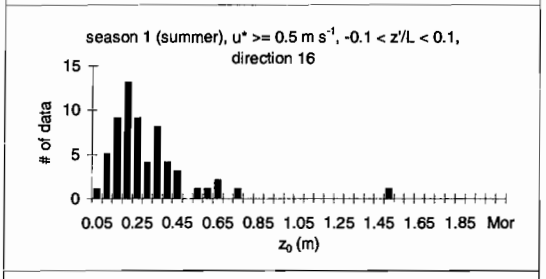

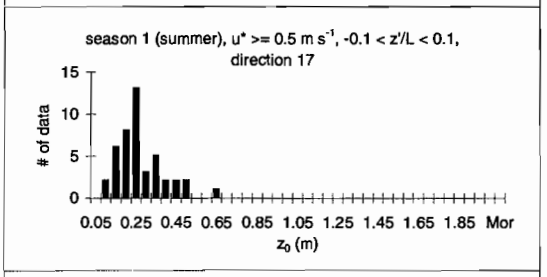

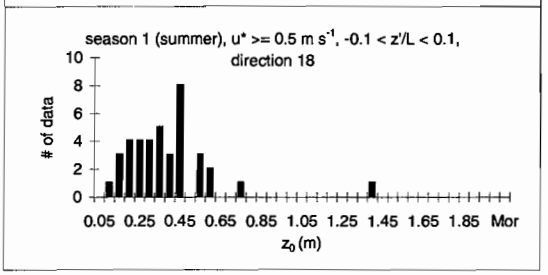

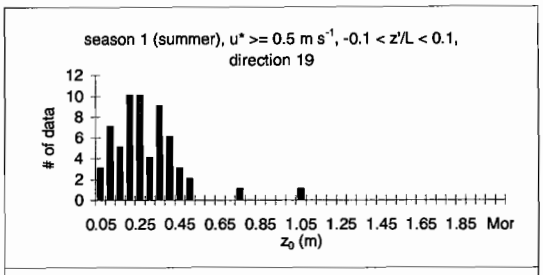

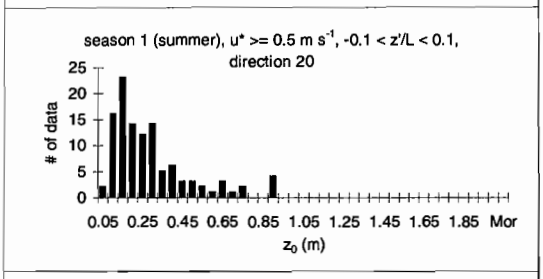

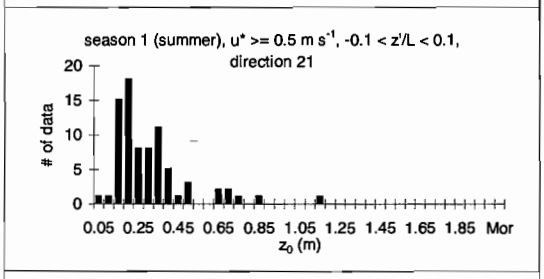

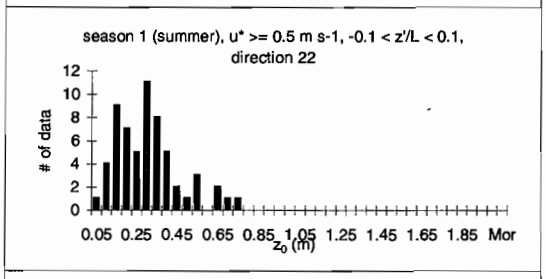

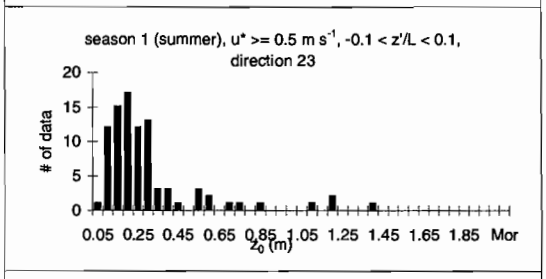

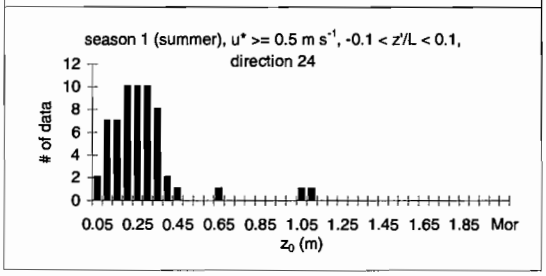

Appendix III: Histograms (z_m = 30 m, z_d = 27 m)

Data are sorted by season and by direction.

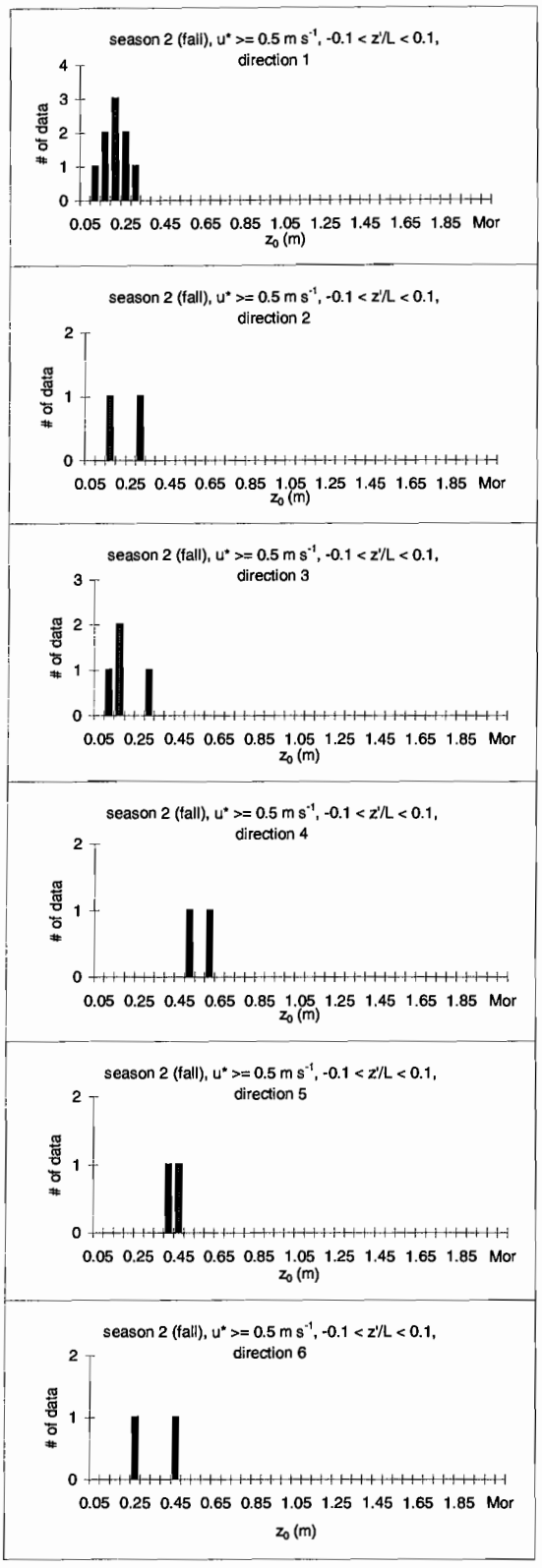

N/A

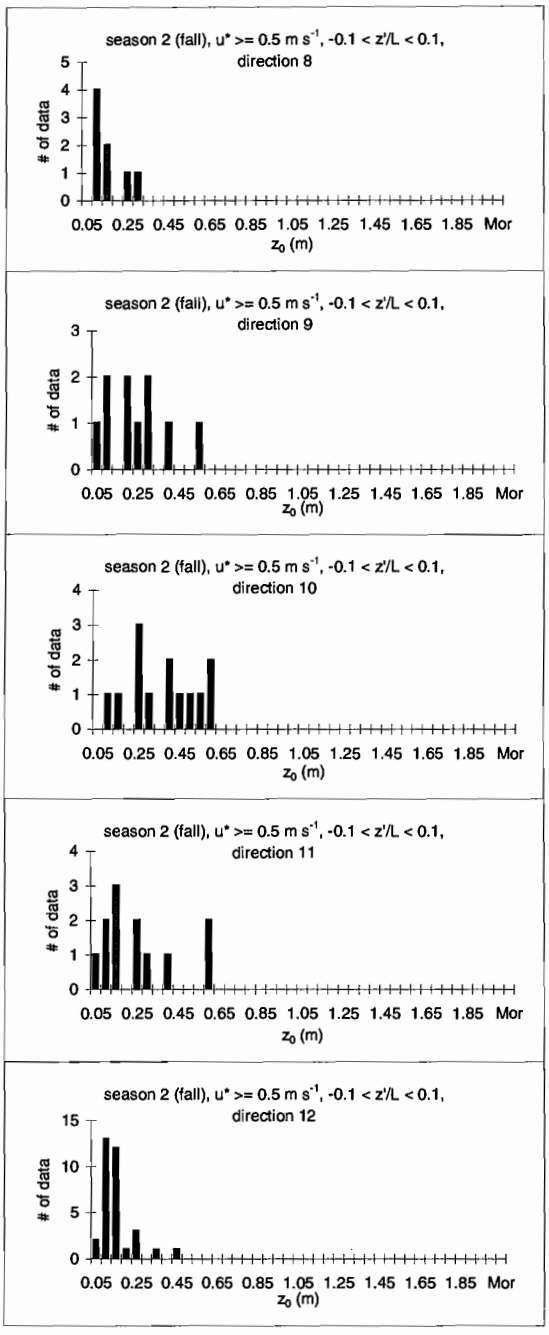

Appendix III: Histograms (z_m = 30 m, z_d = 27 m)

Data are sorted by season and by direction.

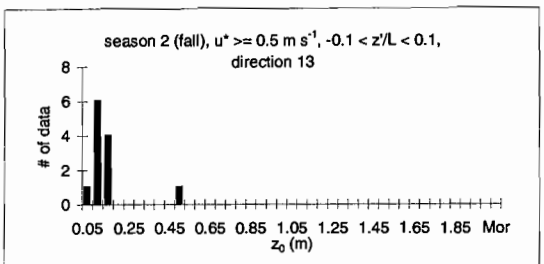

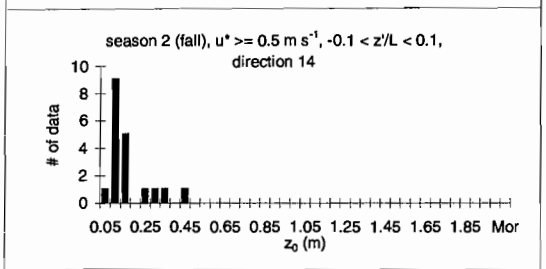

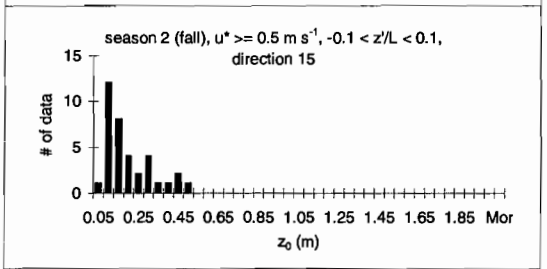

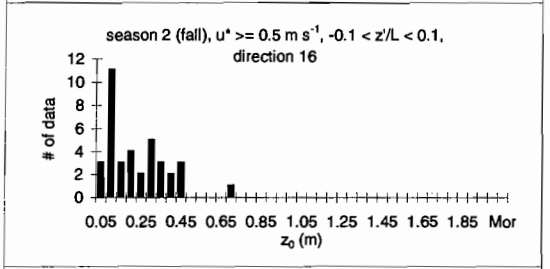

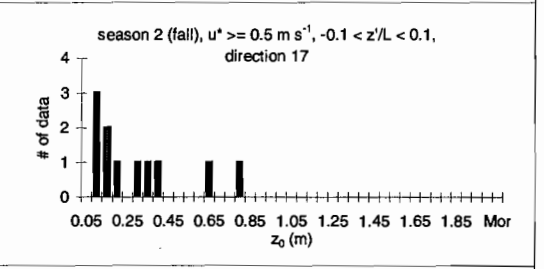

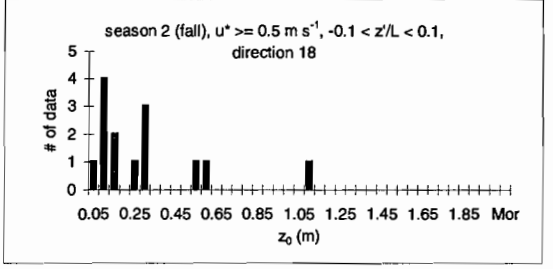

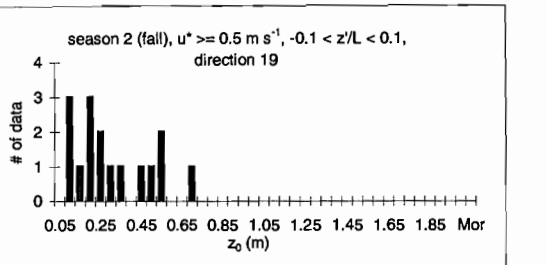

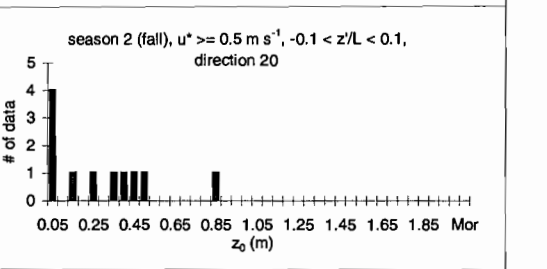

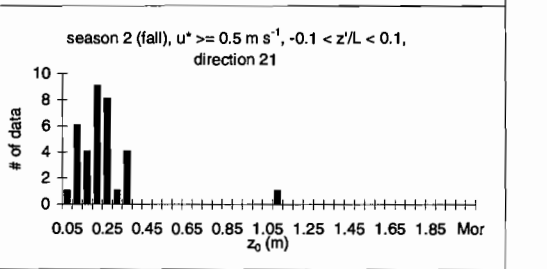

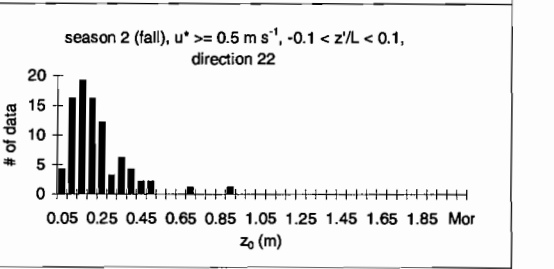

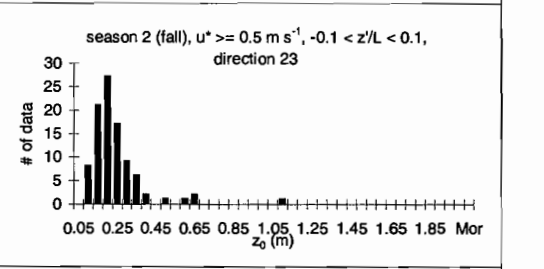

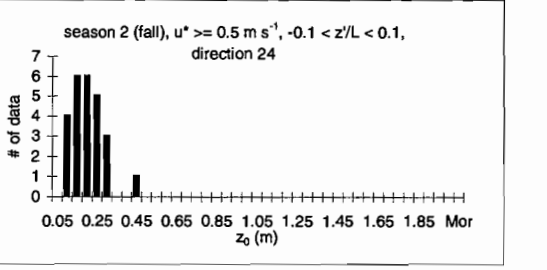

Appendix III: Histograms (z_m = 30 m, z_d = 27 m)

Data are sorted by season and by direction.

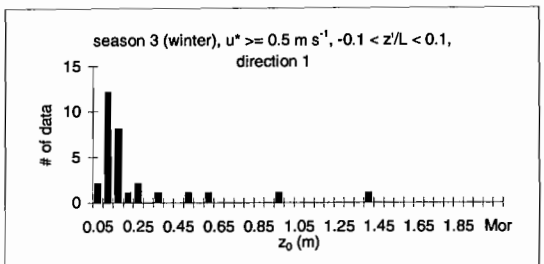

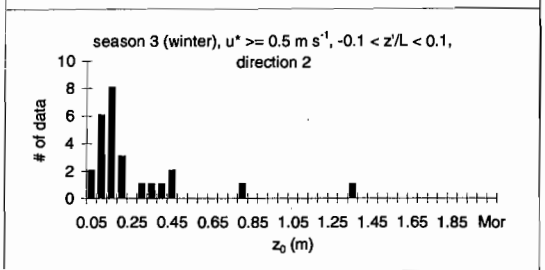

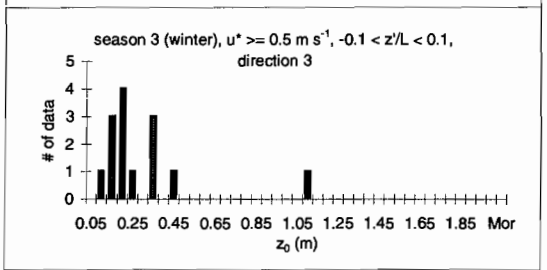

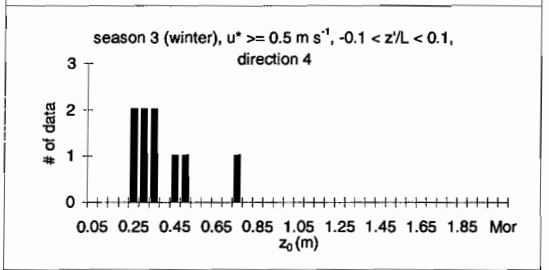

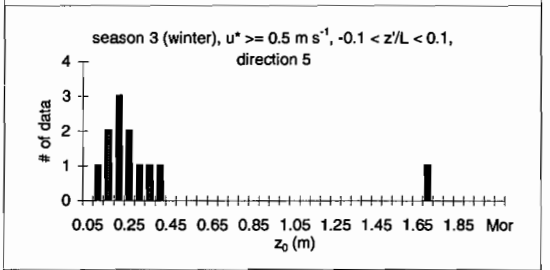

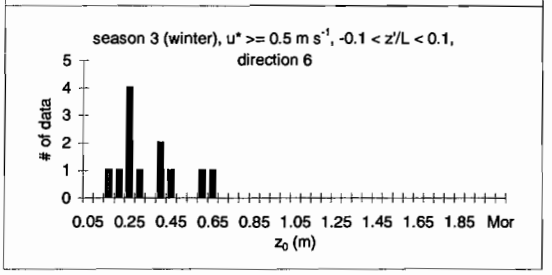

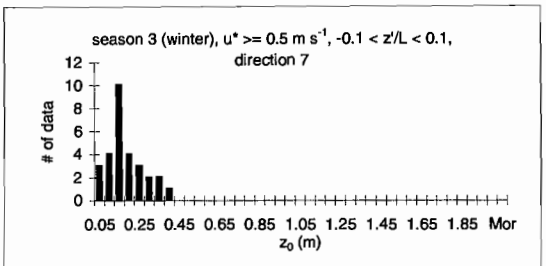

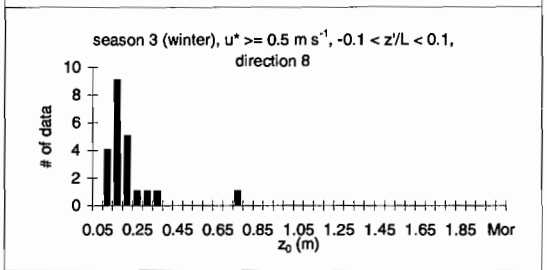

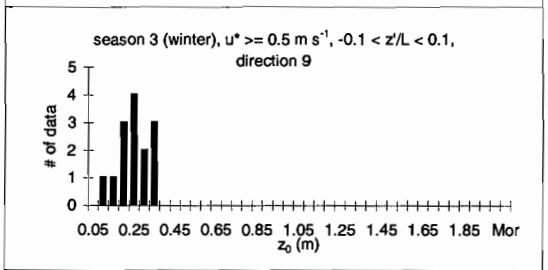

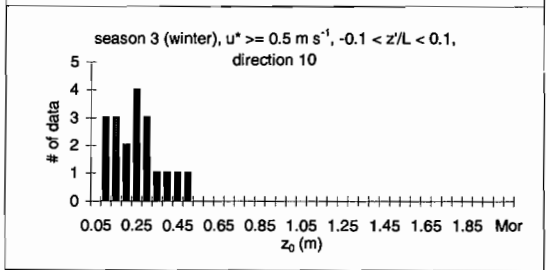

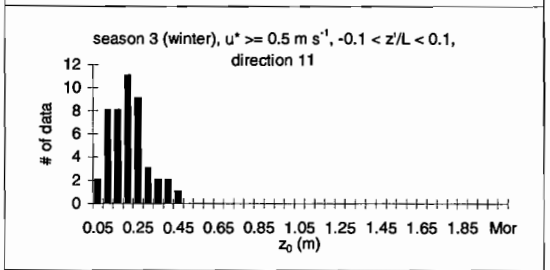

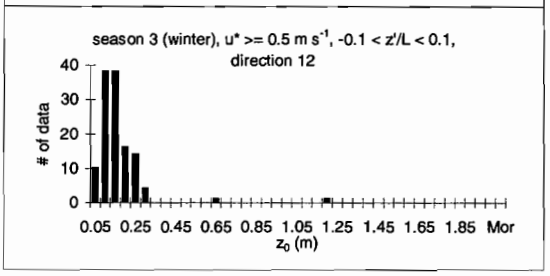

Appendix III: Histograms (z_m = 30 m, z_d = 27 m)

Data are sorted by season and by direction.

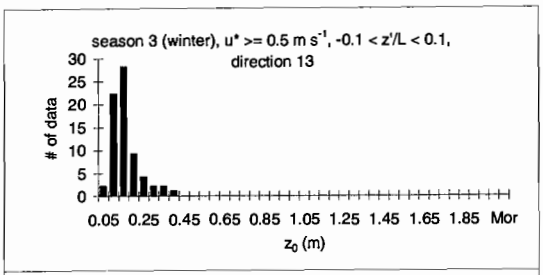

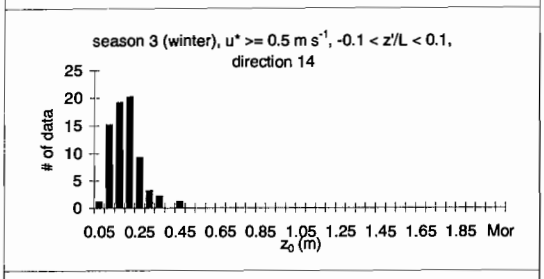

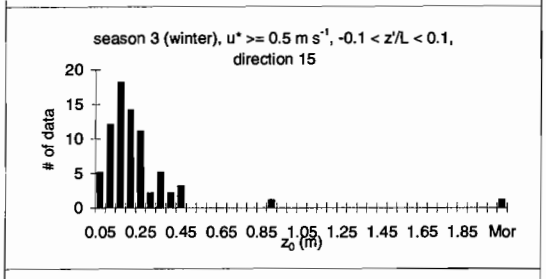

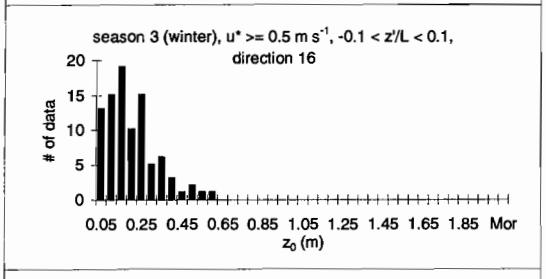

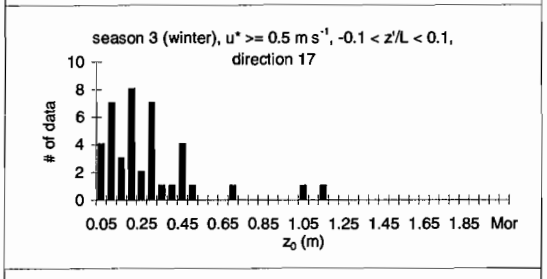

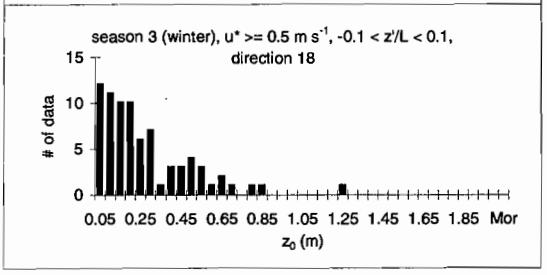

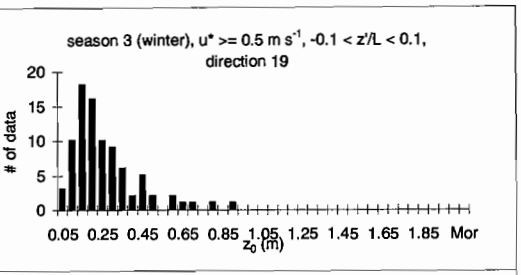

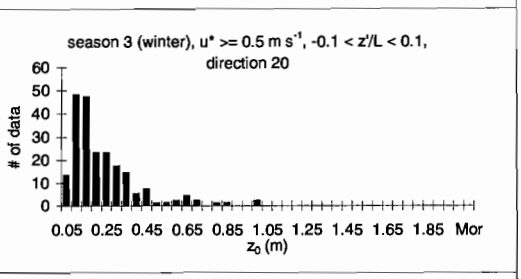

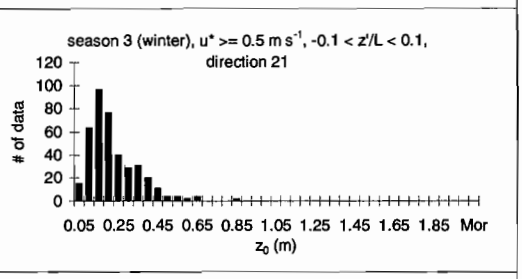

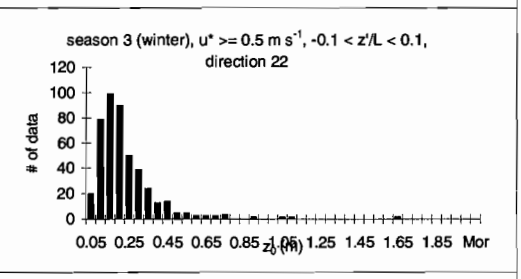

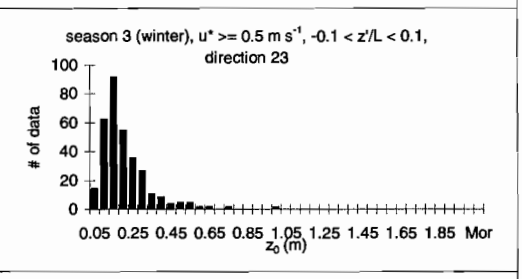

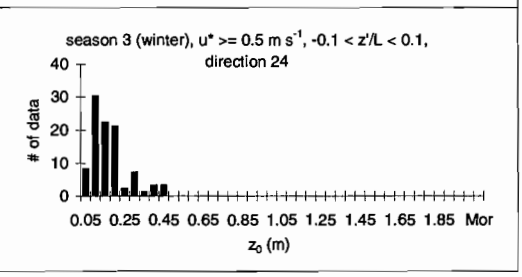

Appendix III: Histograms (z_m = 30 m, z_d = 27 m)

Data are sorted by season and by direction.

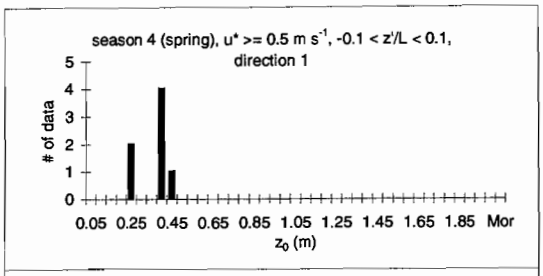

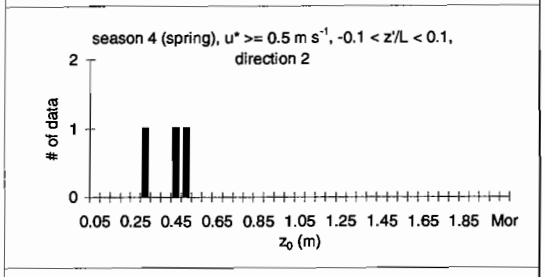

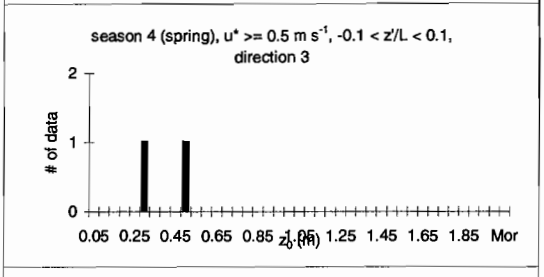

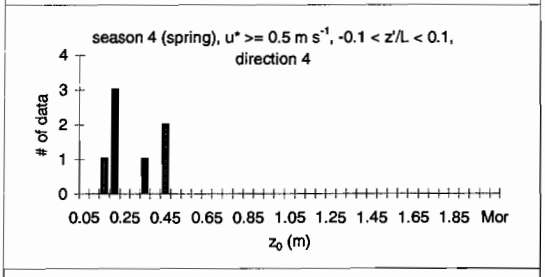

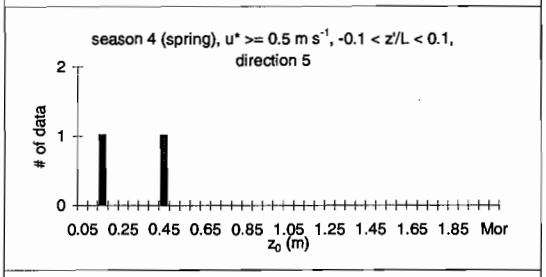

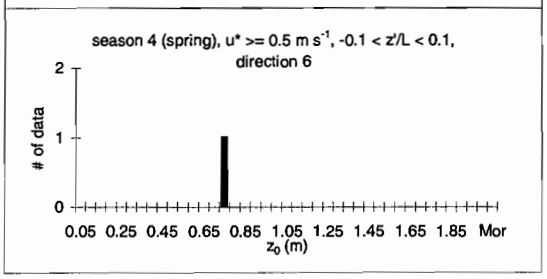

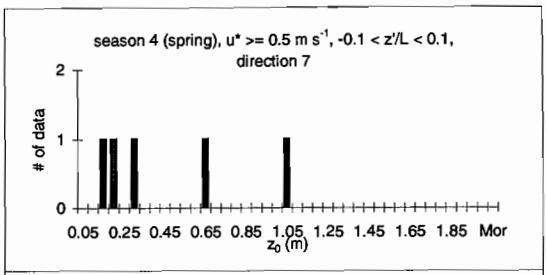

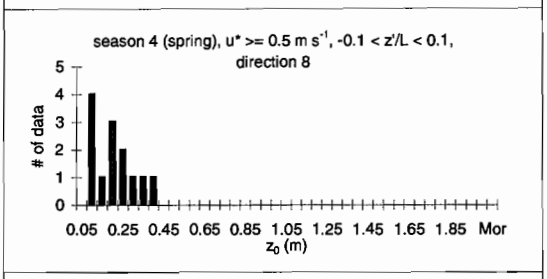

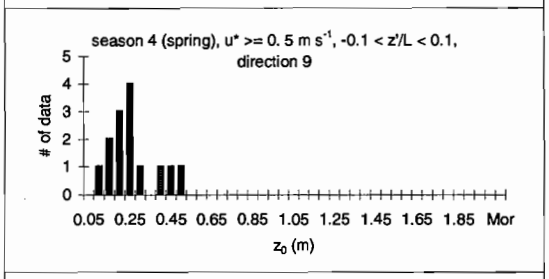

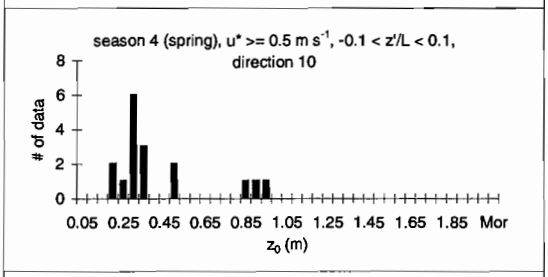

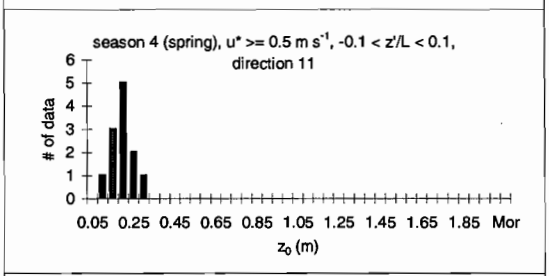

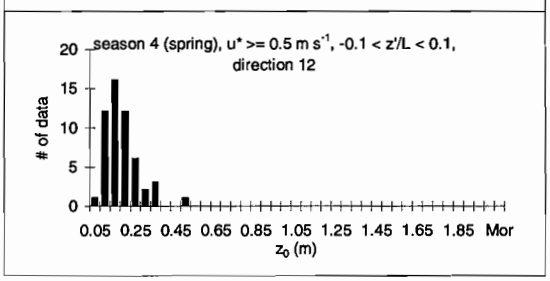

Appendix III: Histograms (z_m = 30 m, z_d = 27 m)

Data are sorted by season and by direction.

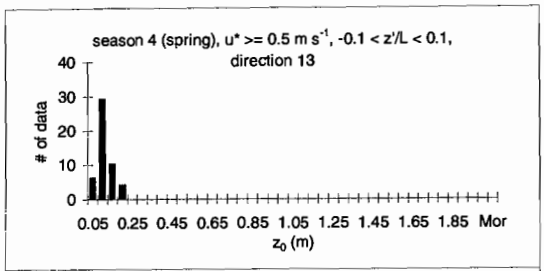

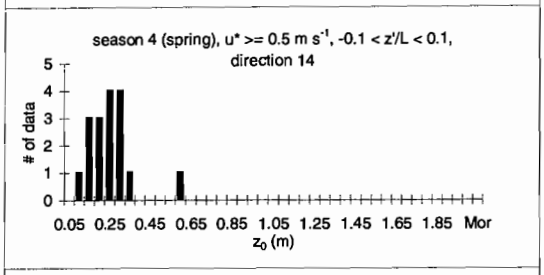

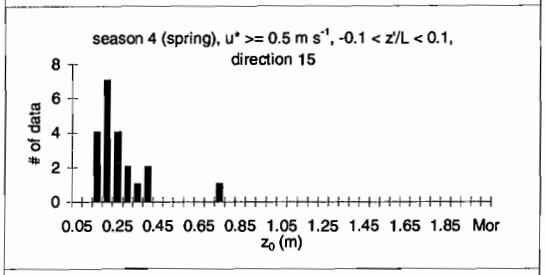

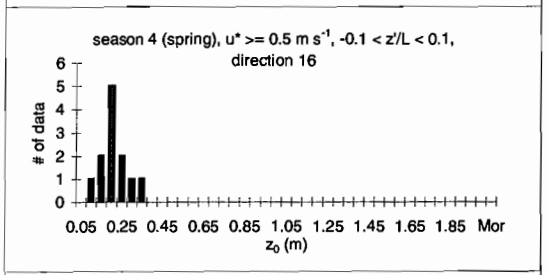

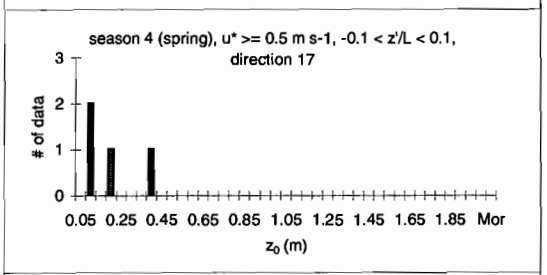

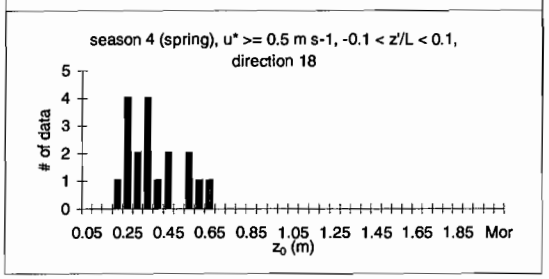

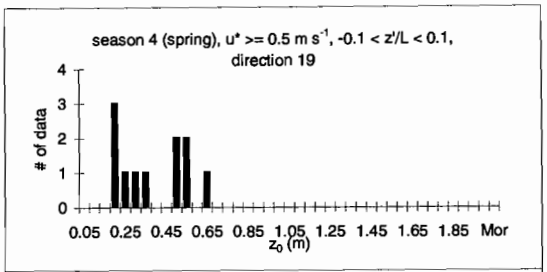

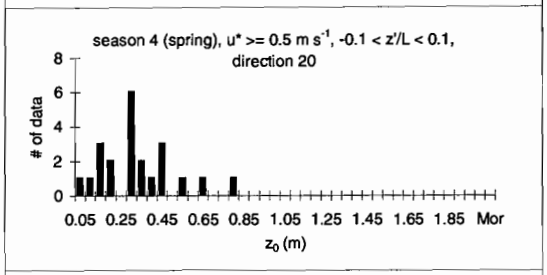

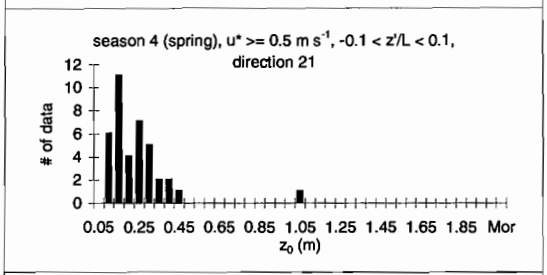

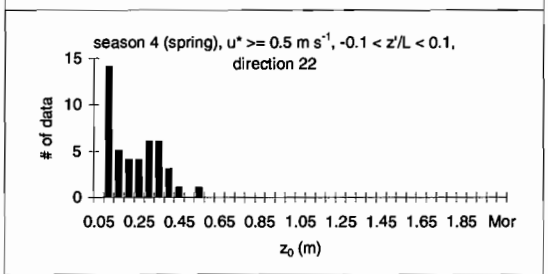

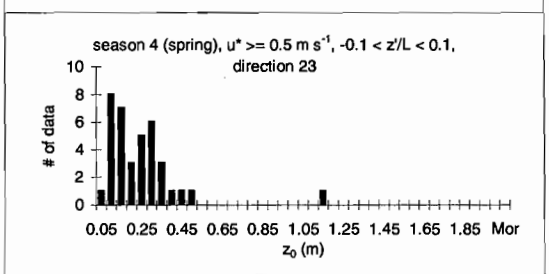

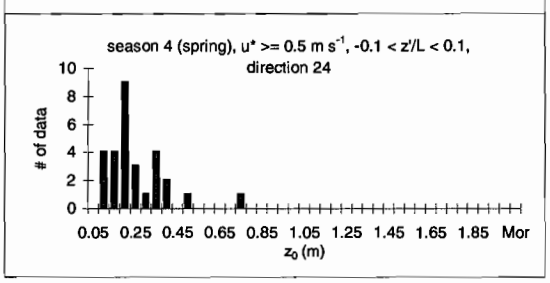

Appendix III: Histograms (z_m = 30 m, z_d = 27 m)

Data are sorted by season and by direction.

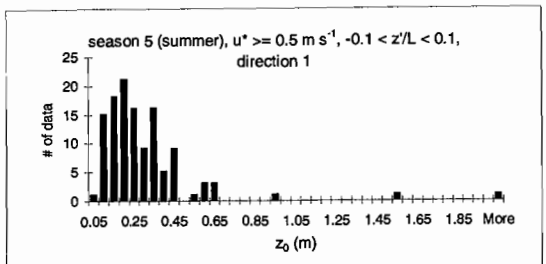

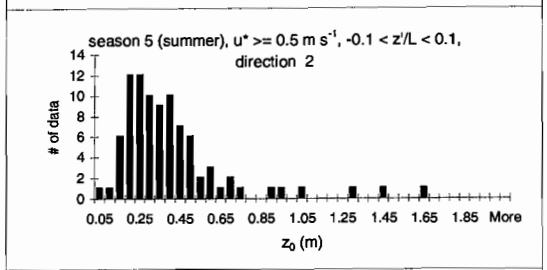

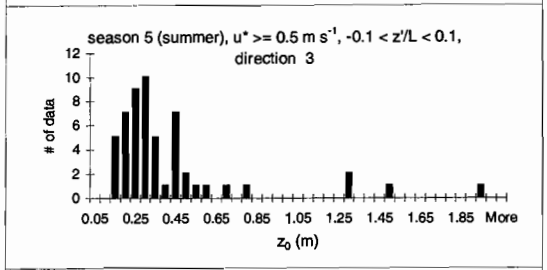

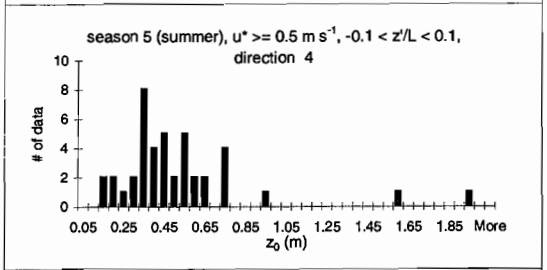

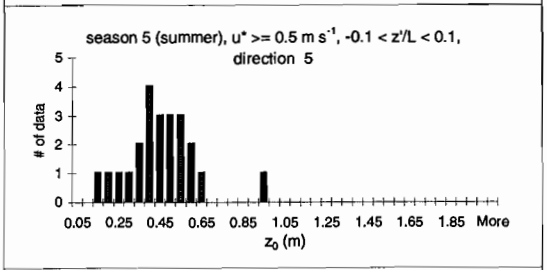

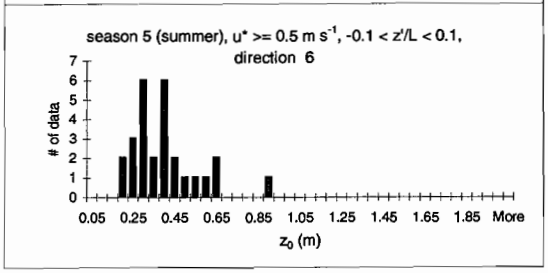

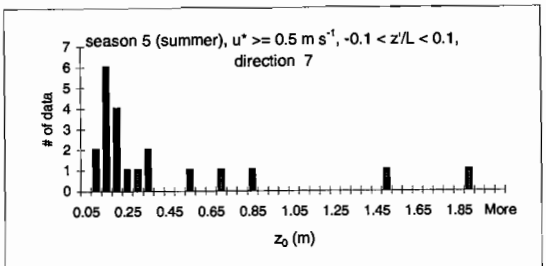

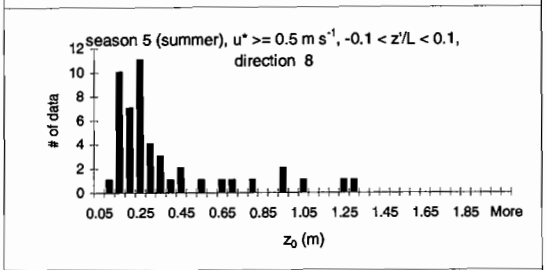

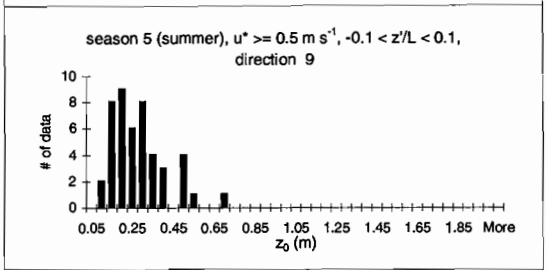

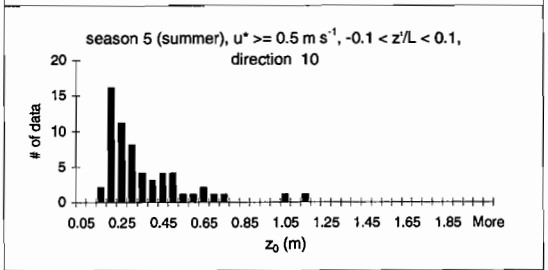

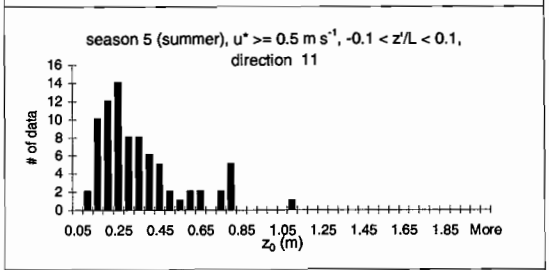

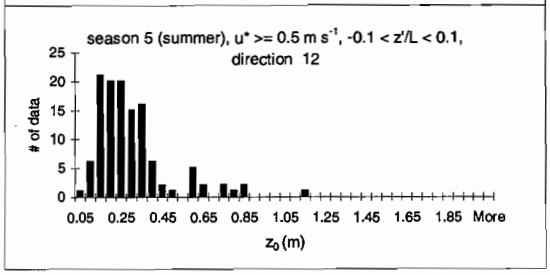

Appendix III: Histograms (z_m = 30 m, z_d = 27 m)

Data are sorted by season and by direction.

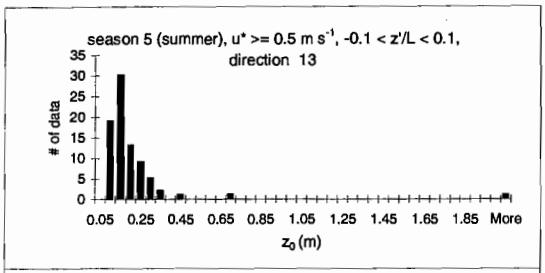

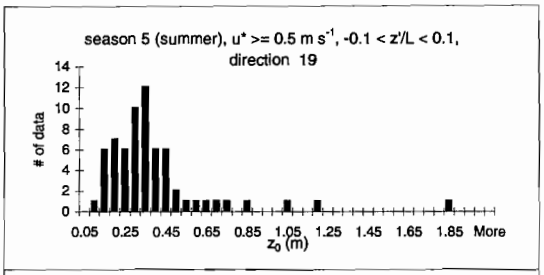

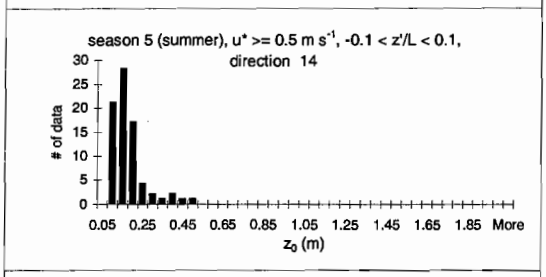

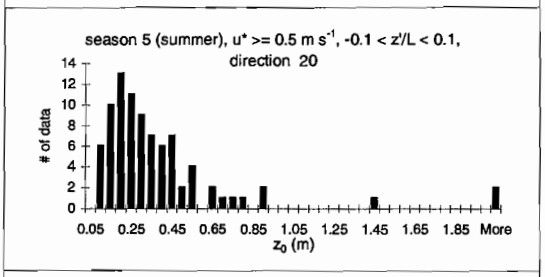

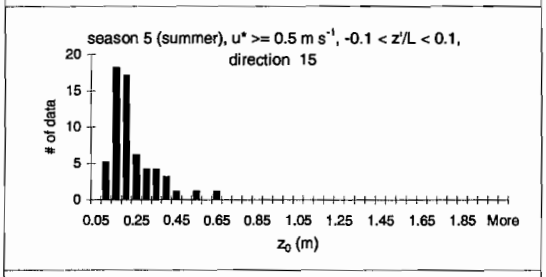

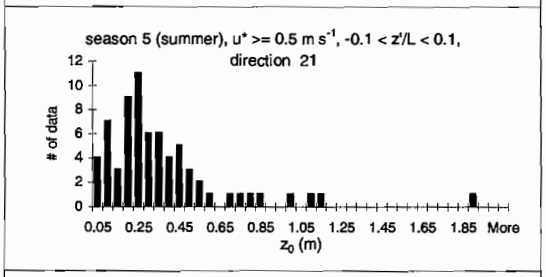

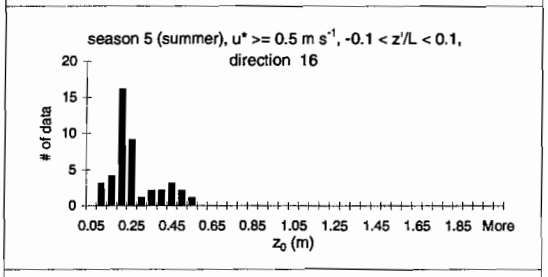

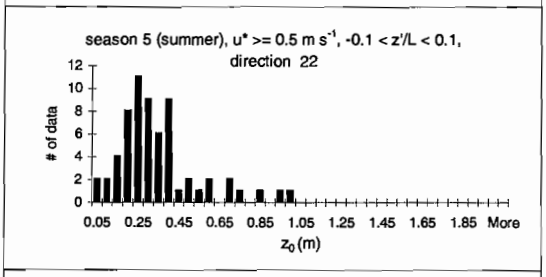

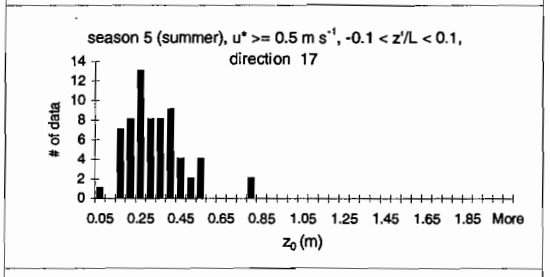

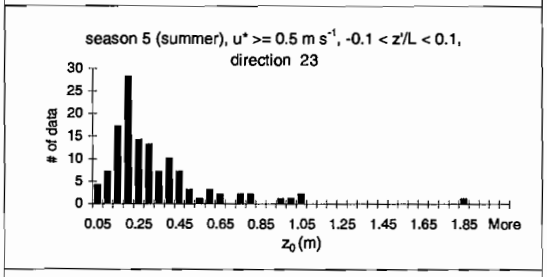

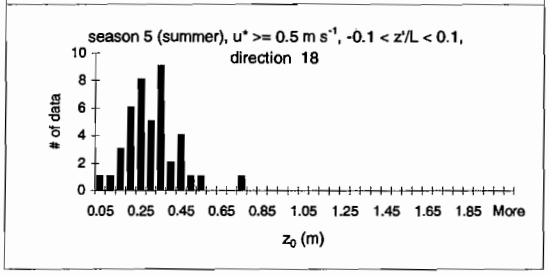

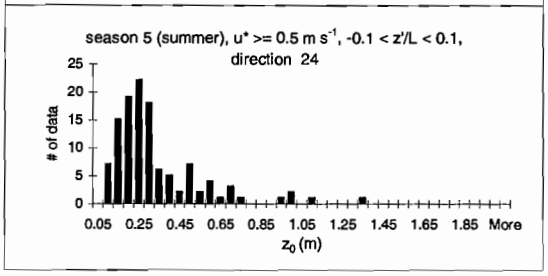

Appendix III: Histograms (z_m = 30 m, z_d = 27 m)

Data are sorted by season and by direction.

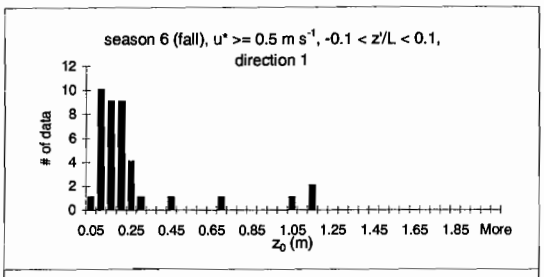

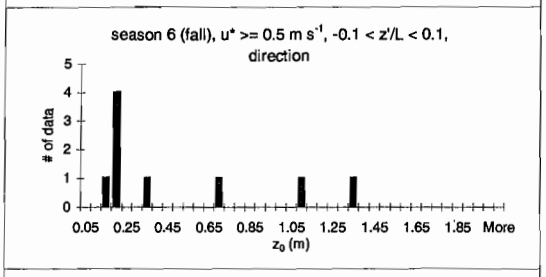

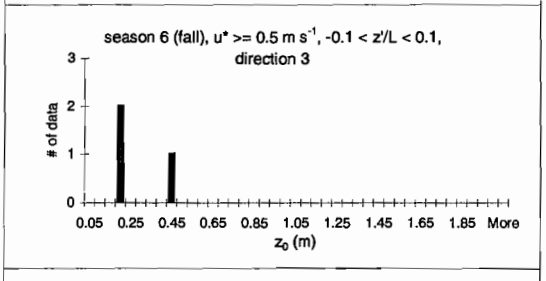

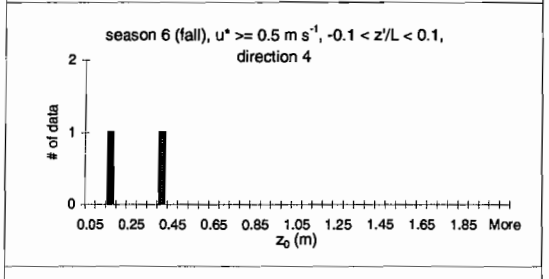

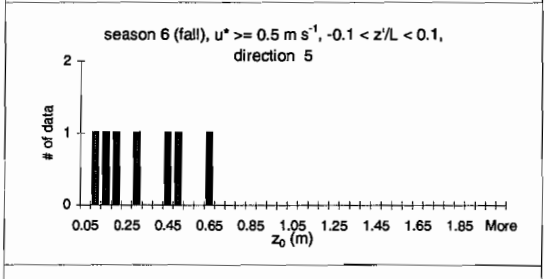

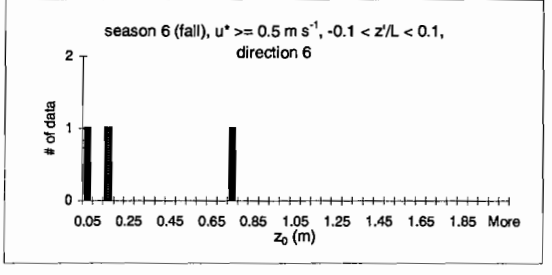

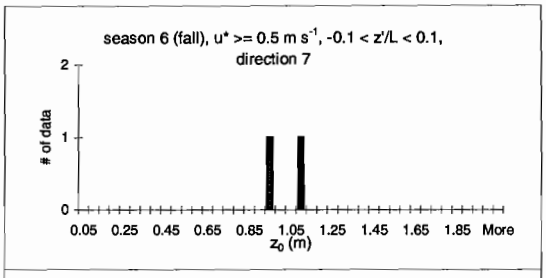

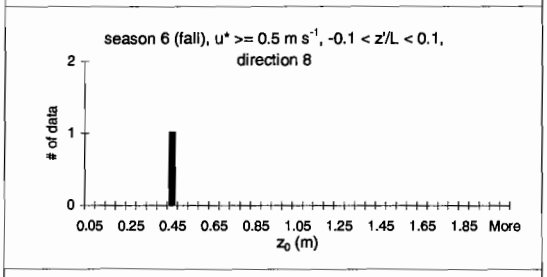

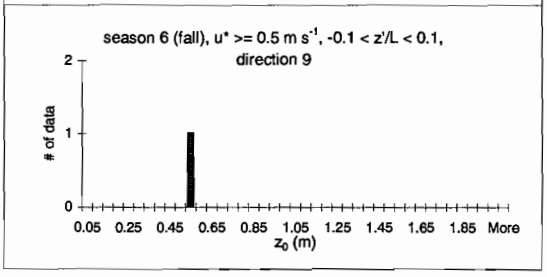

N/A

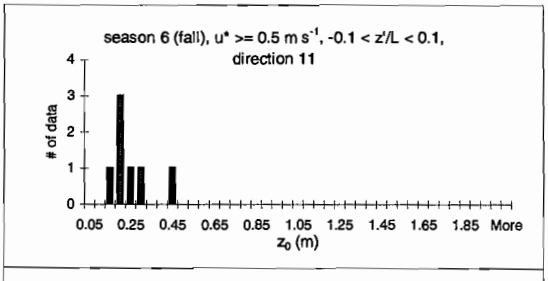

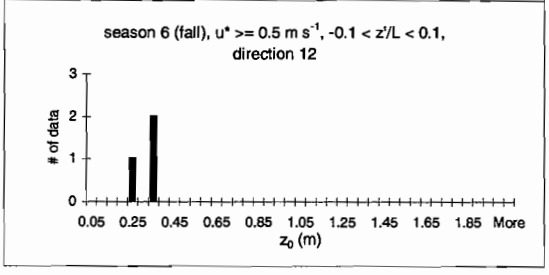

Appendix III: Histograms (z_m = 30 m, z_d = 27 m)

Data are sorted by season and by direction.

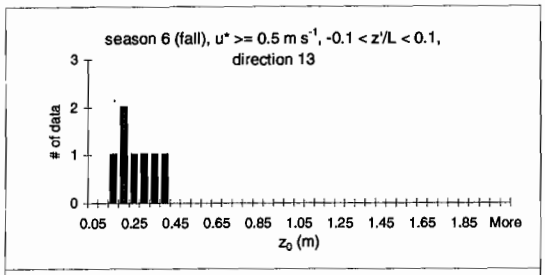

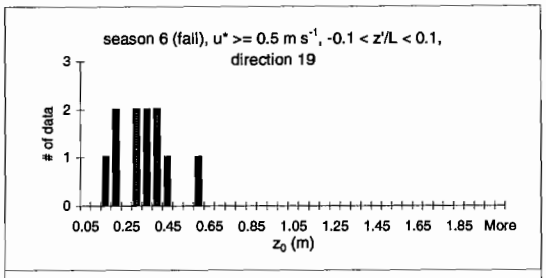

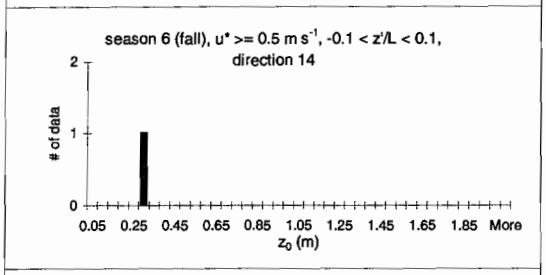

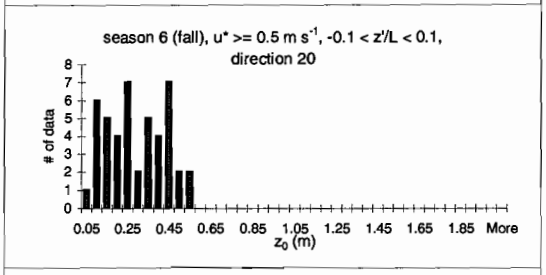

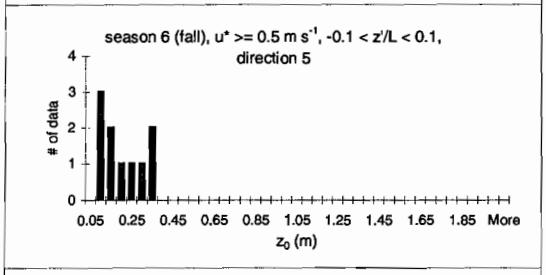

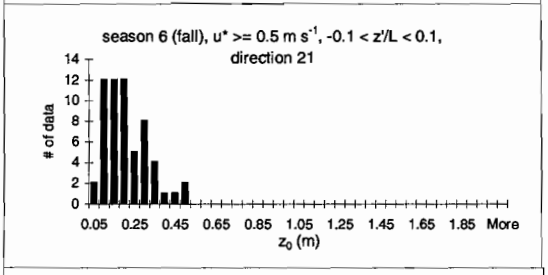

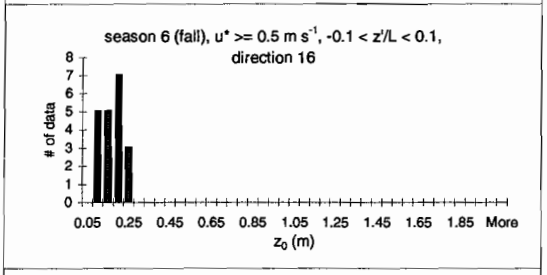

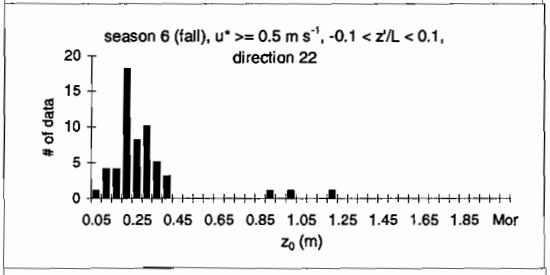

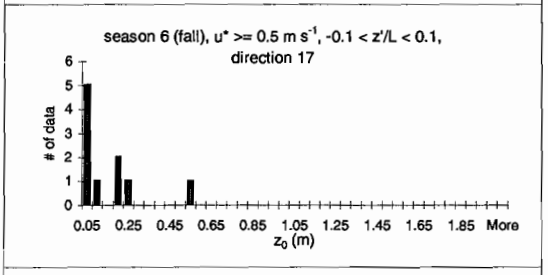

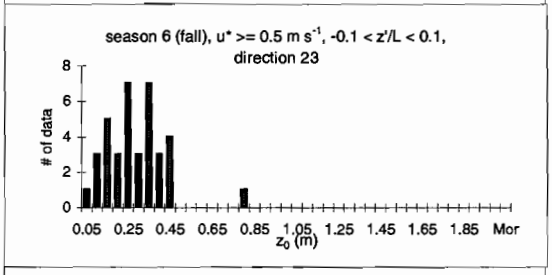

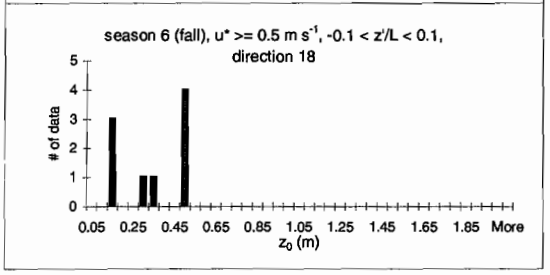

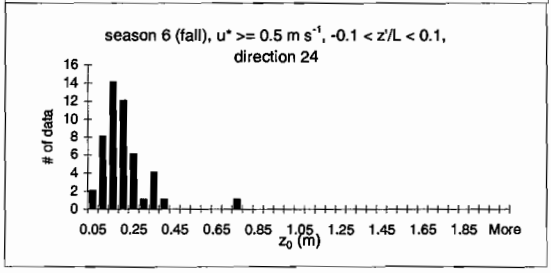

Appendix III: Histograms (z_m = 30 m, z_d = 27 m)

Data are sorted by season and by direction.

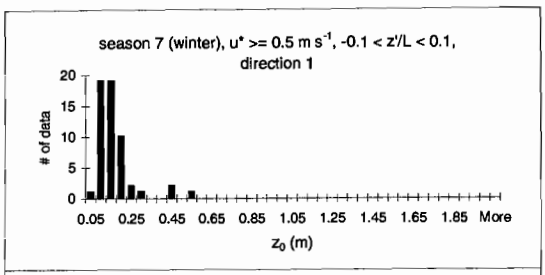

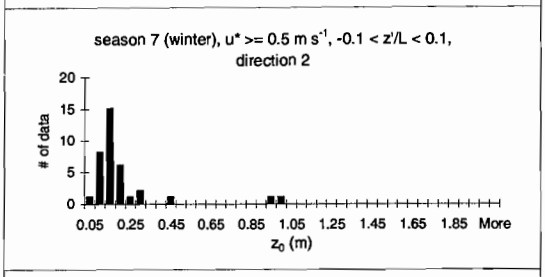

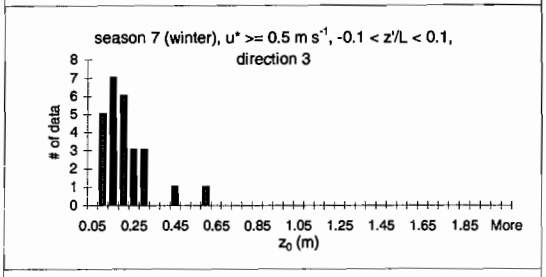

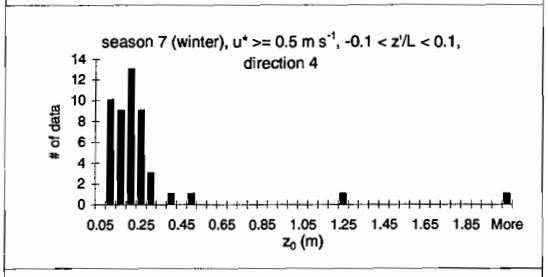

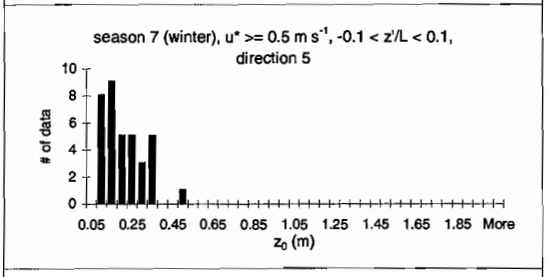

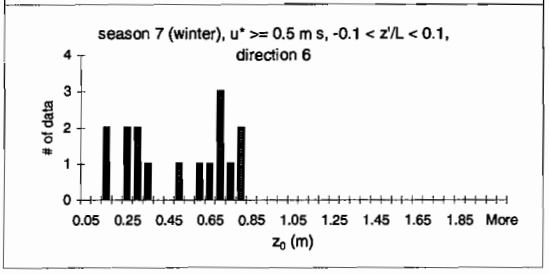

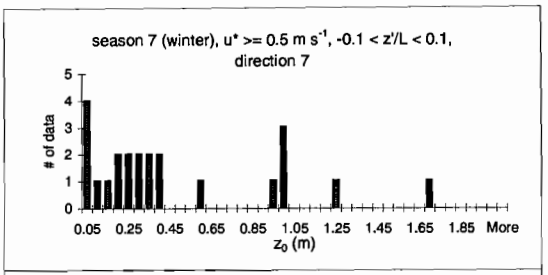

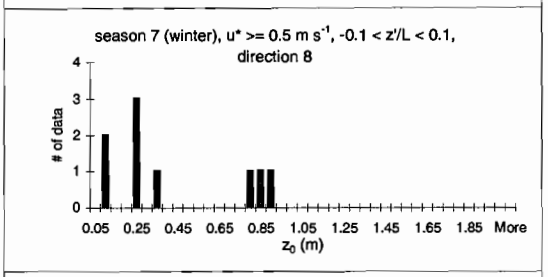

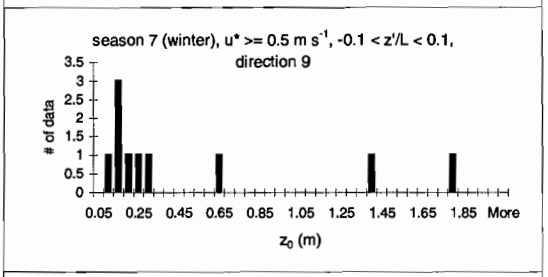

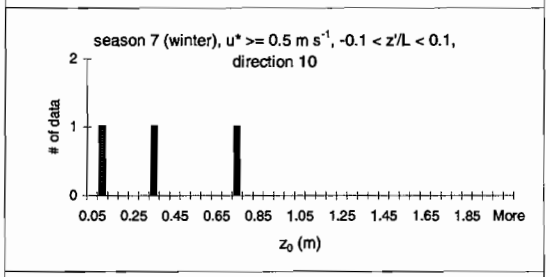

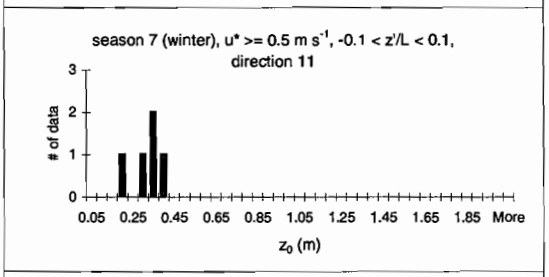

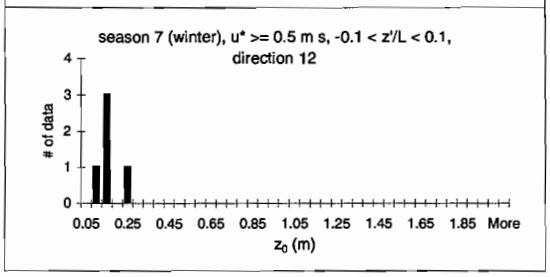

Appendix III: Histograms (z_m = 30 m, z_d = 27 m)

Data are sorted by season and by direction.

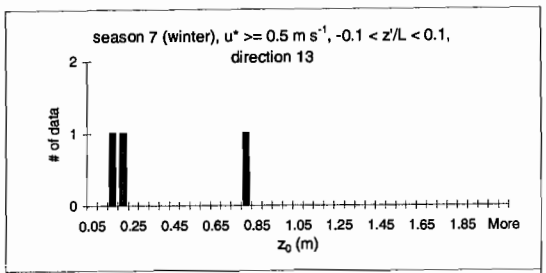

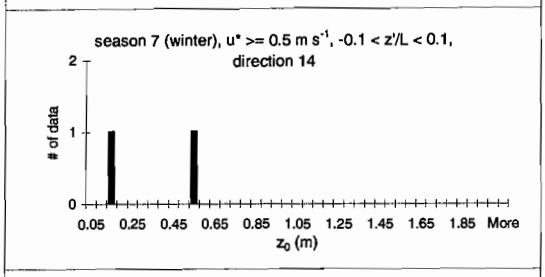

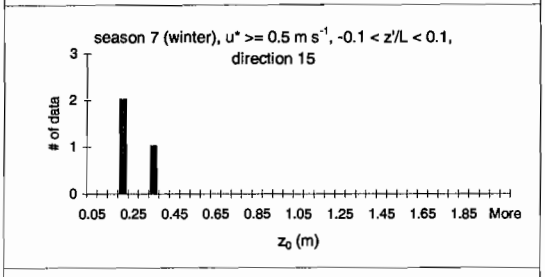

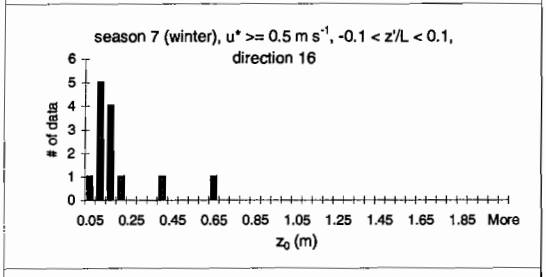

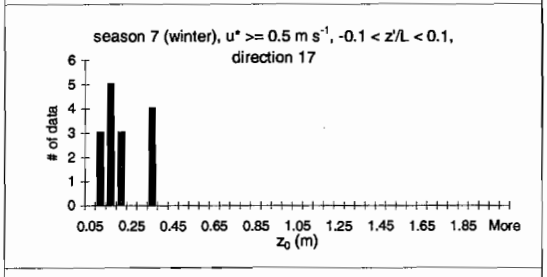

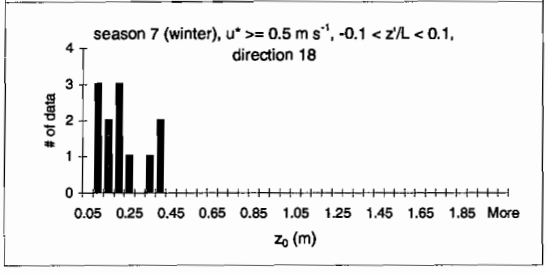

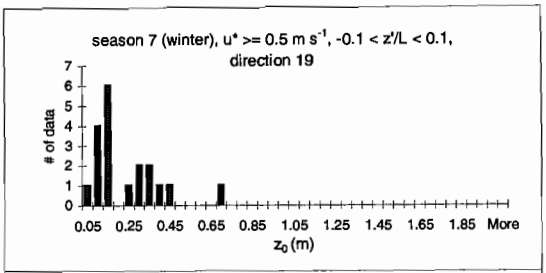

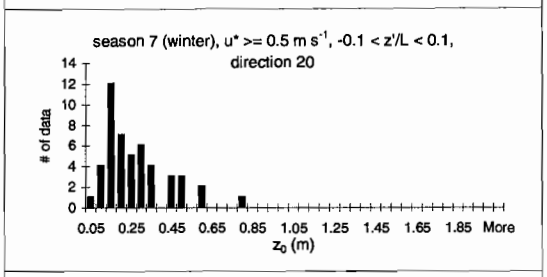

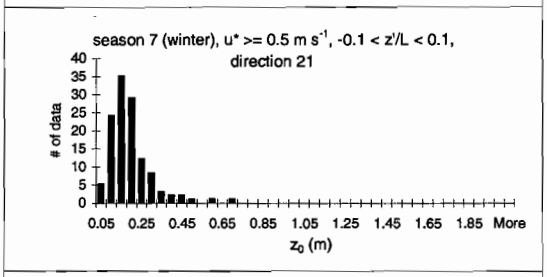

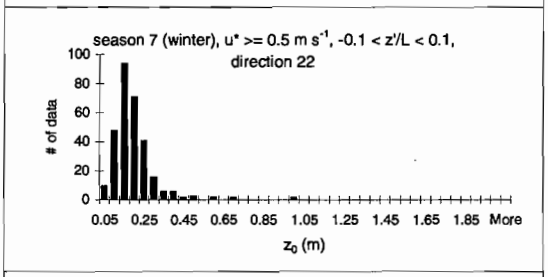

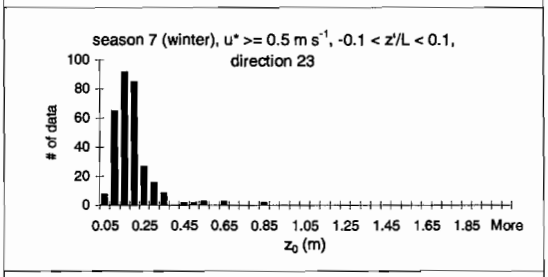

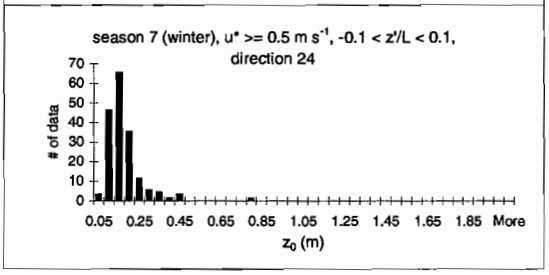

Appendix III: Histograms (z_m = 30 m, z_d = 27 m)

Data are sorted by season and by direction.

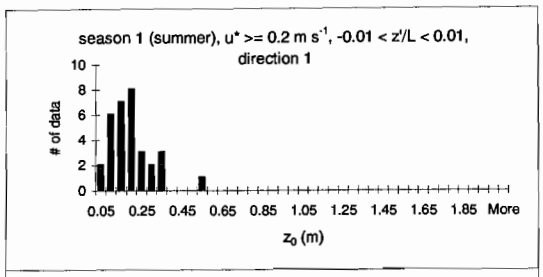

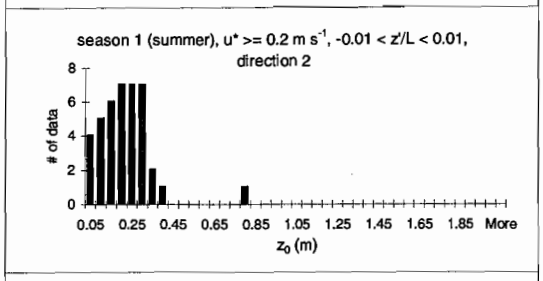

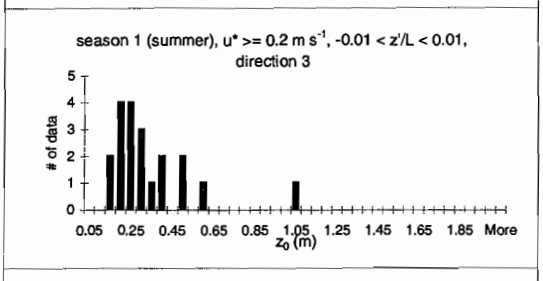

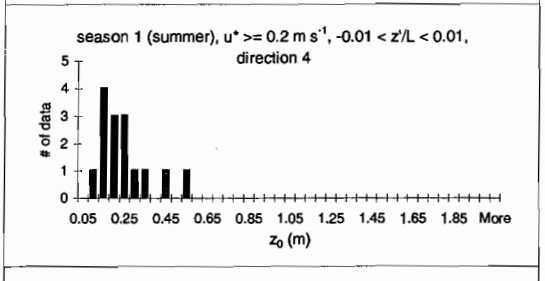

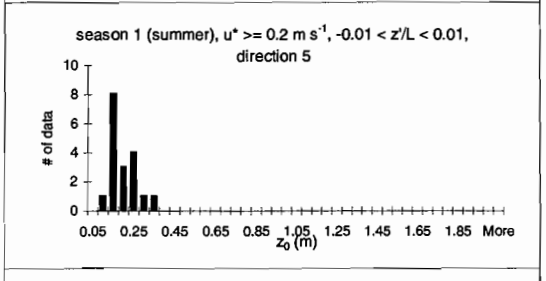

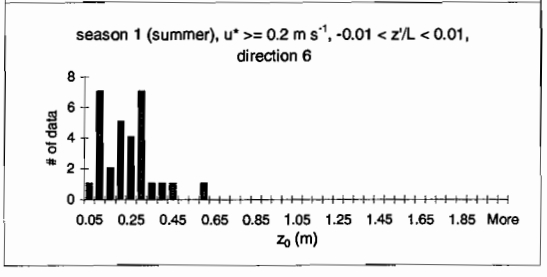

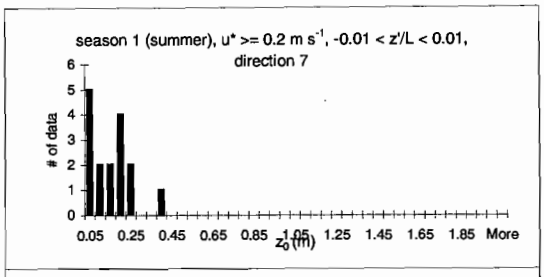

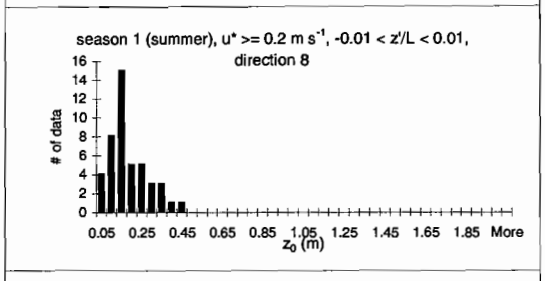

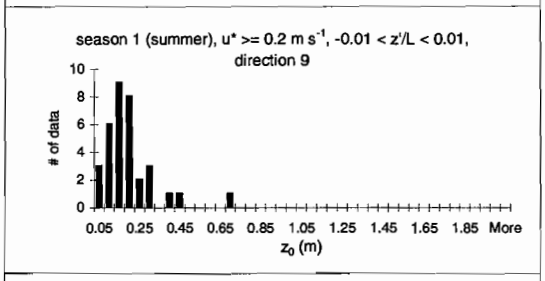

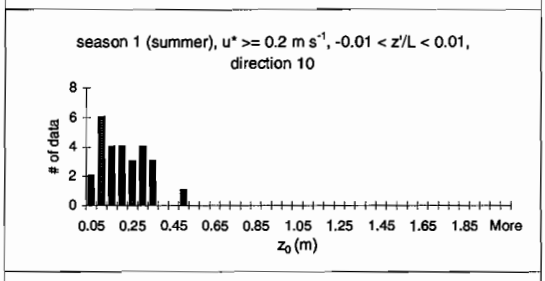

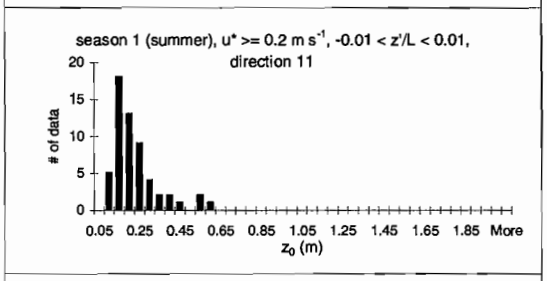

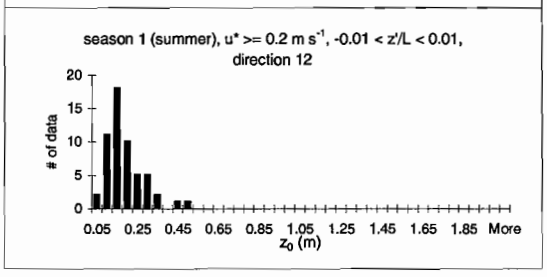

Appendix III: Histograms (z_m = 30 m, z_d = 27 m)

Data are sorted by season and by direction.

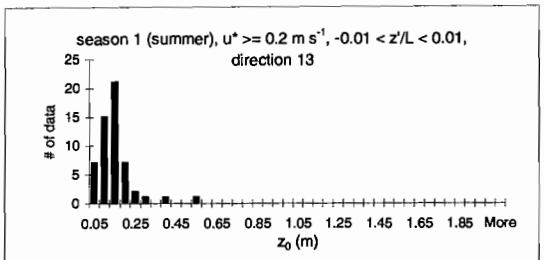

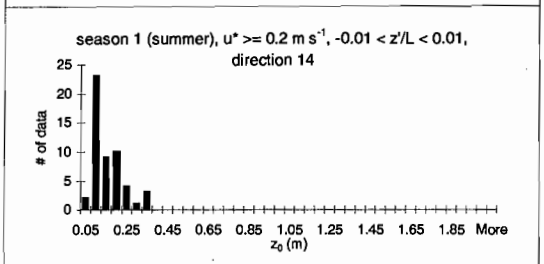

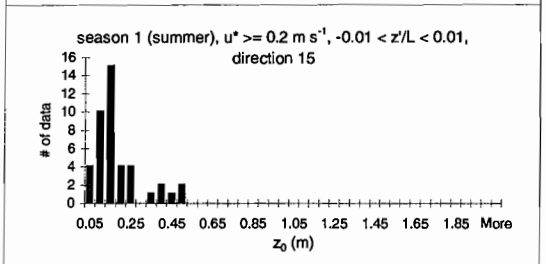

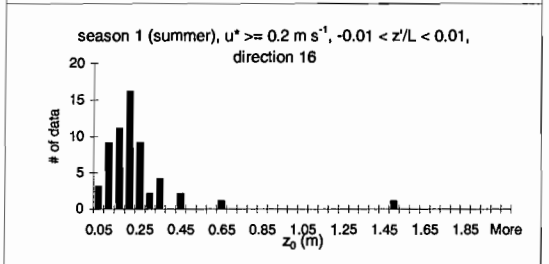

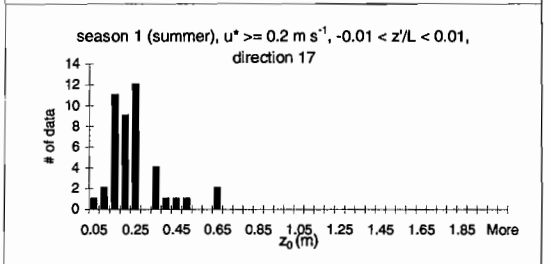

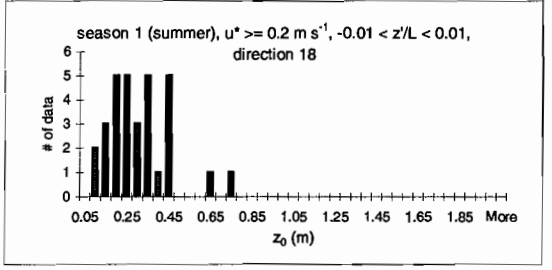

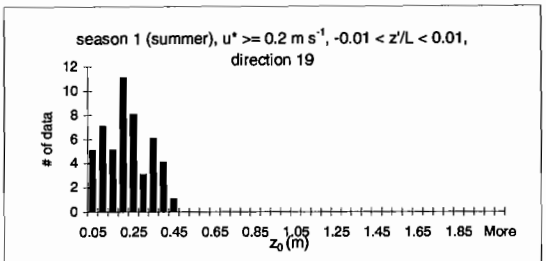

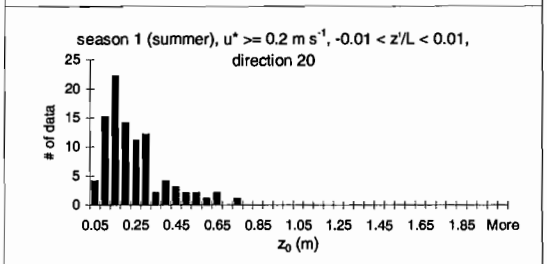

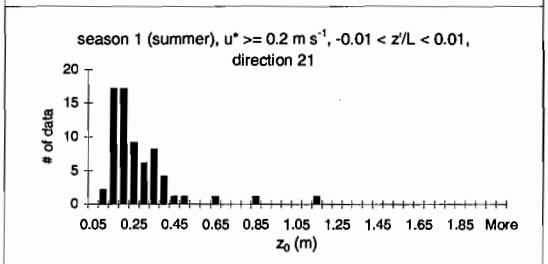

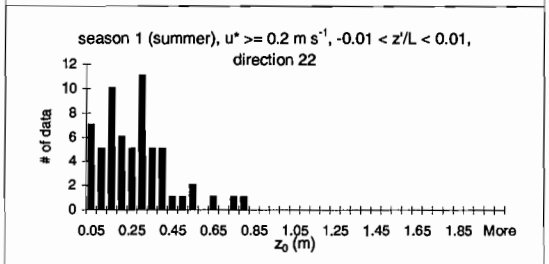

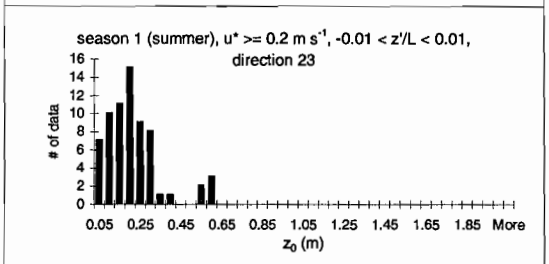

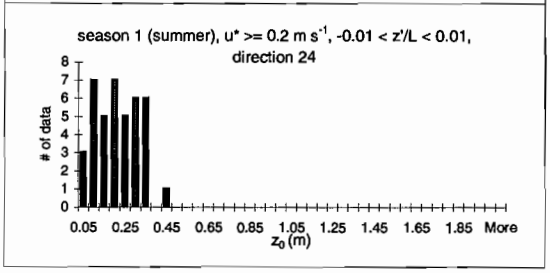

Appendix III: Histograms (z_m = 30 m, z_d = 27 m)

Data are sorted by season and by direction.

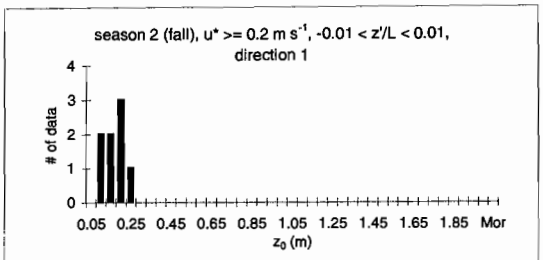

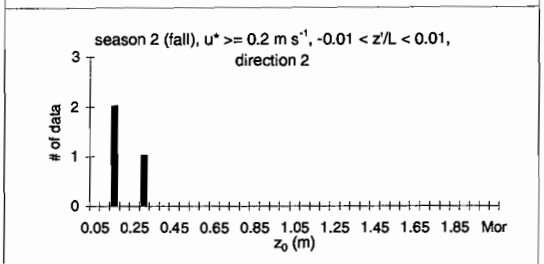

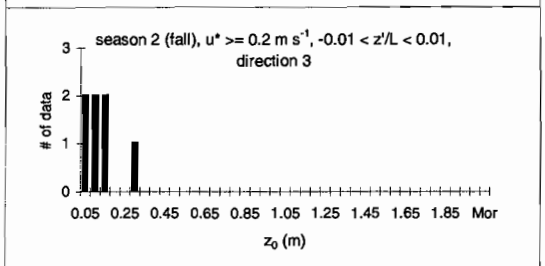

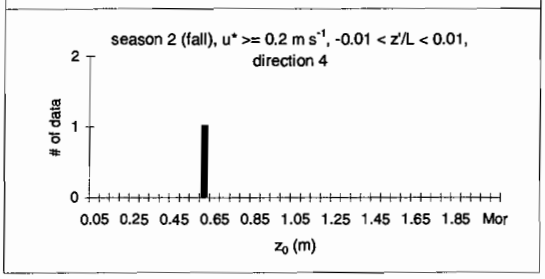

N/A

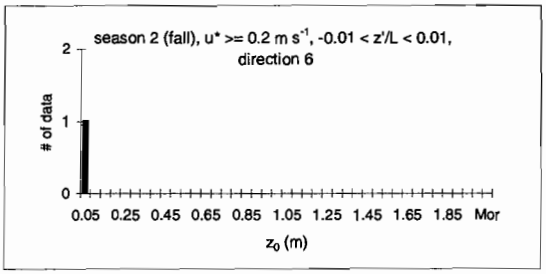

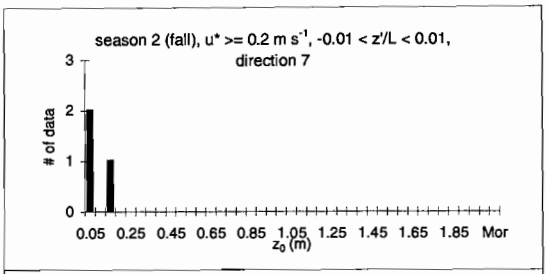

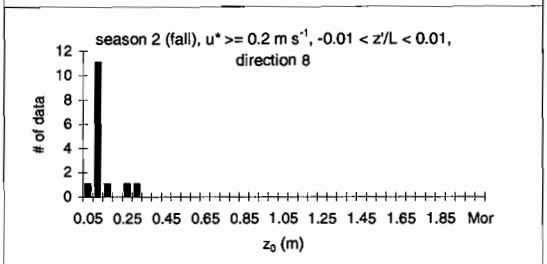

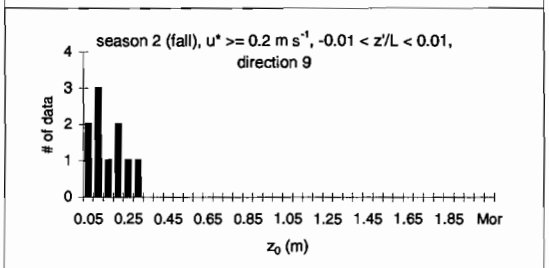

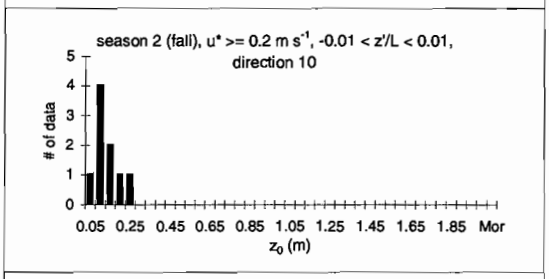

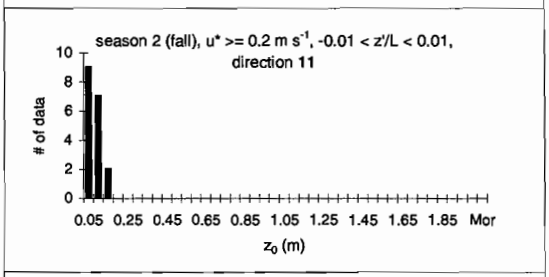

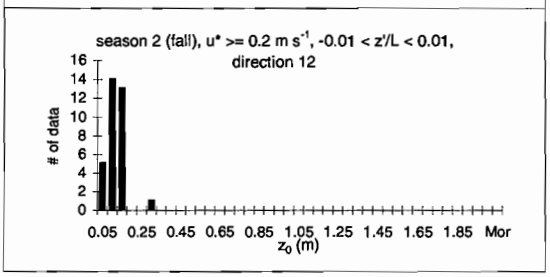

Appendix III: Histograms (z_m = 30 m, z_d = 27 m)

Data are sorted by season and by direction.

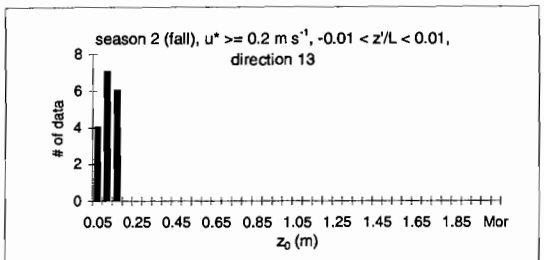

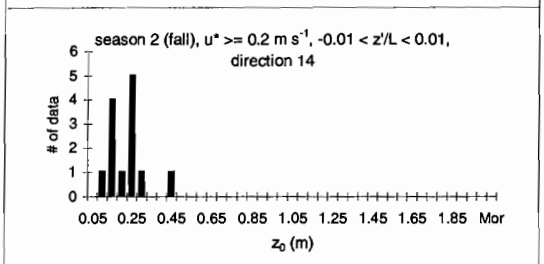

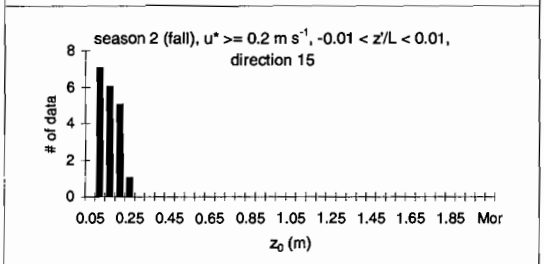

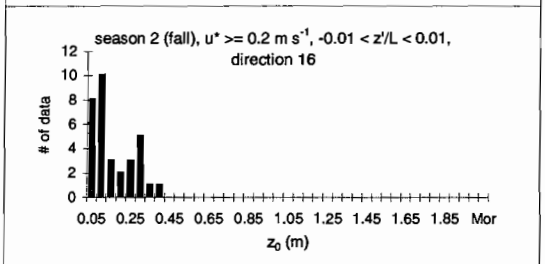

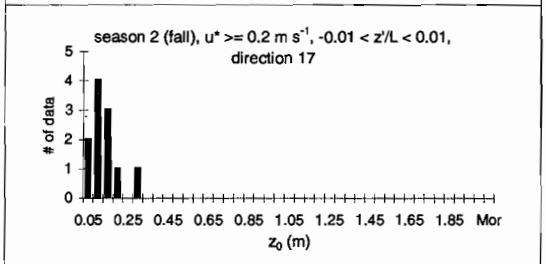

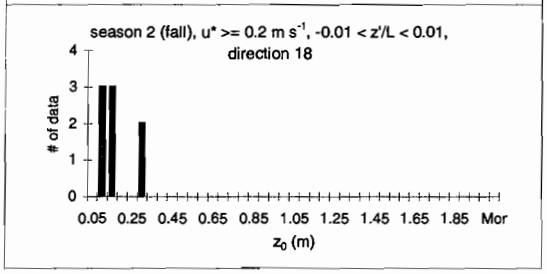

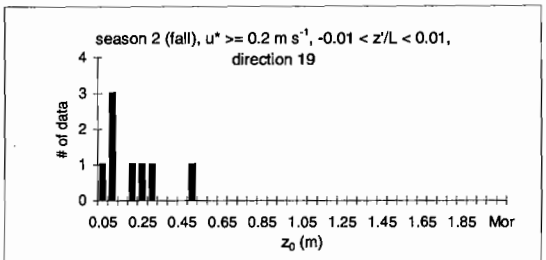

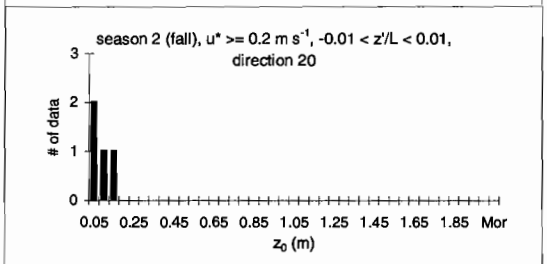

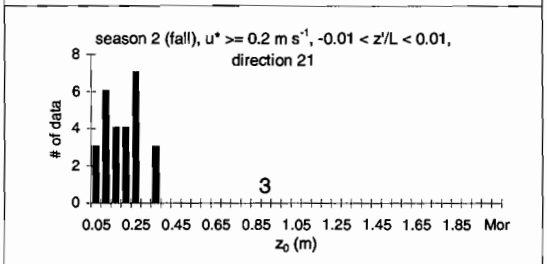

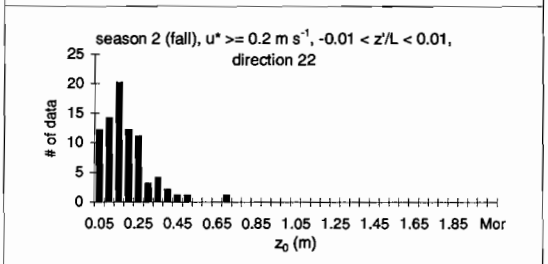

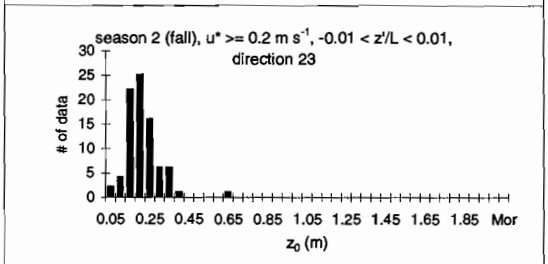

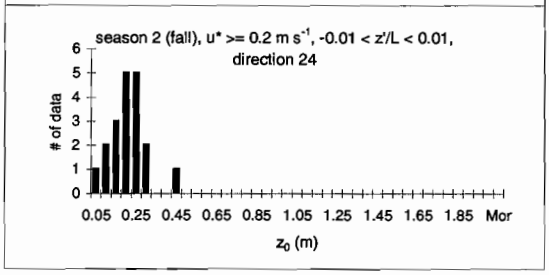

Appendix III: Histograms (z_m = 30 m, z_d = 27 m)

Data are sorted by season and by direction.

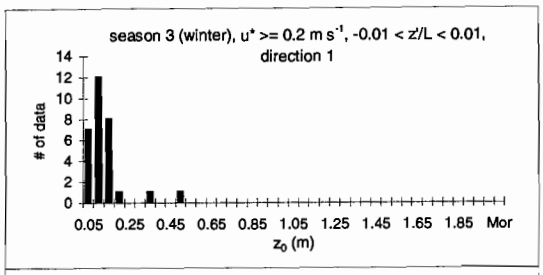

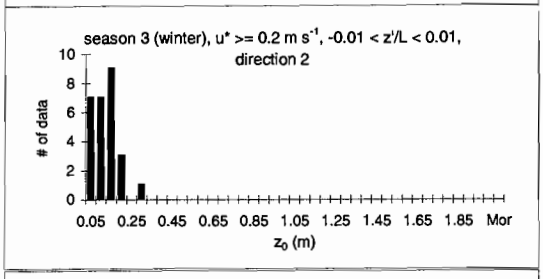

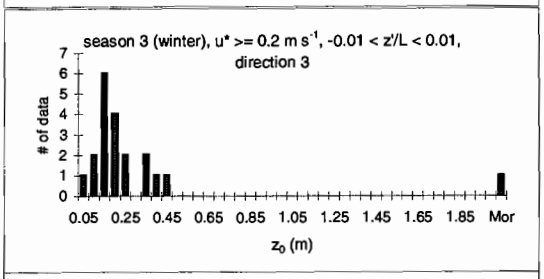

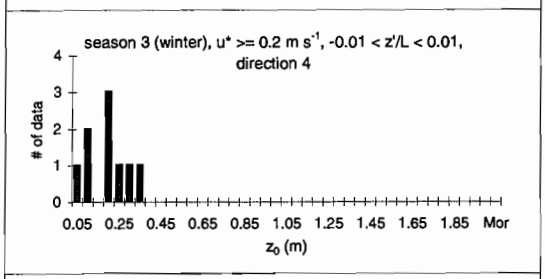

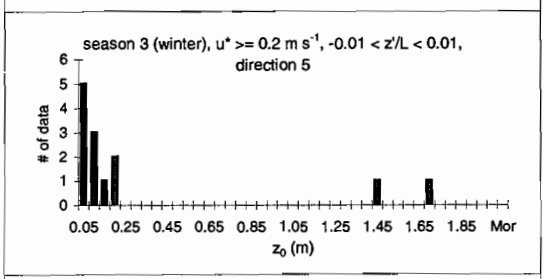

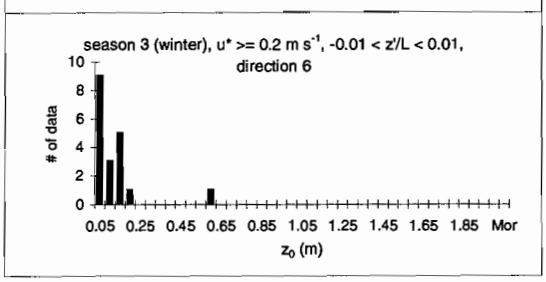

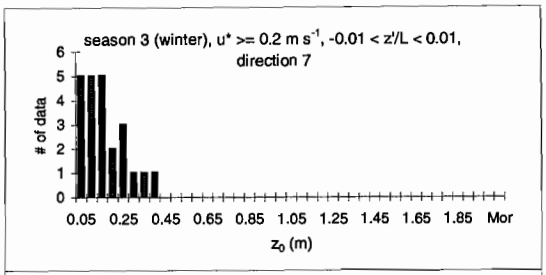

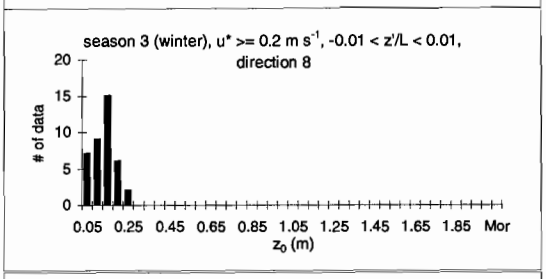

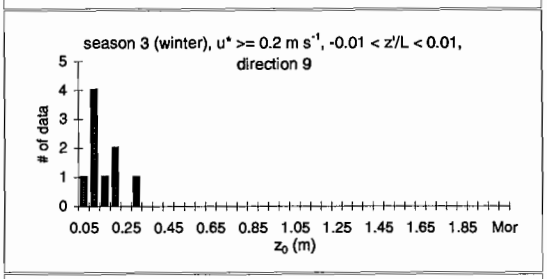

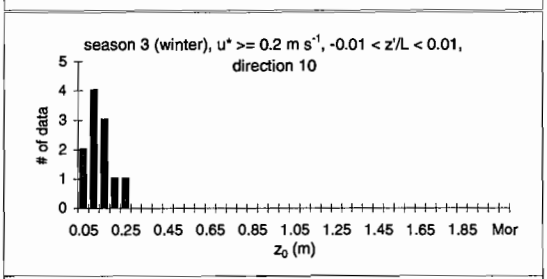

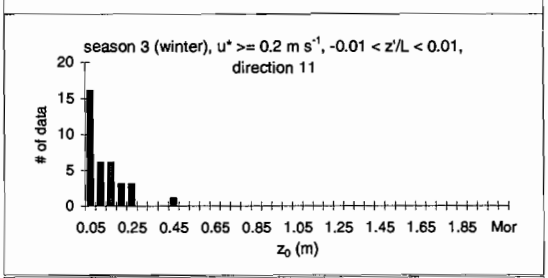

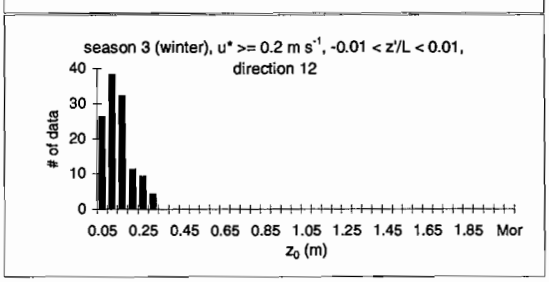

Appendix III: Histograms (z_m = 30 m, z_d = 27 m)

Data are sorted by season and by direction.

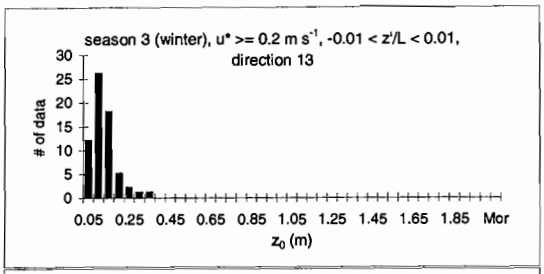

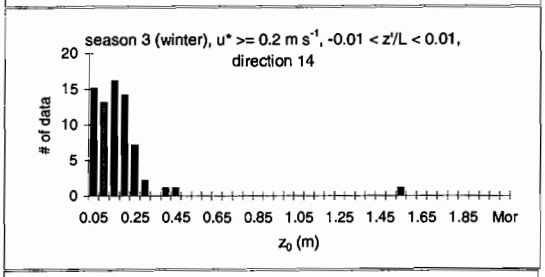

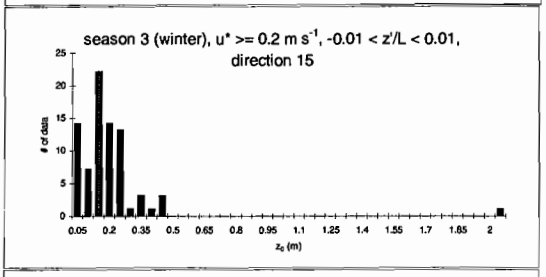

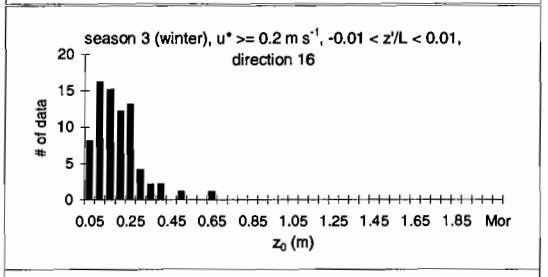

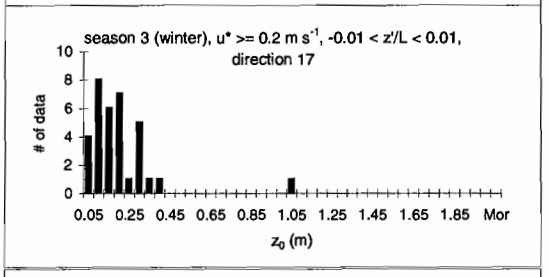

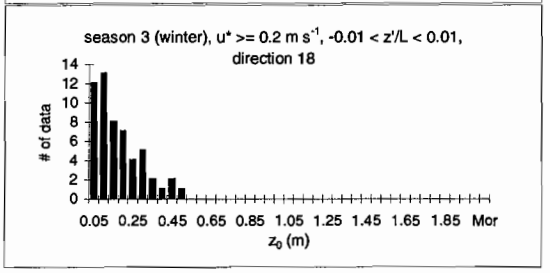

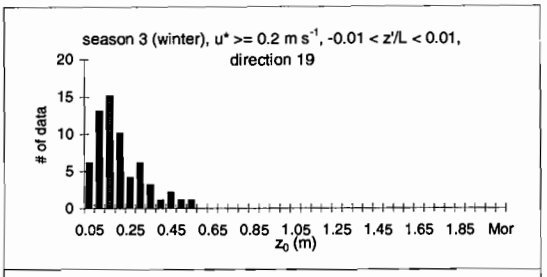

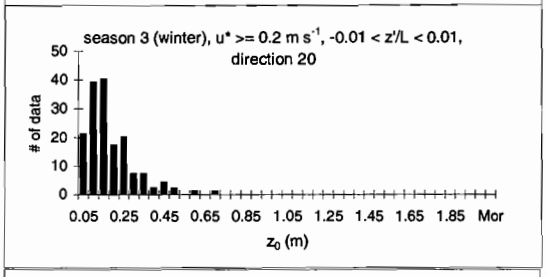

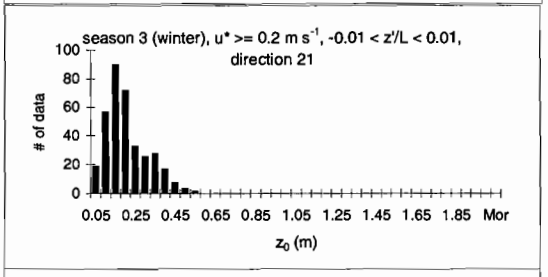

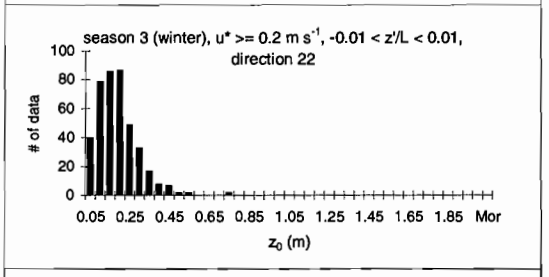

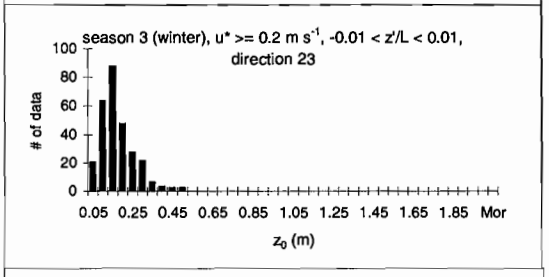

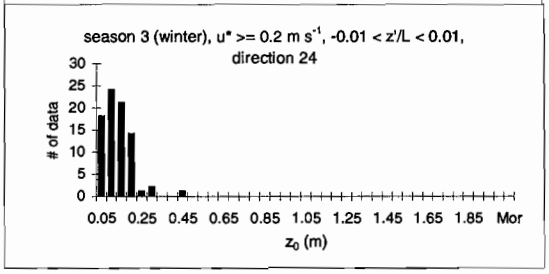

Appendix III: Histograms (z_m = 30 m, z_d = 27 m)

Data are sorted by season and by direction.

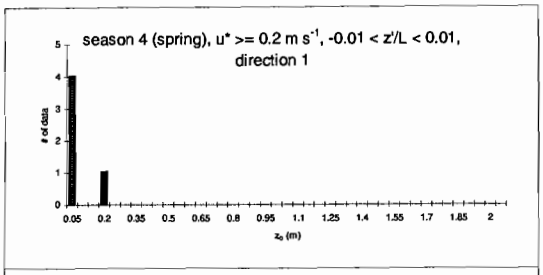

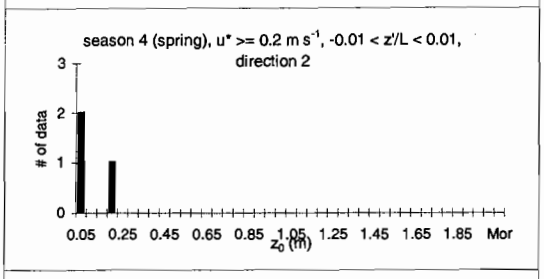

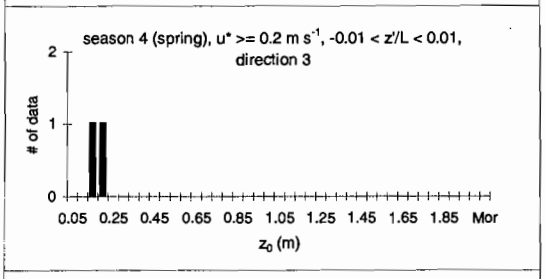

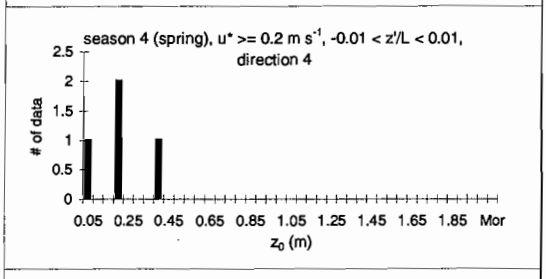

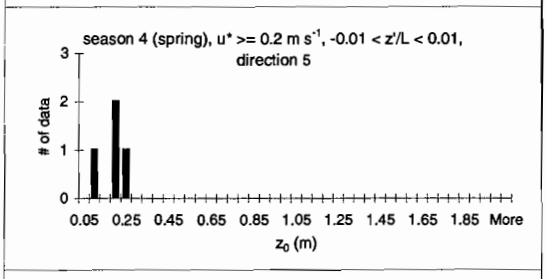

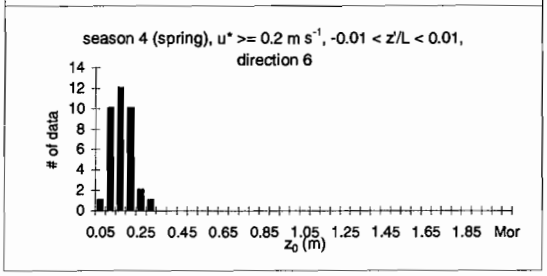

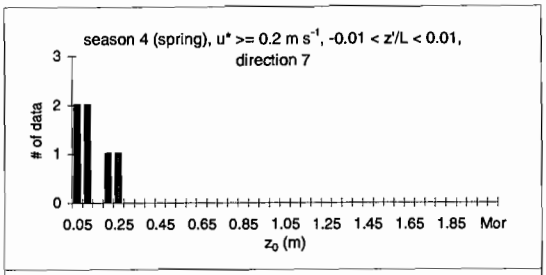

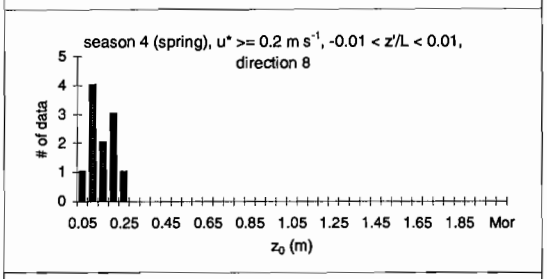

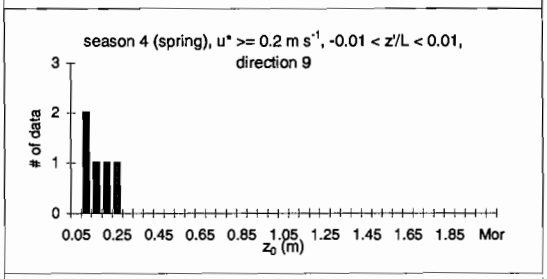

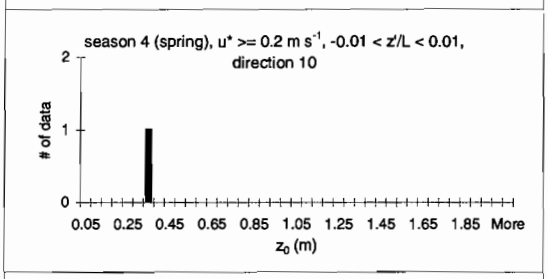

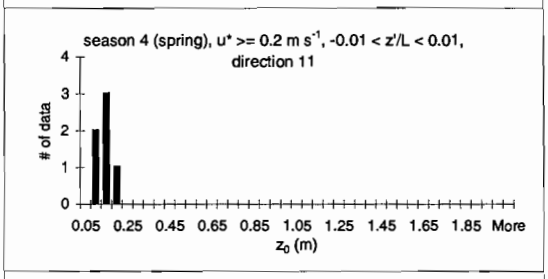

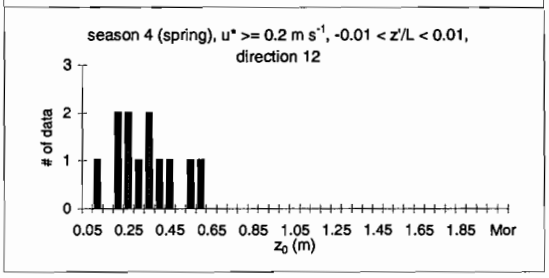

Appendix III: Histograms (z_m = 30 m, z_d = 27 m)

Data are sorted by season and by direction.

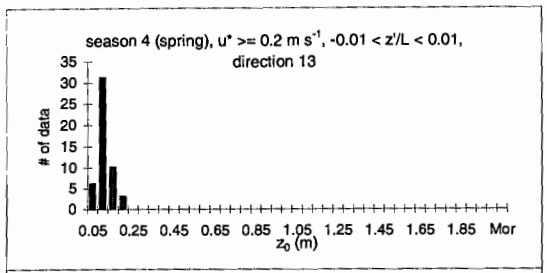

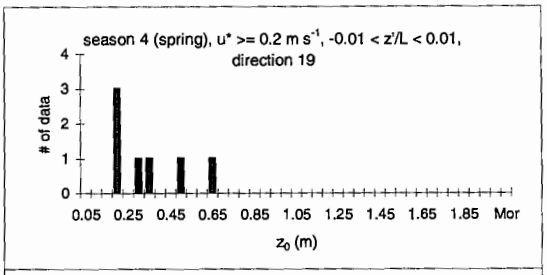

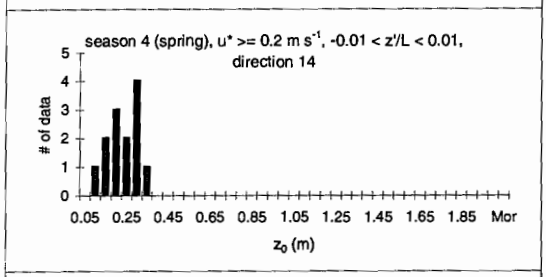

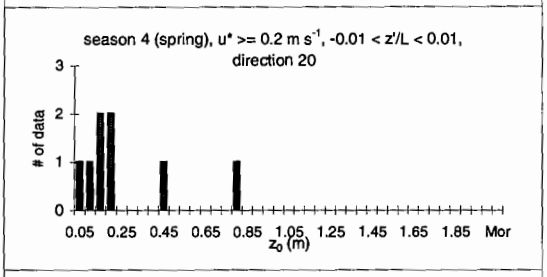

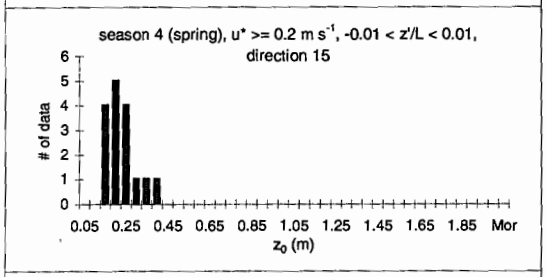

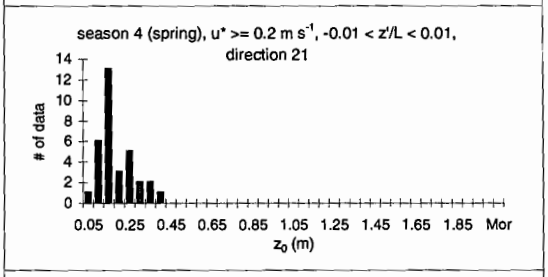

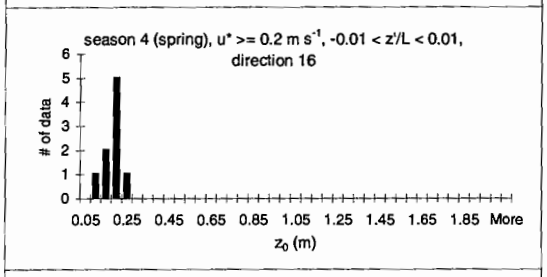

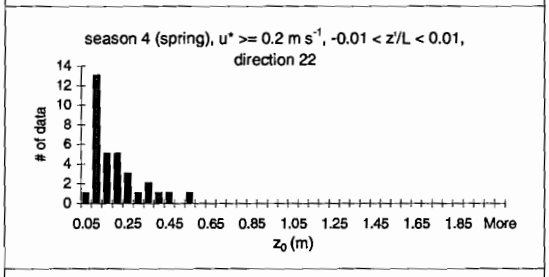

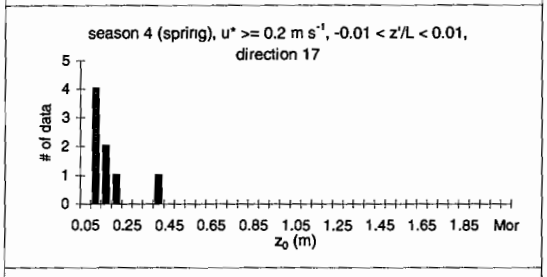

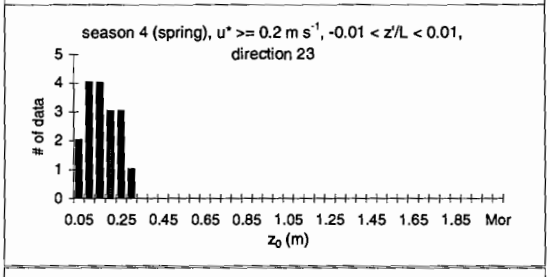

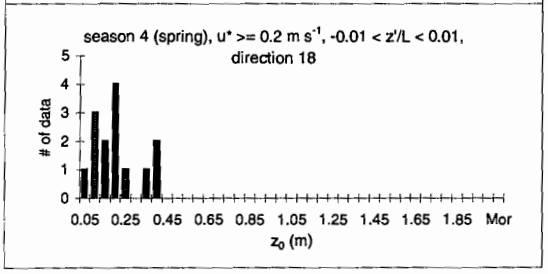

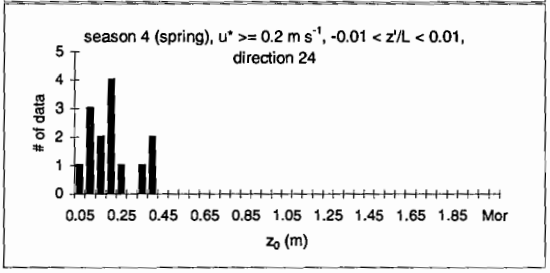

Appendix III: Histograms (z_m = 30 m, z_d = 27 m)

Data are sorted by season and by direction.

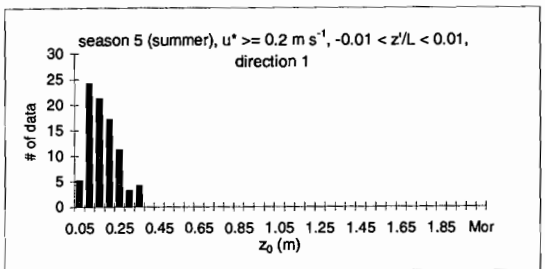

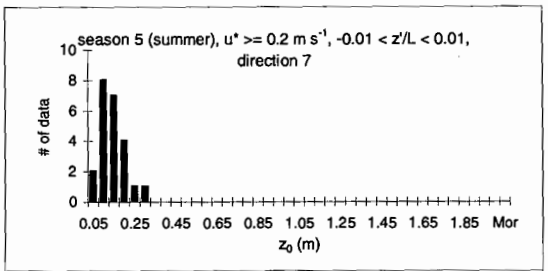

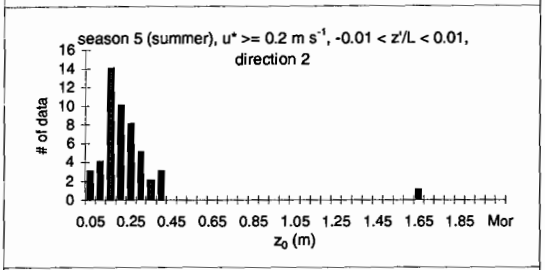

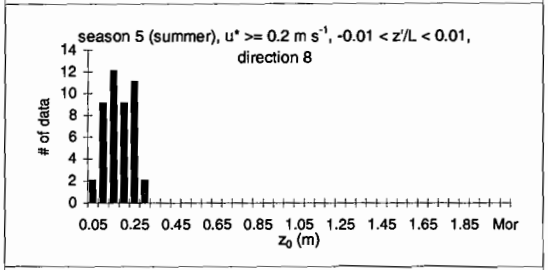

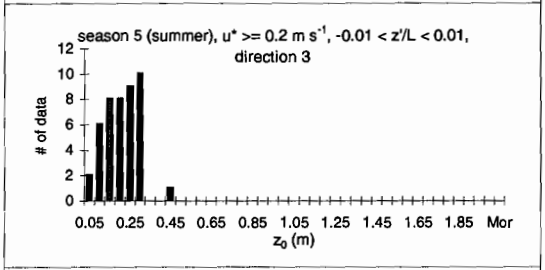

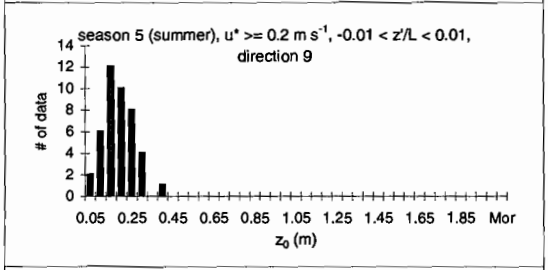

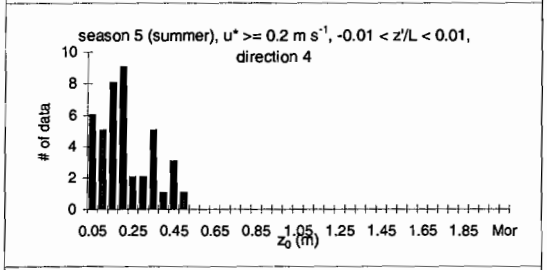

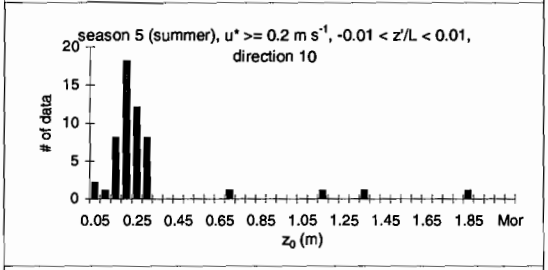

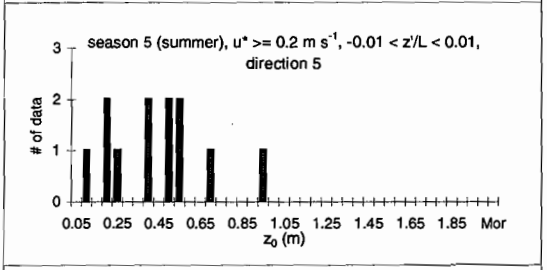

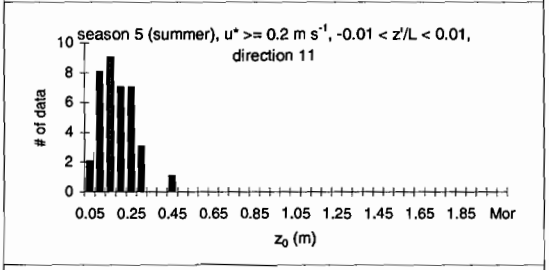

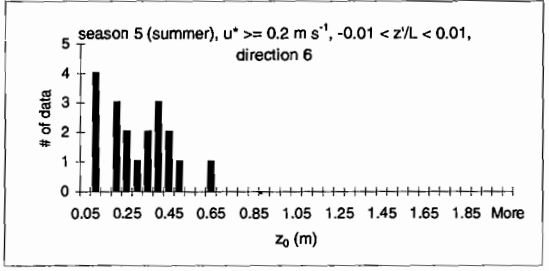

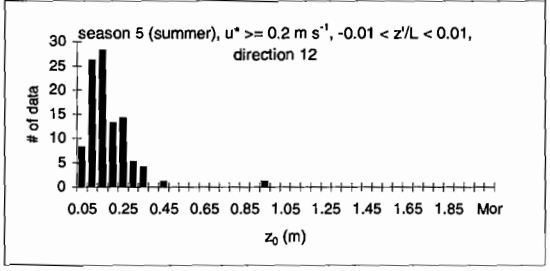

Appendix III: Histograms (z_m = 30 m, z_d = 27 m)

Data are sorted by season and by direction.

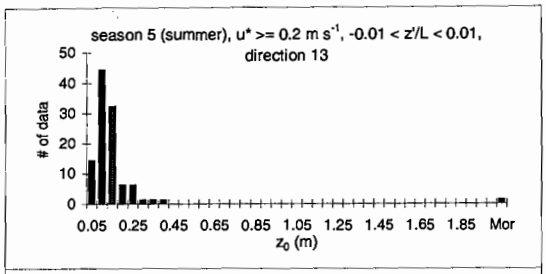

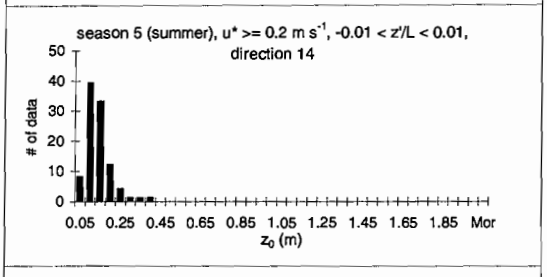

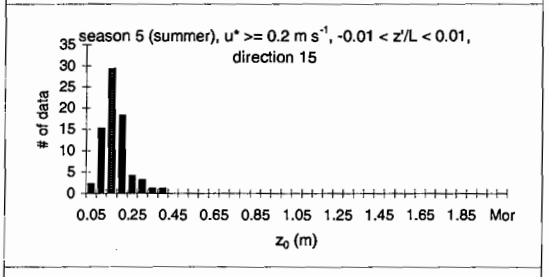

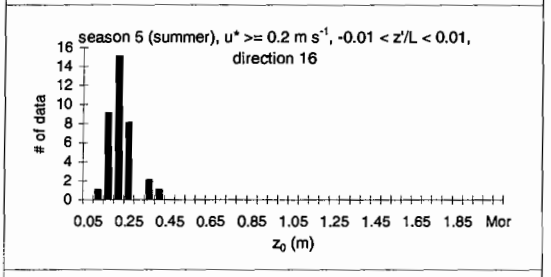

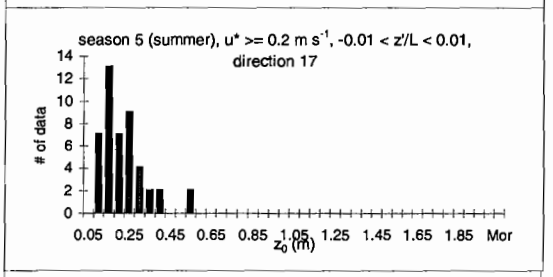

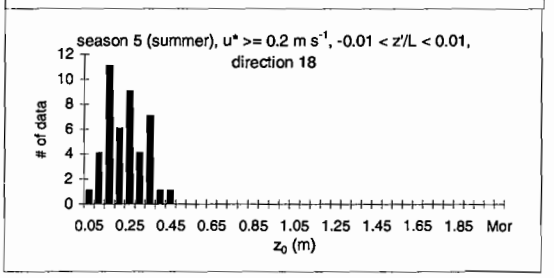

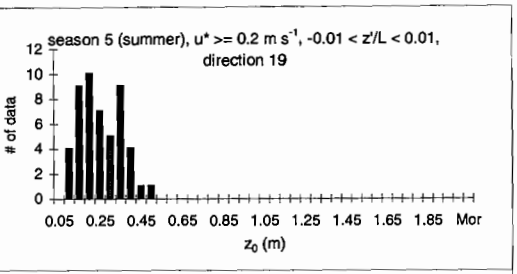

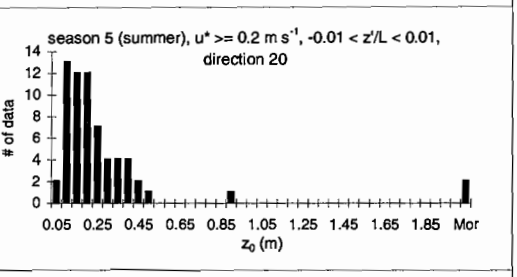

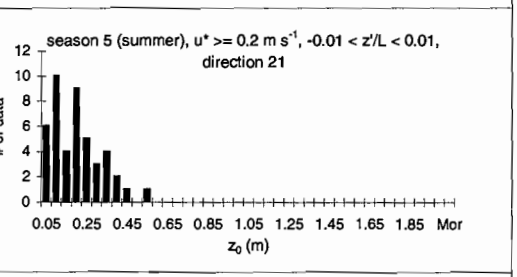

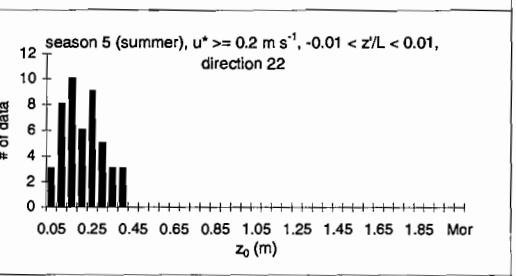

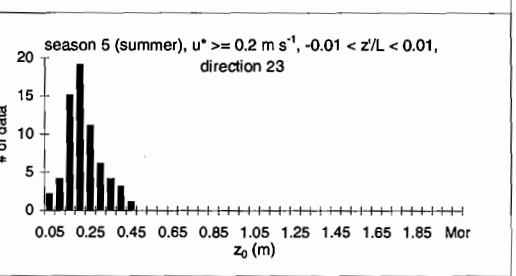

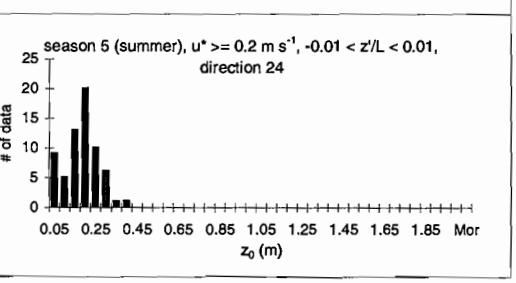

Appendix III: Histograms (z_m = 30 m, z_d = 27 m)

Data are sorted by season and by direction.

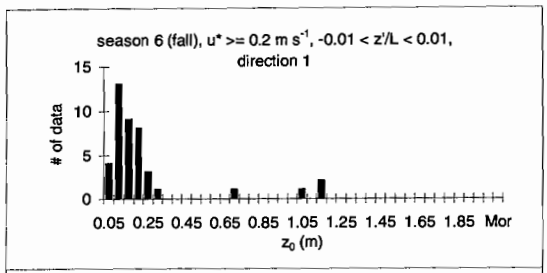

N/A

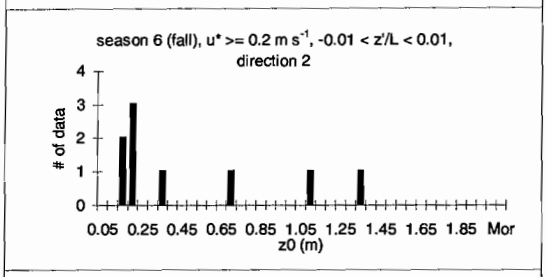

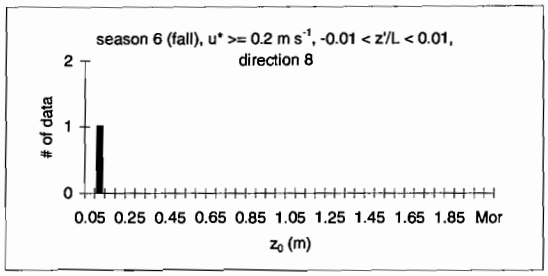

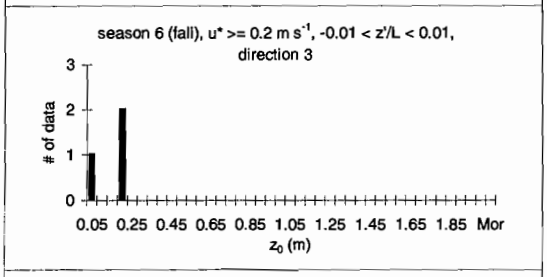

N/A

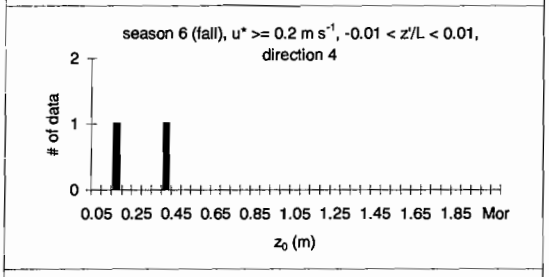

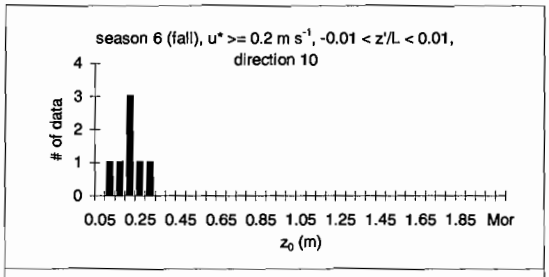

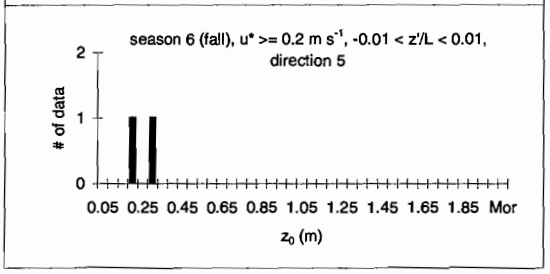

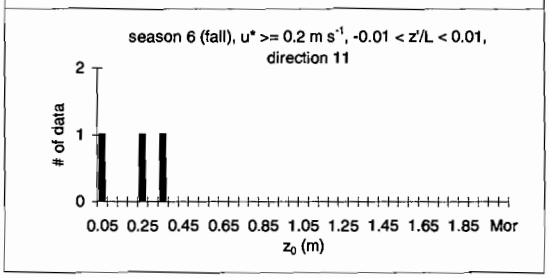

N/A

N/A

Appendix III: Histograms (z_m = 30 m, z_d = 27 m)

Data are sorted by season and by direction.

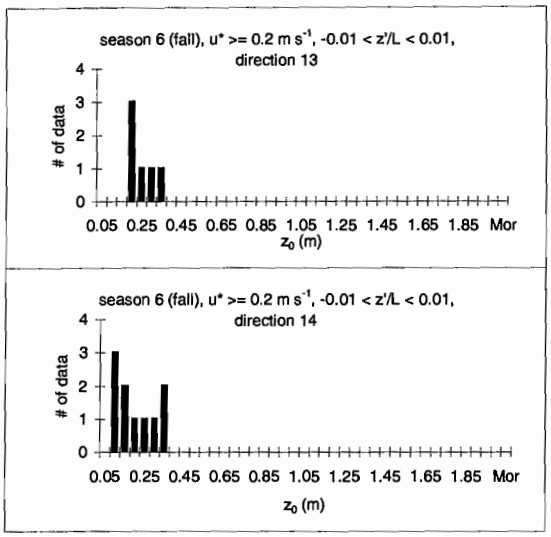

N/A

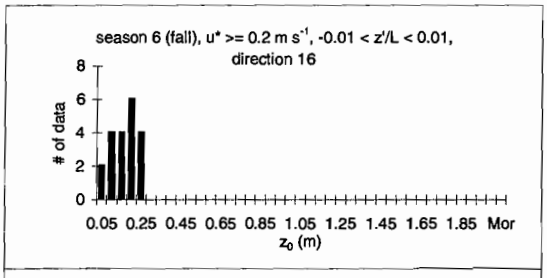

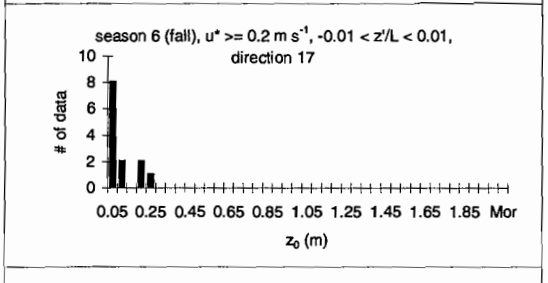

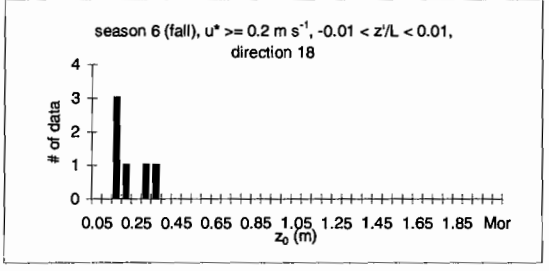

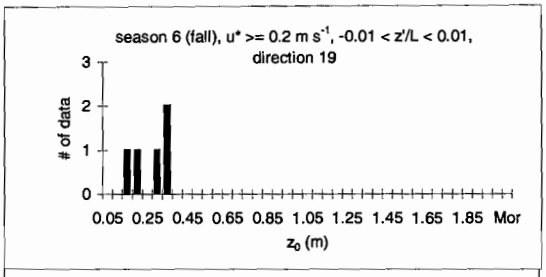

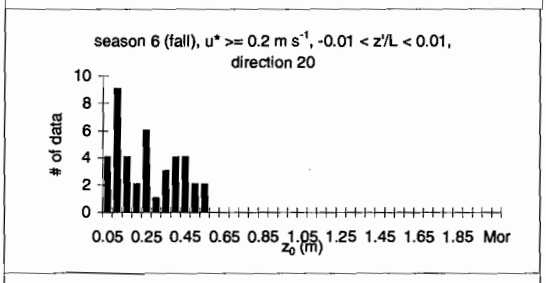

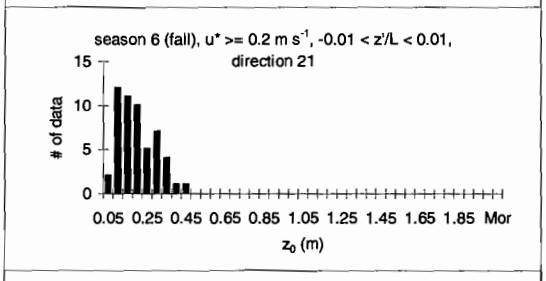

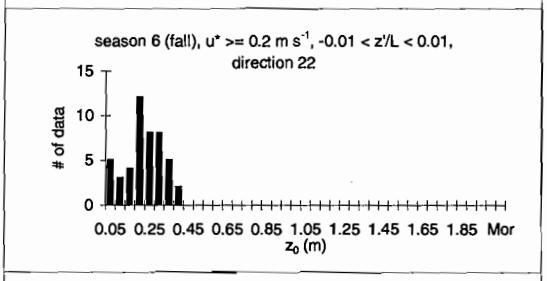

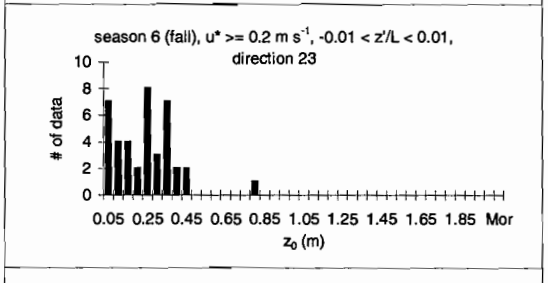

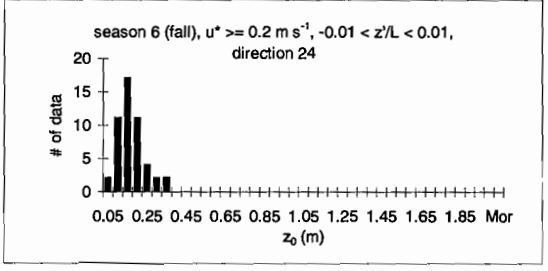

Appendix III: Histograms (z_m = 30 m, z_d = 27 m)

Data are sorted by season and by direction.

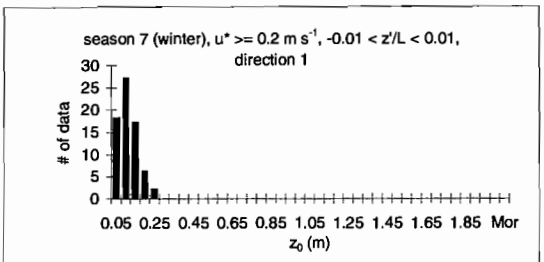

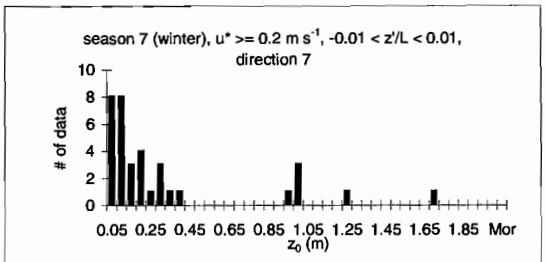

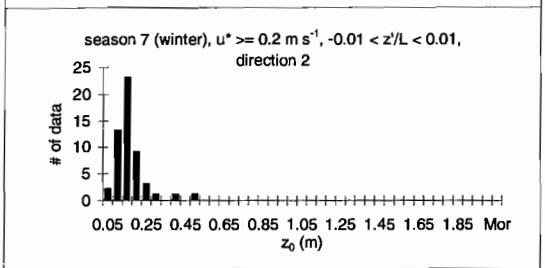

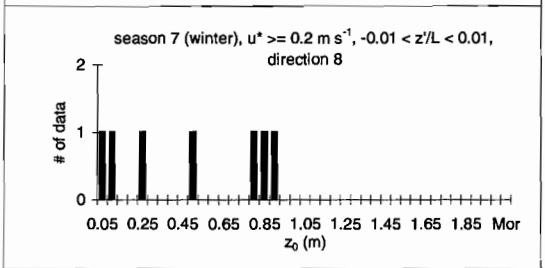

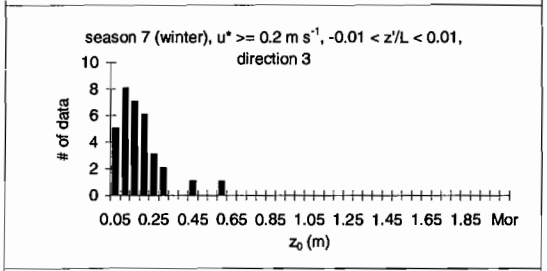

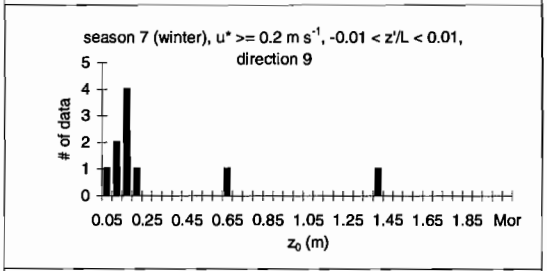

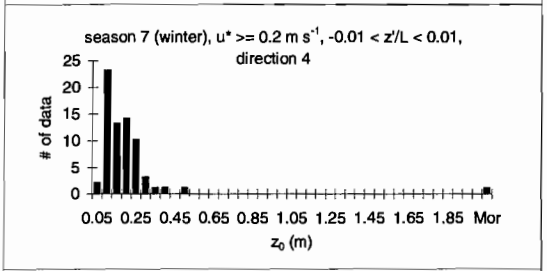

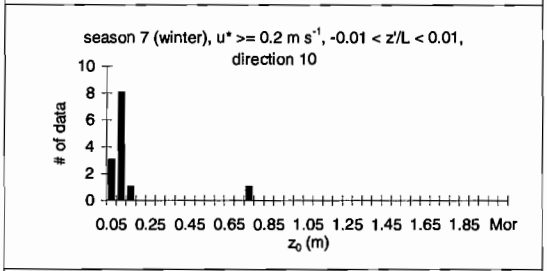

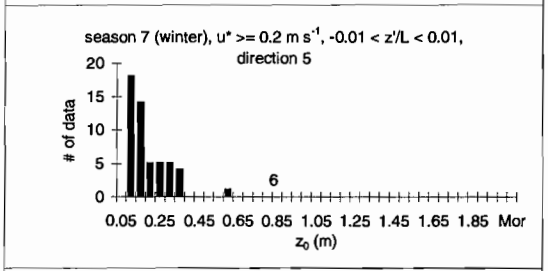

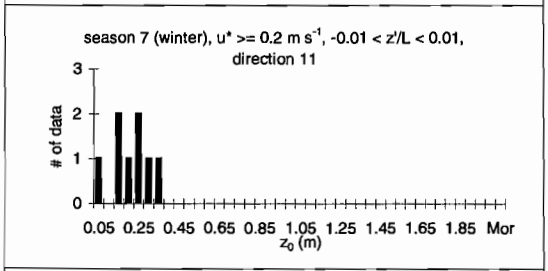

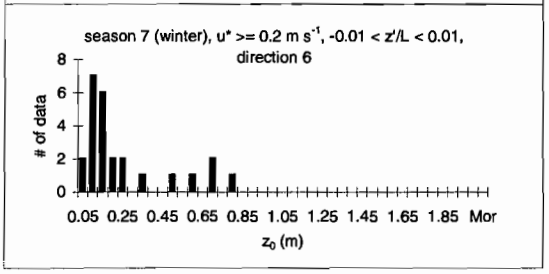

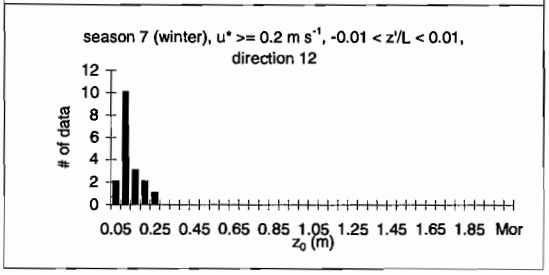

Appendix III: Histograms (z_m = 30 m, z_d = 27 m)

Data are sorted by season and by direction.

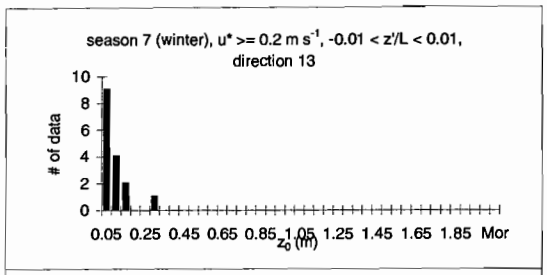

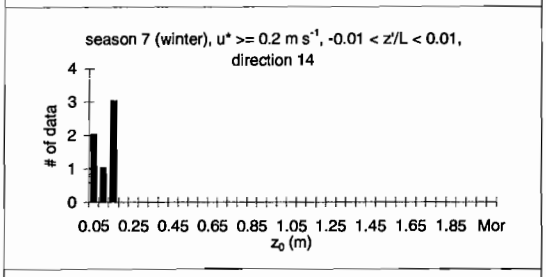

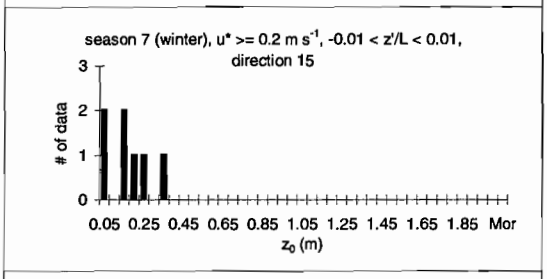

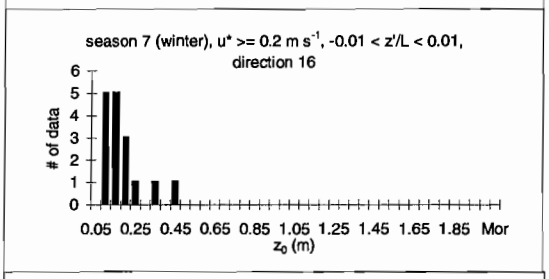

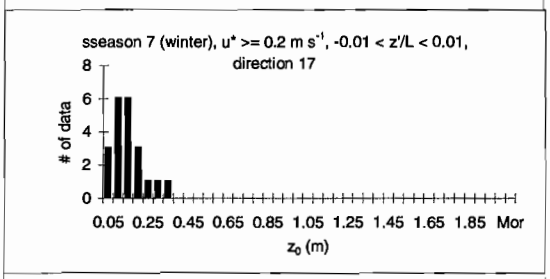

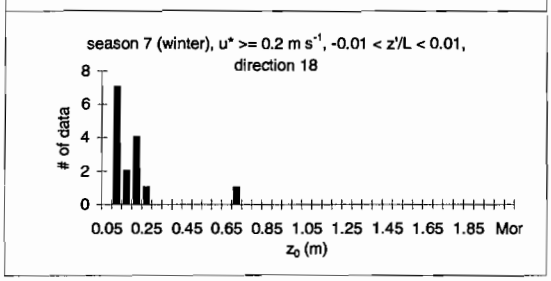

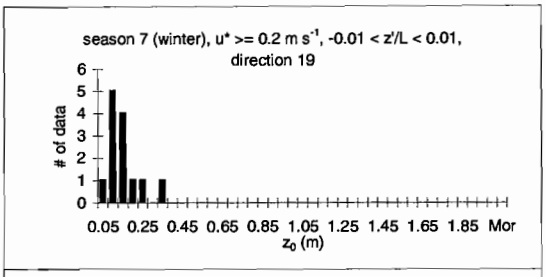

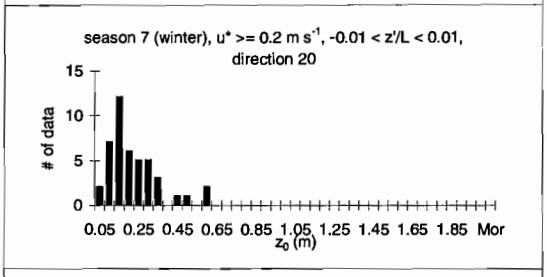

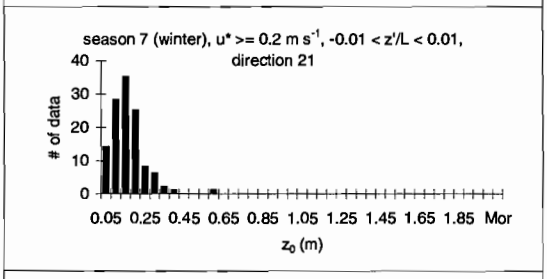

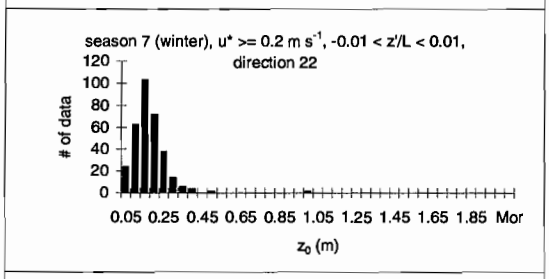

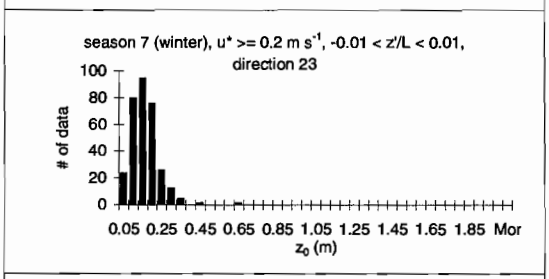

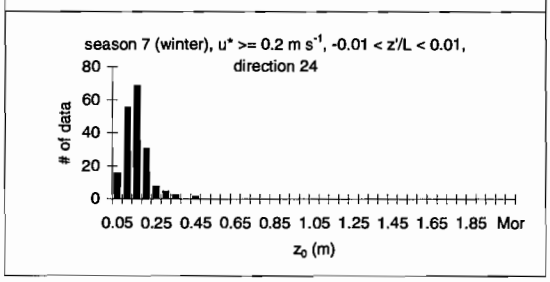

Appendix III: Histograms (z_m = 30 m, z_d = 27 m)

Data are sorted by season and by direction.

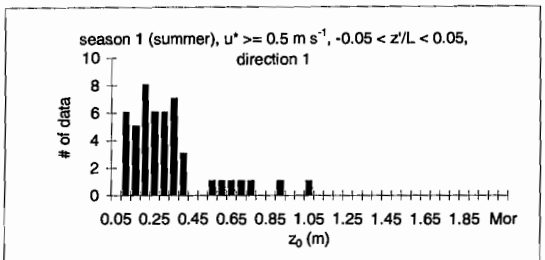

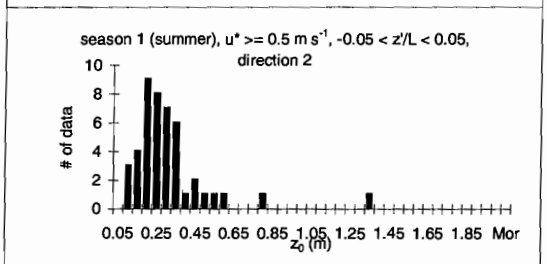

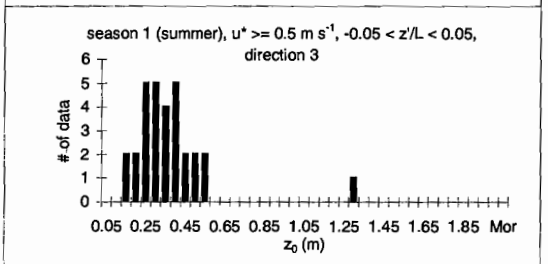

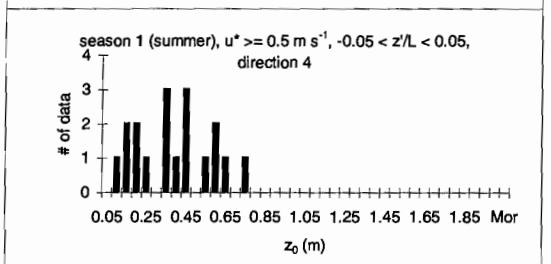

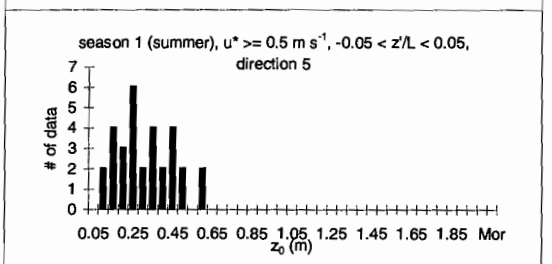

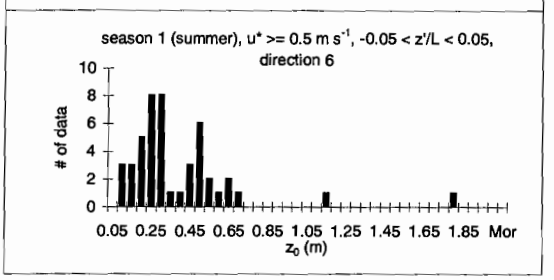

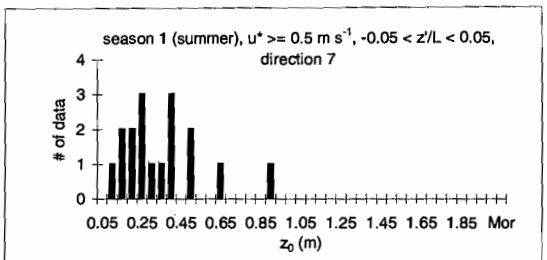

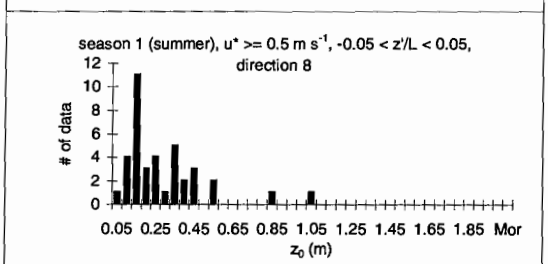

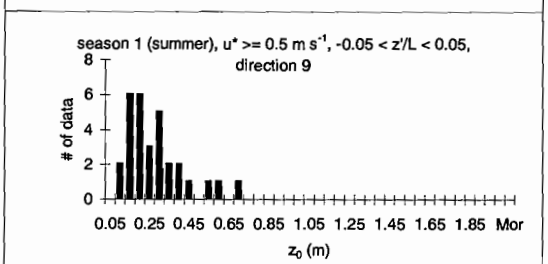

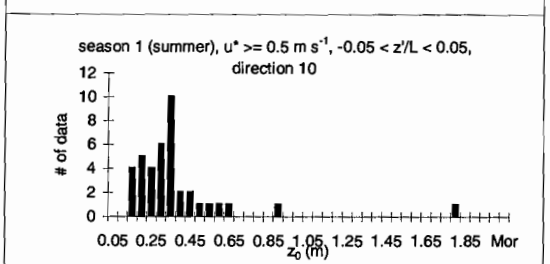

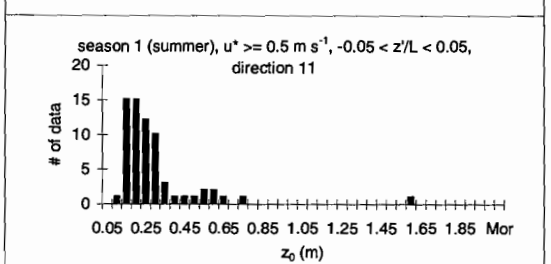

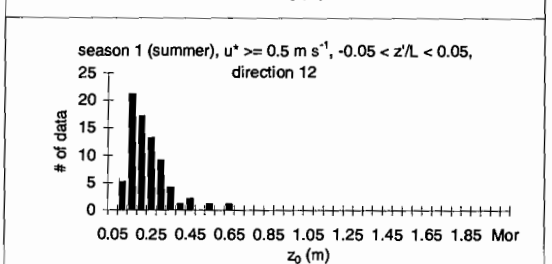

Appendix III: Histograms (z_m = 30 m, z_d = 27 m)

Data are sorted by season and by direction.

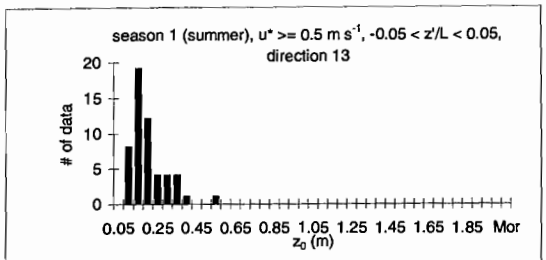

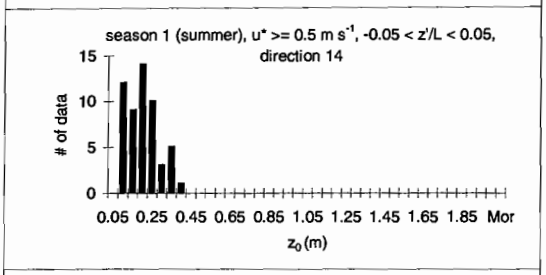

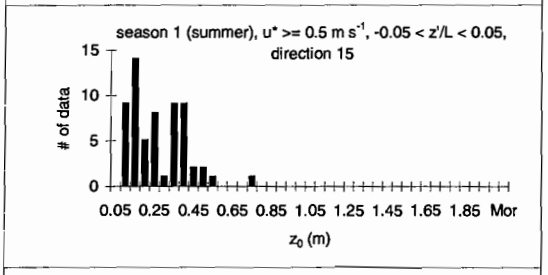

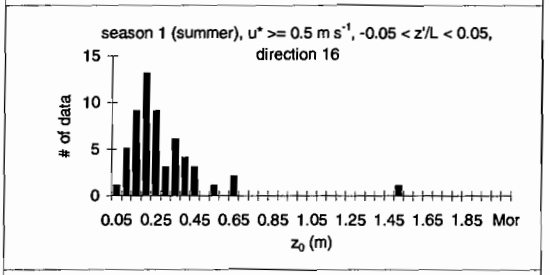

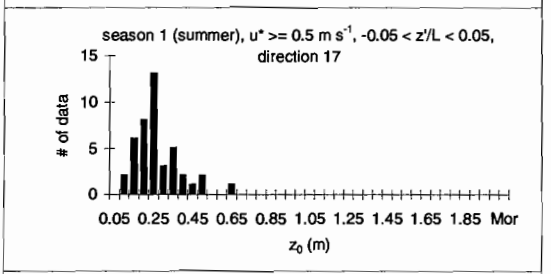

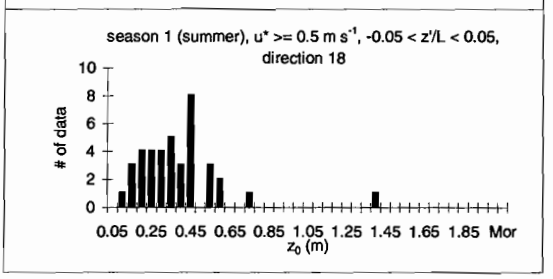

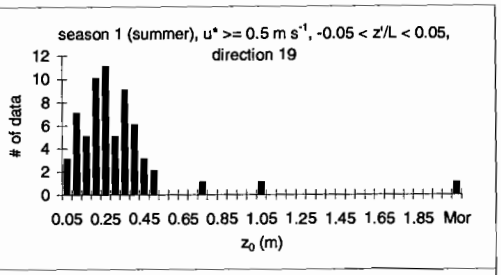

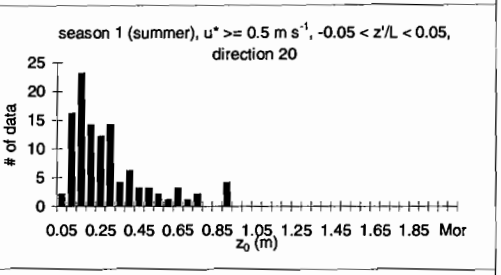

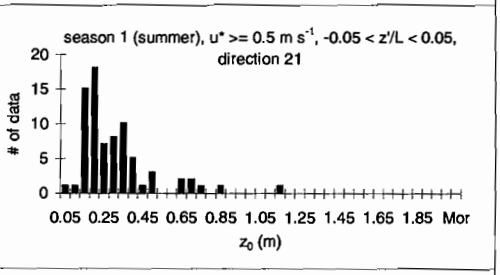

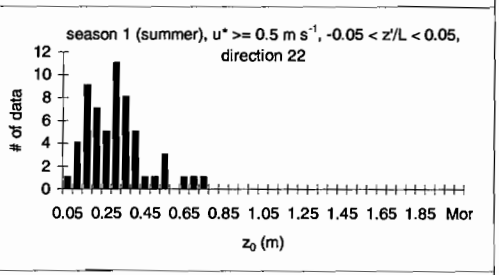

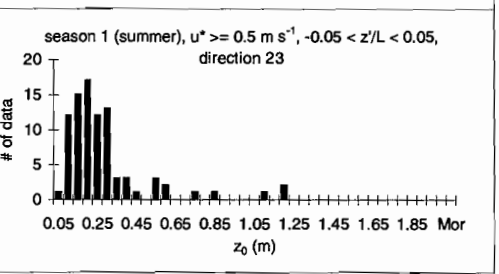

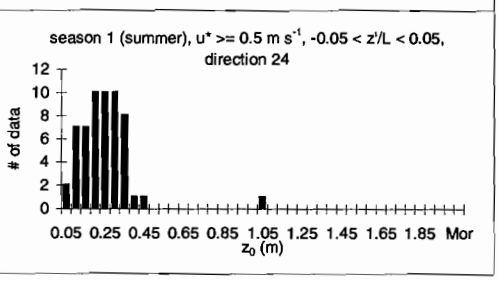

Appendix III: Histograms (z_m = 30 m, z_d = 27 m)

Data are sorted by season and by direction.

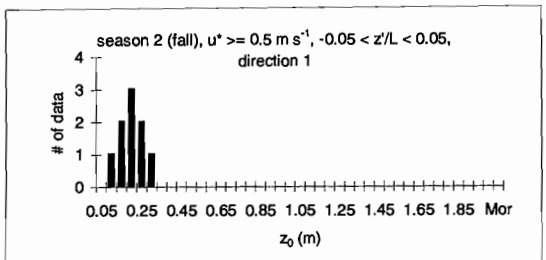

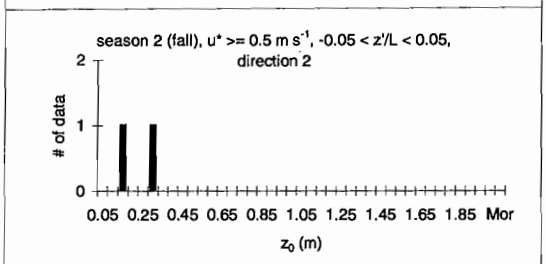

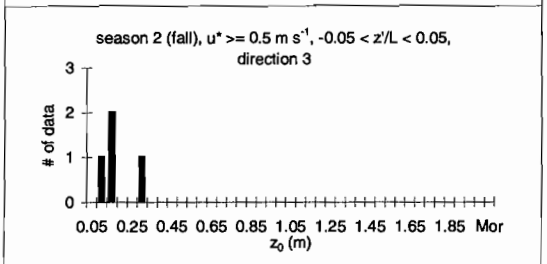

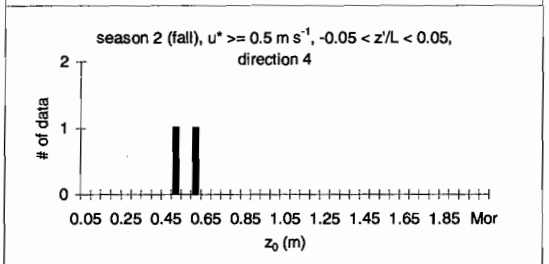

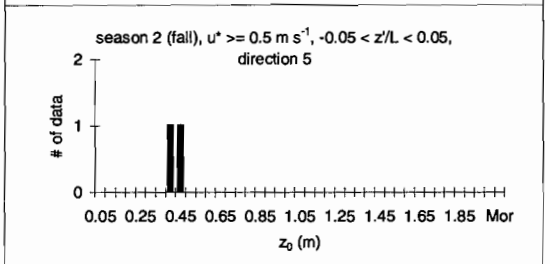

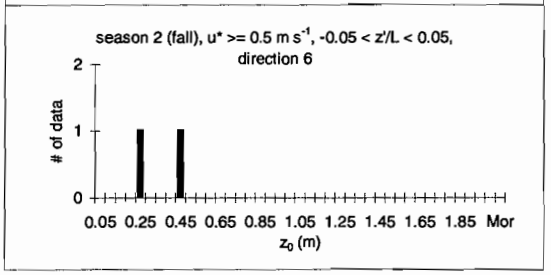

N/A

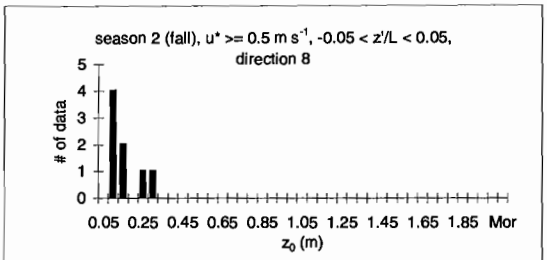

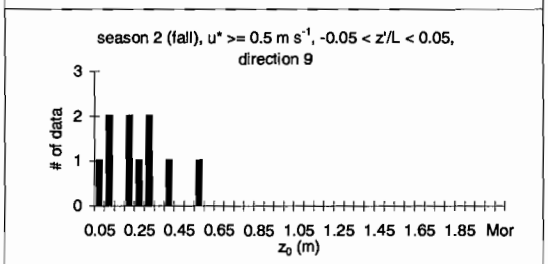

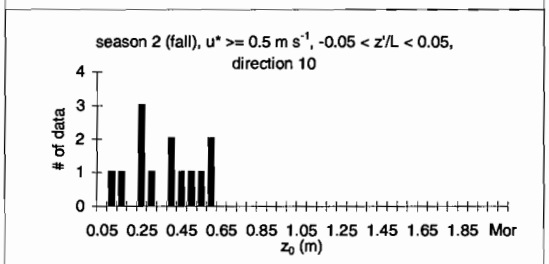

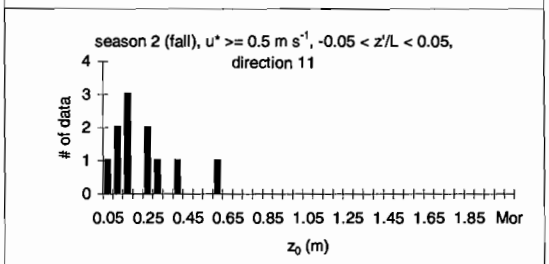

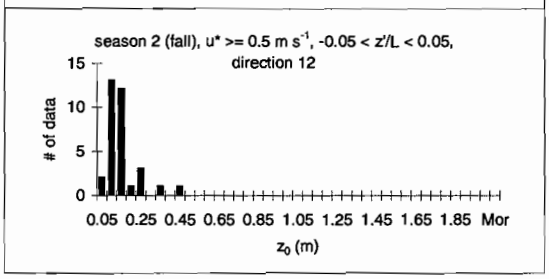

Appendix III: Histograms (z_m = 30 m, z_d = 27 m)

Data are sorted by season and by direction.

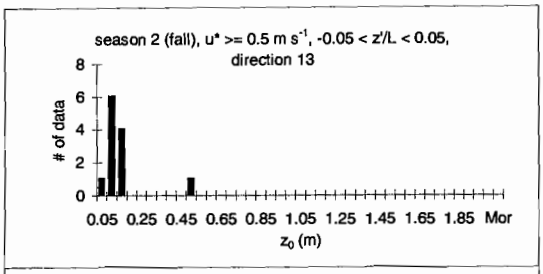

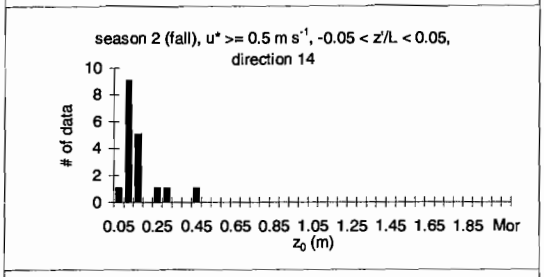

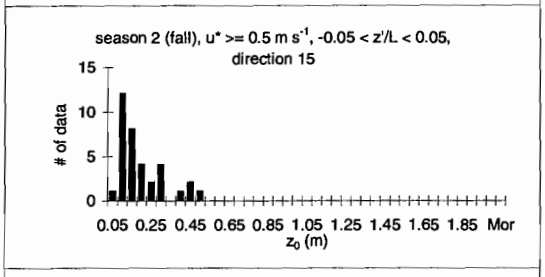

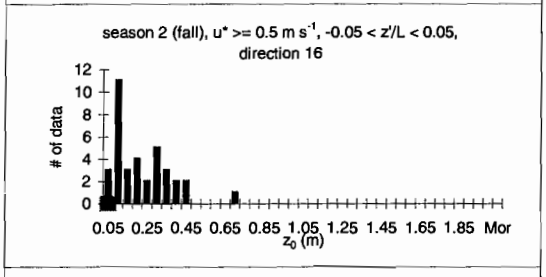

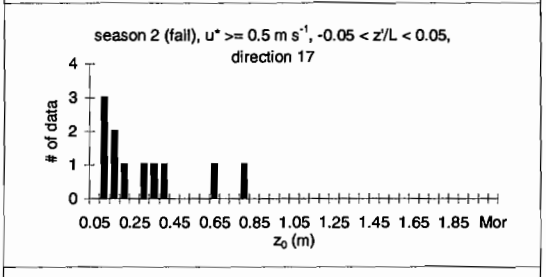

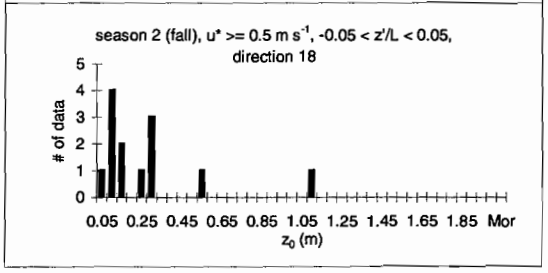

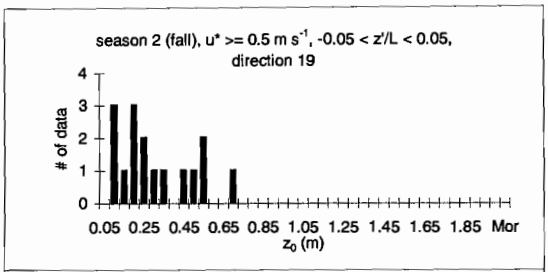

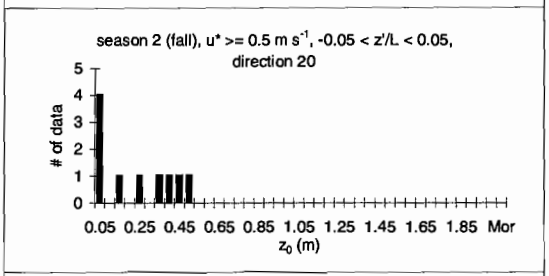

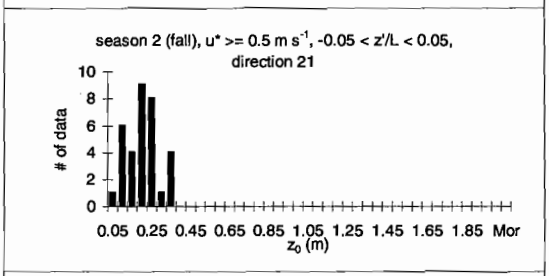

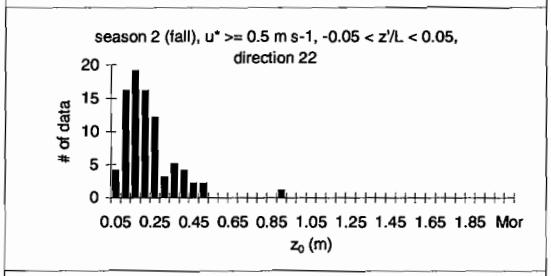

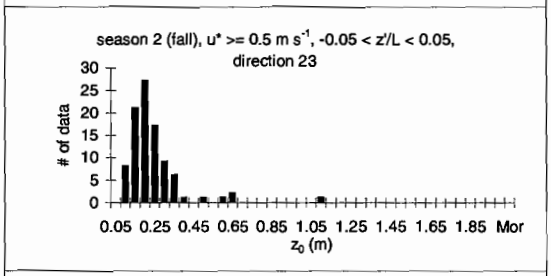

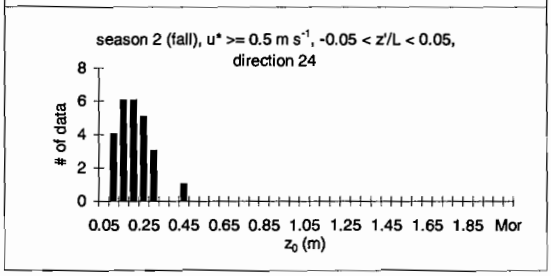

Appendix III: Histograms (z_m = 30 m, z_d = 27 m)

Data are sorted by season and by direction.

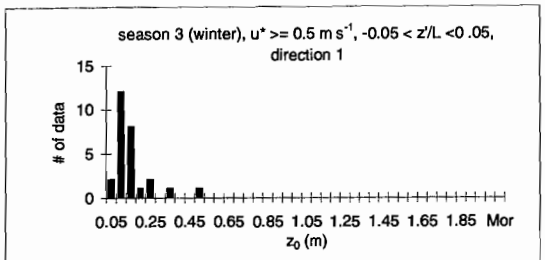

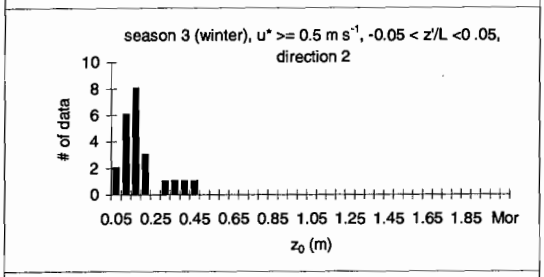

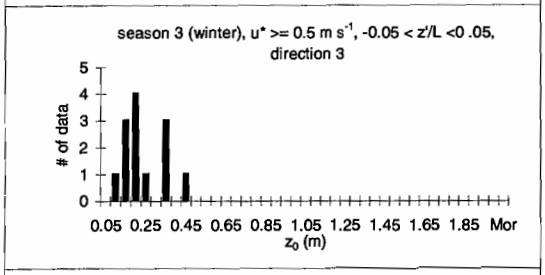

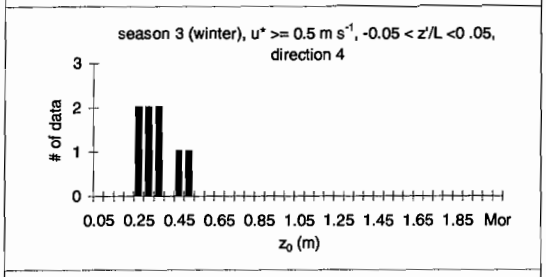

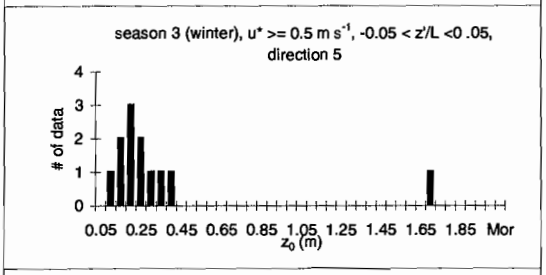

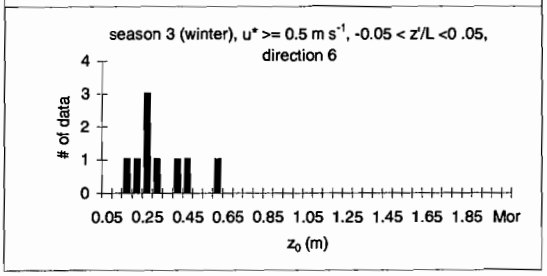

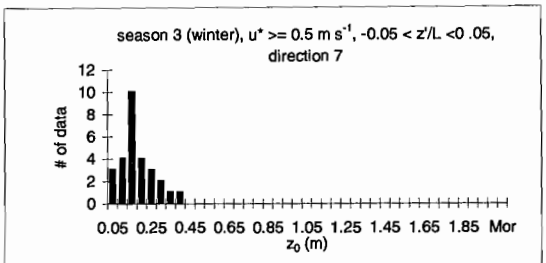

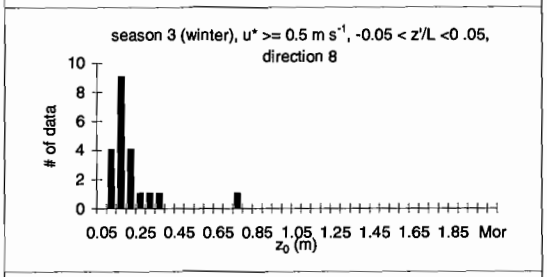

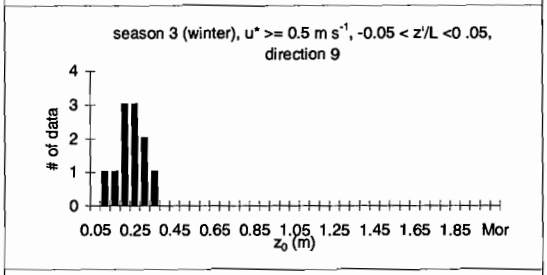

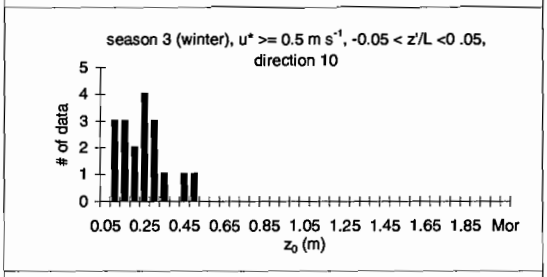

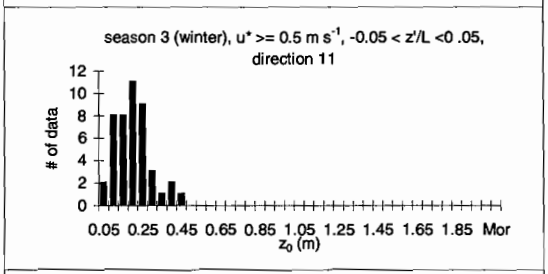

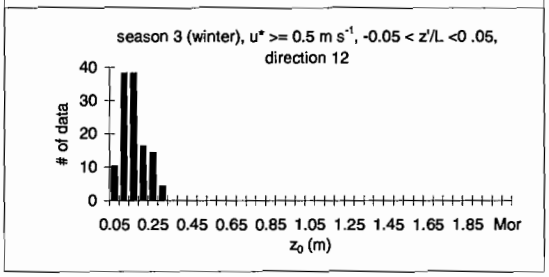

Appendix III: Histograms (z_m = 30 m, z_d = 27 m)

Data are sorted by season and by direction.

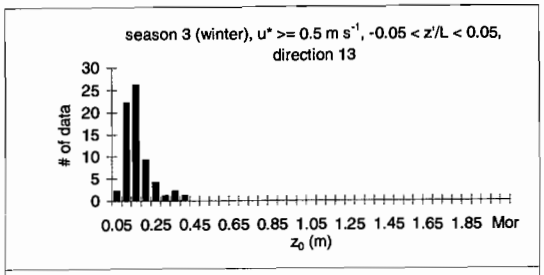

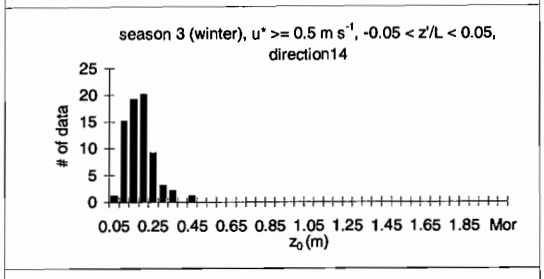

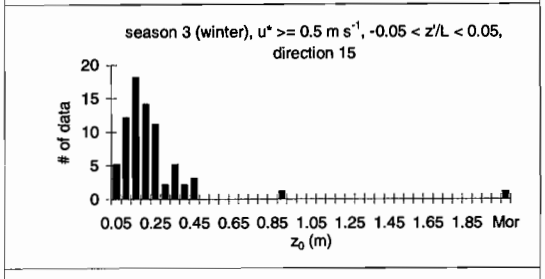

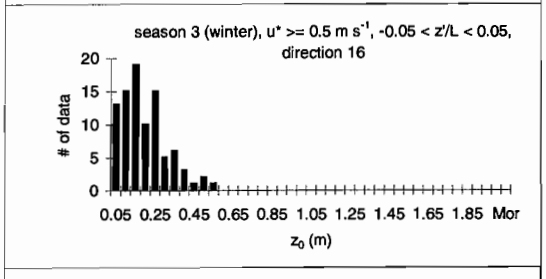

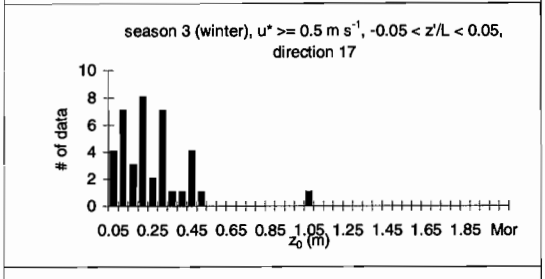

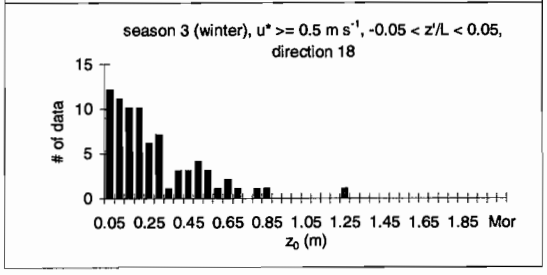

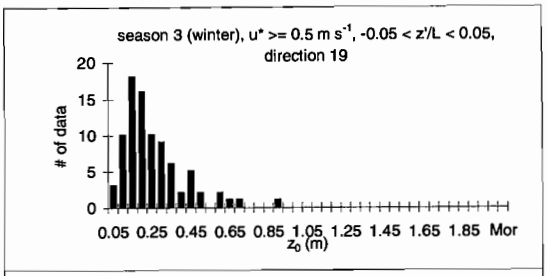

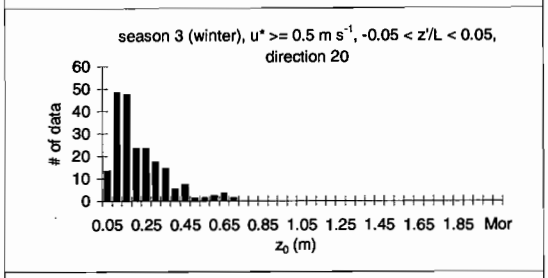

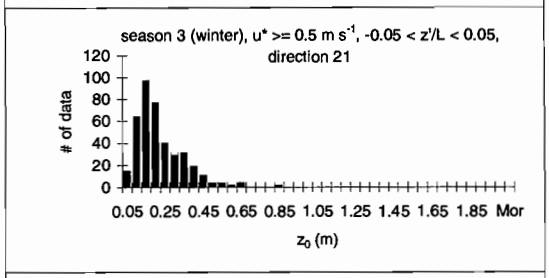

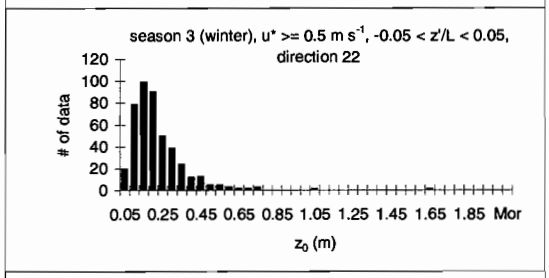

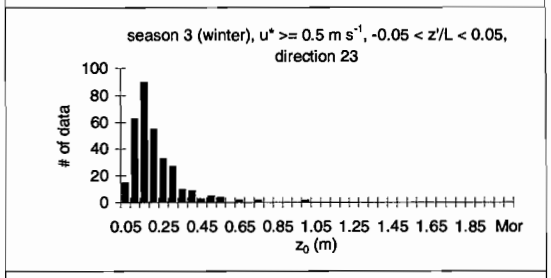

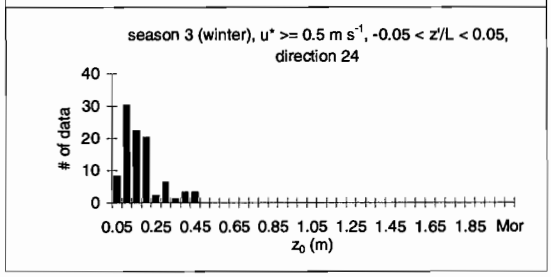

Appendix III: Histograms (z_m = 30 m, z_d = 27 m)

Data are sorted by season and by direction.

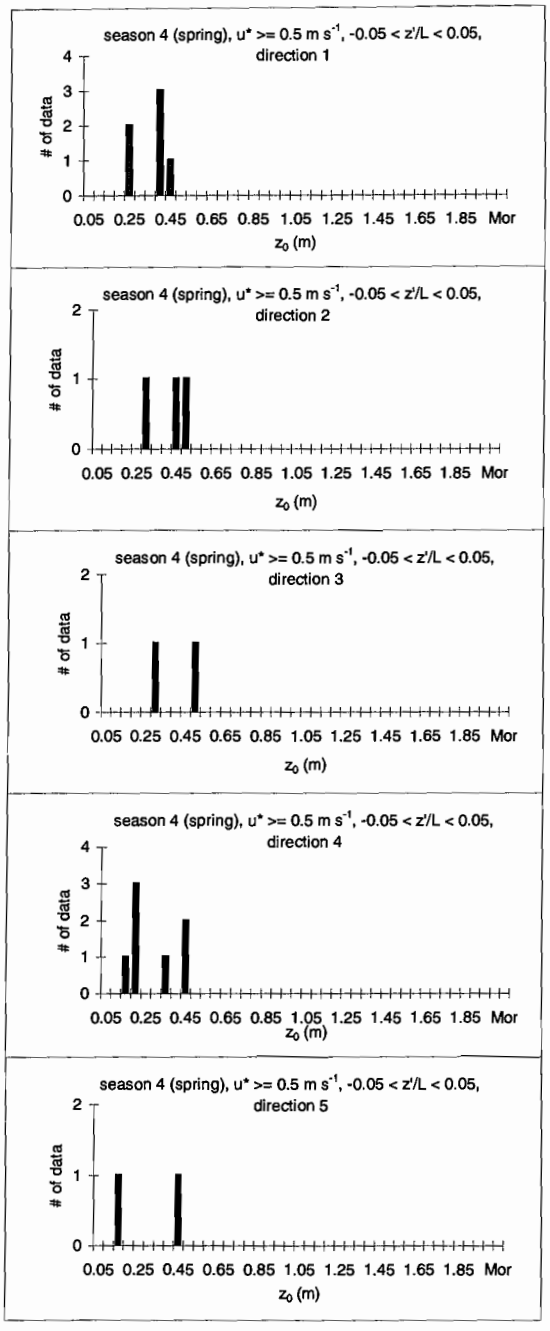

N/A

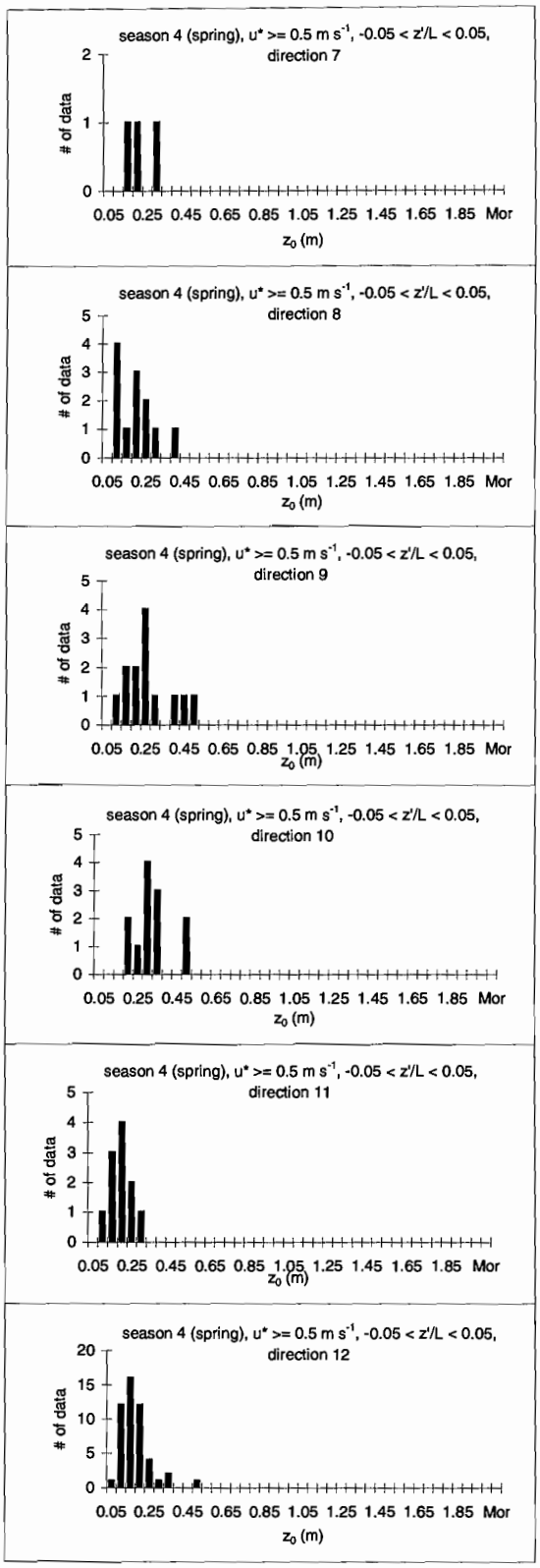

Appendix III: Histograms (z_m = 30 m, z_d = 27 m)

Data are sorted by season and by direction.

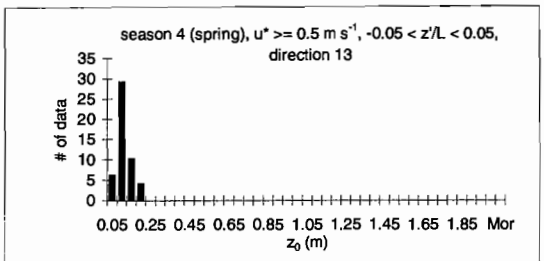

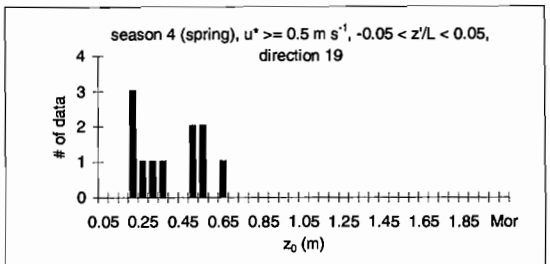

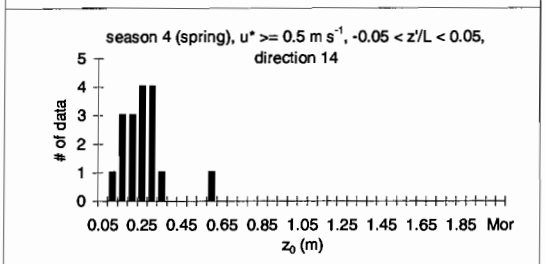

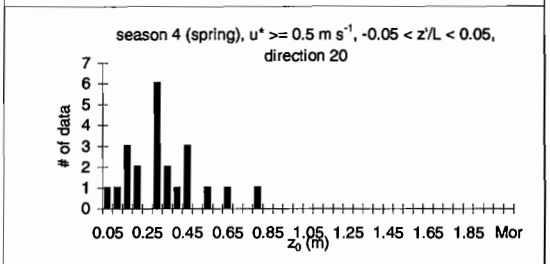

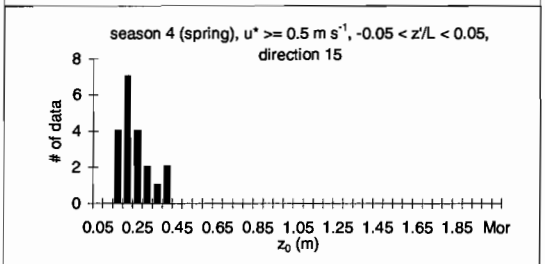

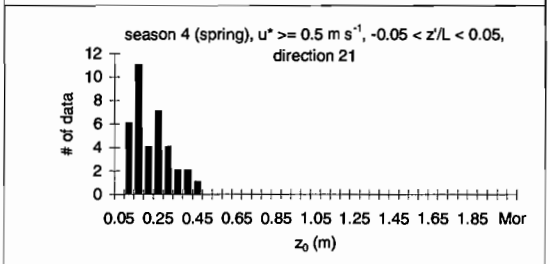

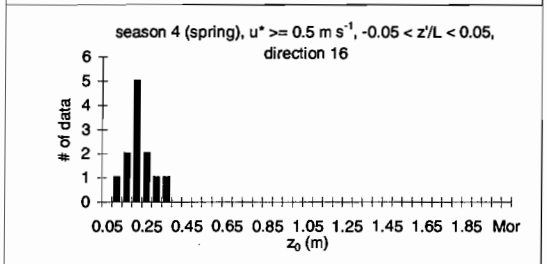

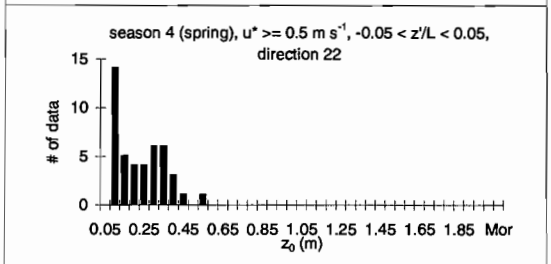

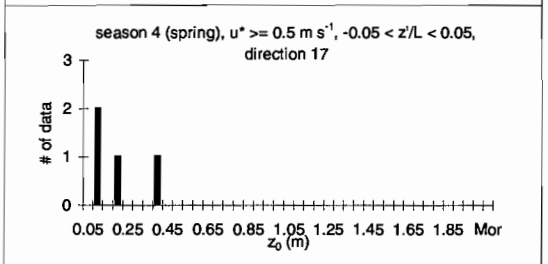

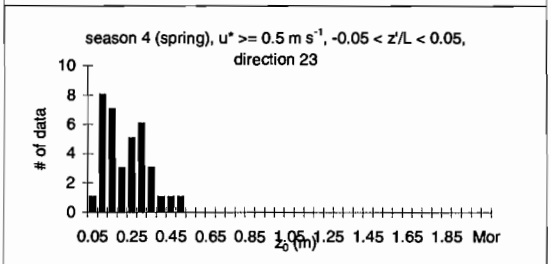

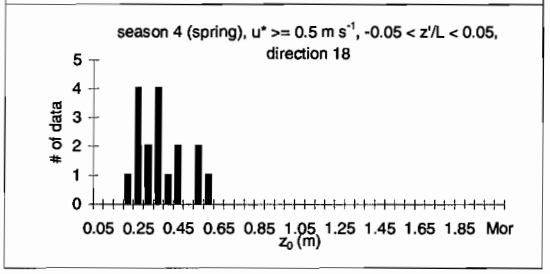

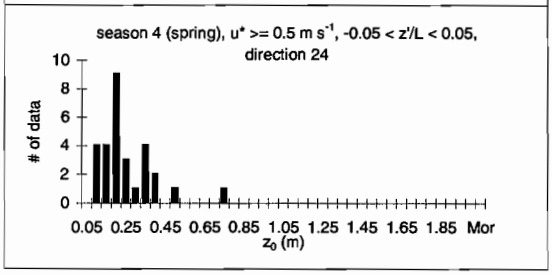

Appendix III: Histograms (z_m = 30 m, z_d = 27 m)

Data are sorted by season and by direction.

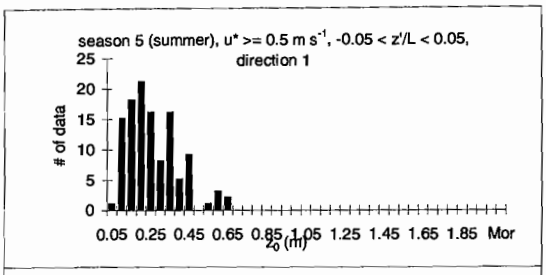

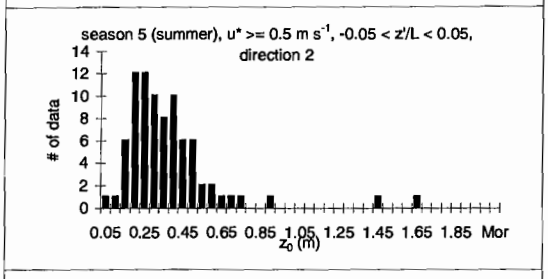

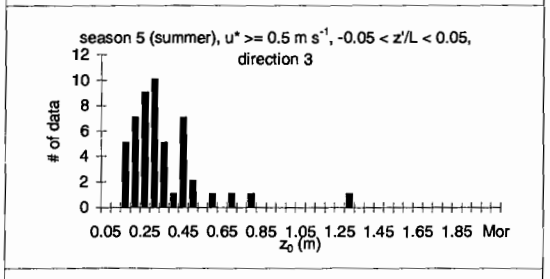

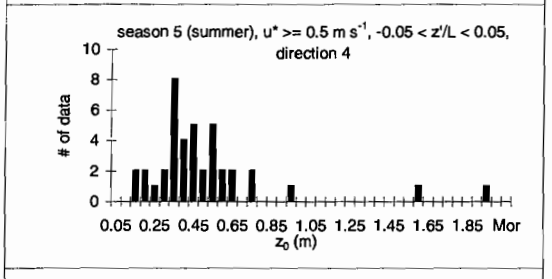

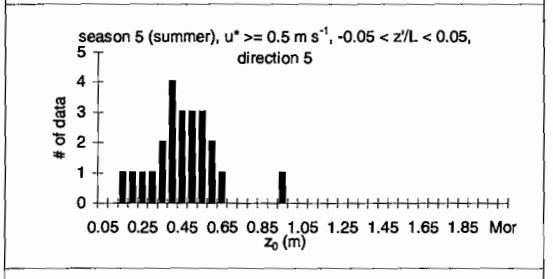

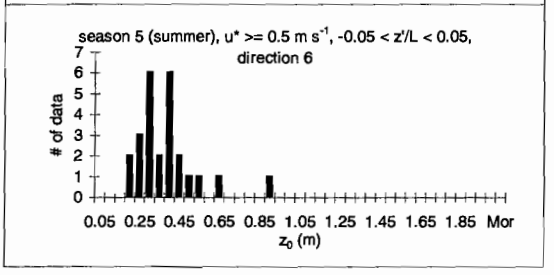

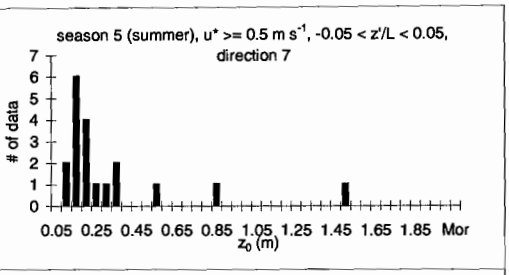

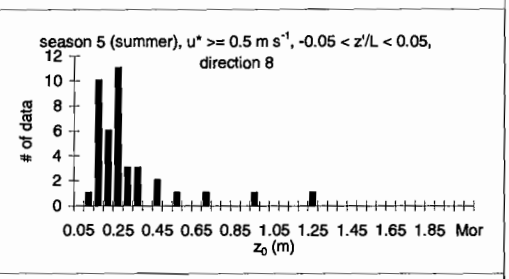

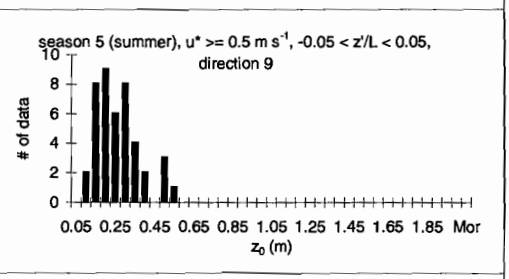

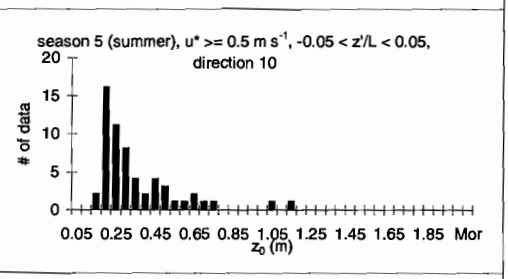

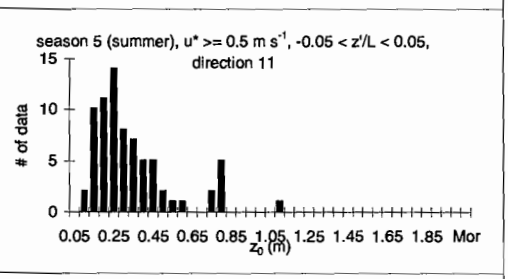

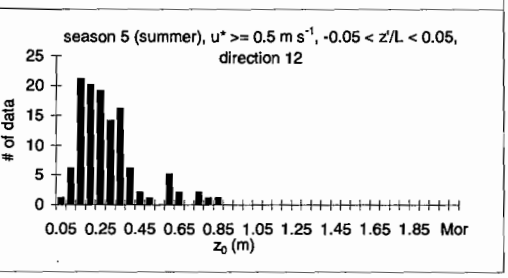

Appendix III: Histograms (z_m = 30 m, z_d = 27 m)

Data are sorted by season and by direction.

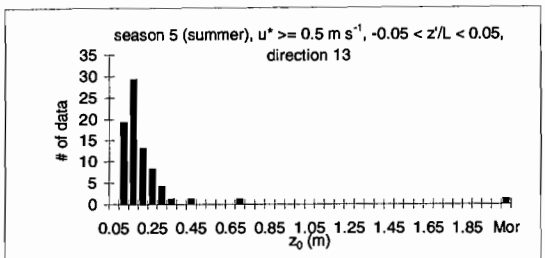

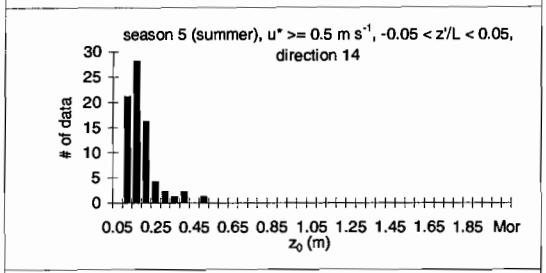

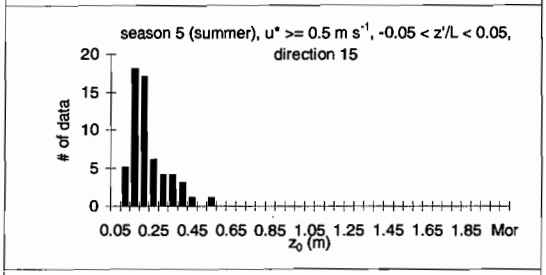

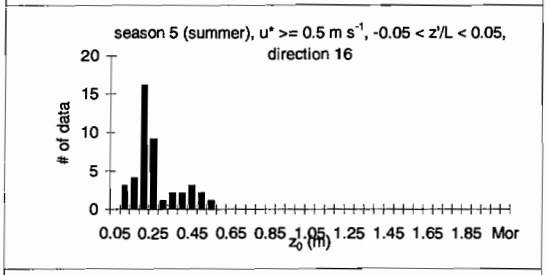

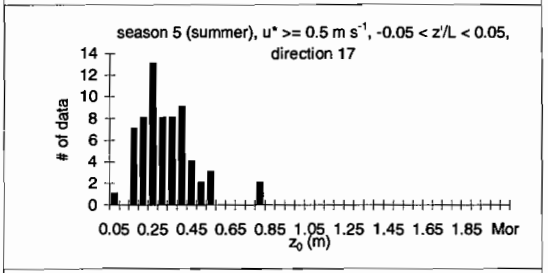

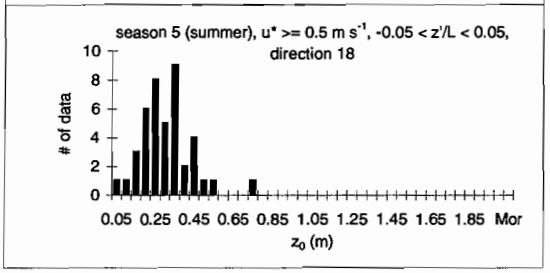

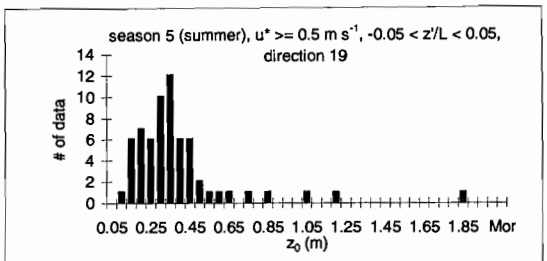

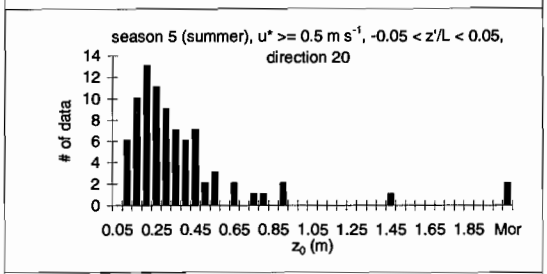

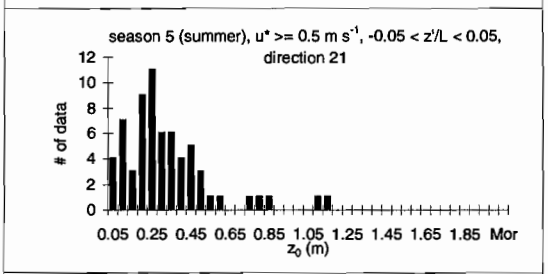

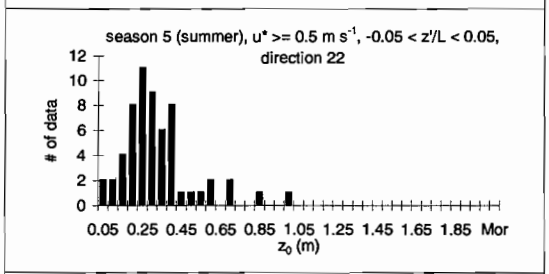

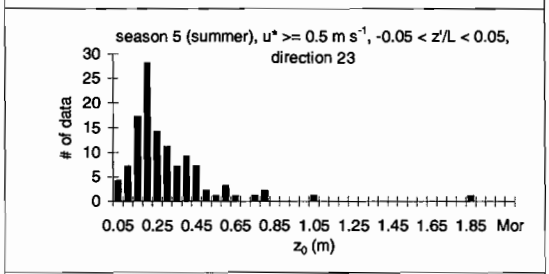

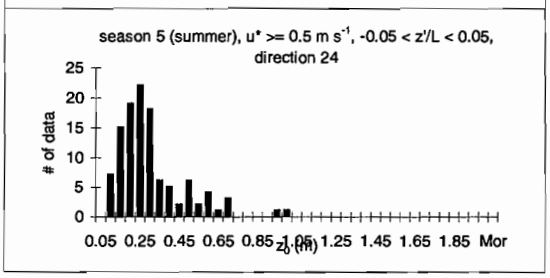

Appendix III: Histograms (z_m = 30 m, z_d = 27 m)

Data are sorted by season and by direction.

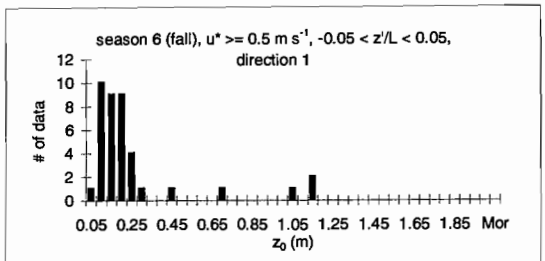

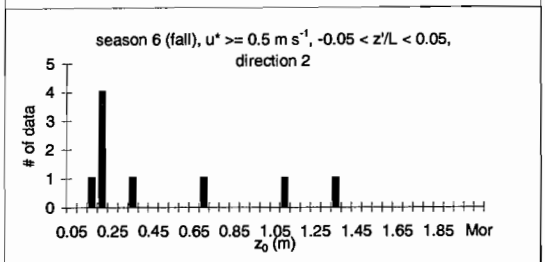

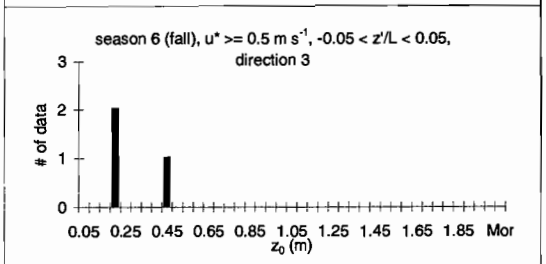

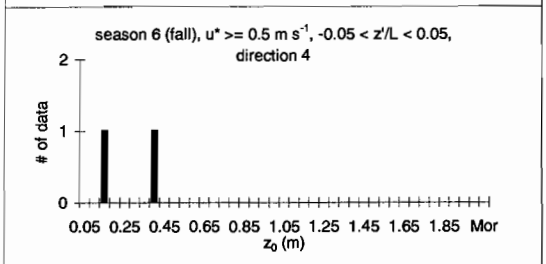

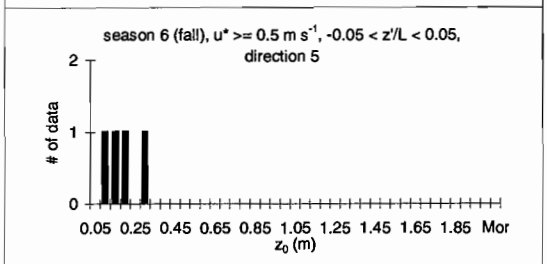

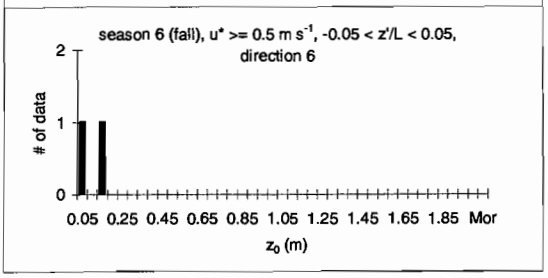

N/A

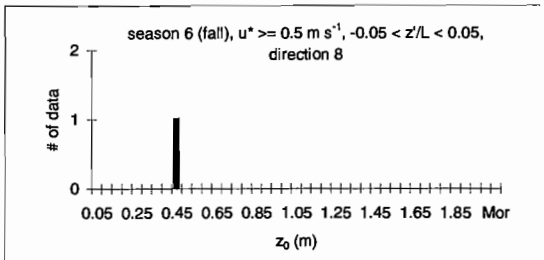

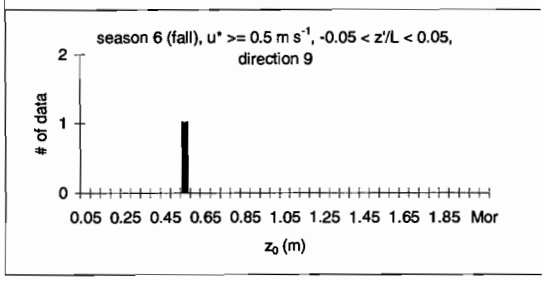

N/A

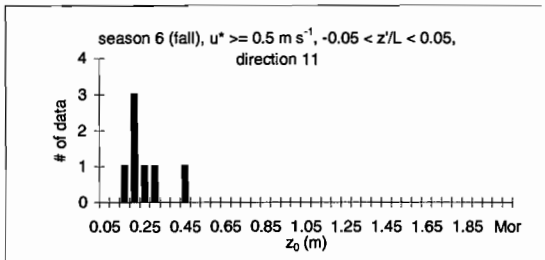

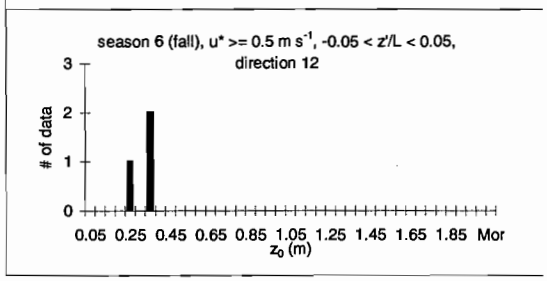

Appendix III: Histograms (z_m = 30 m, z_d = 27 m)

Data are sorted by season and by direction.

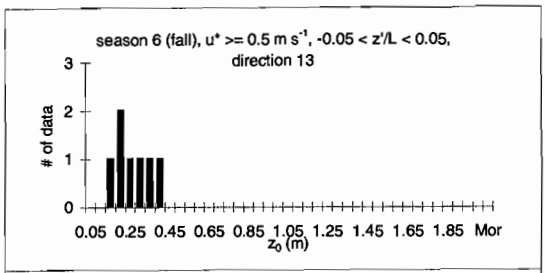

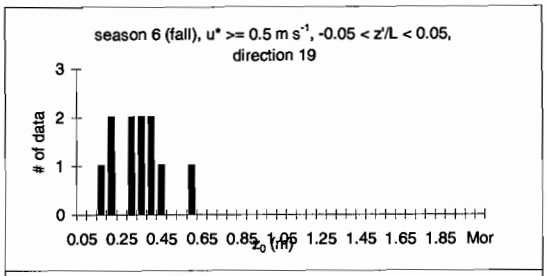

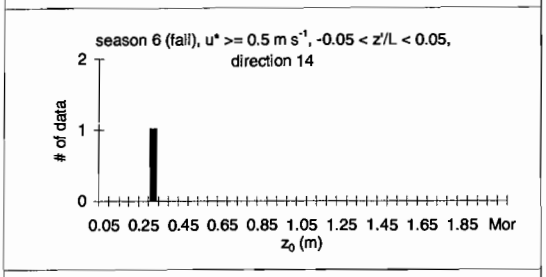

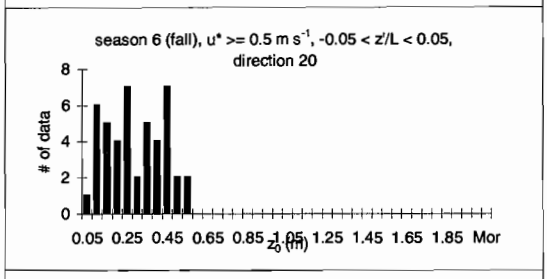

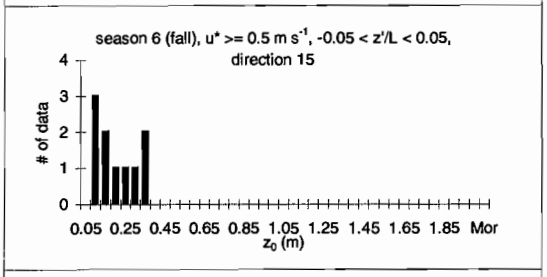

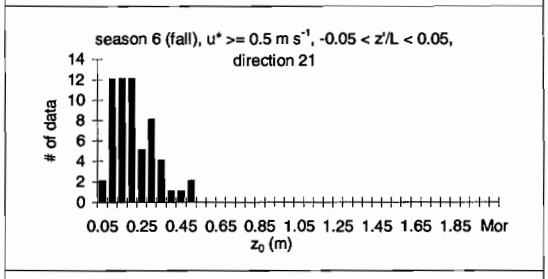

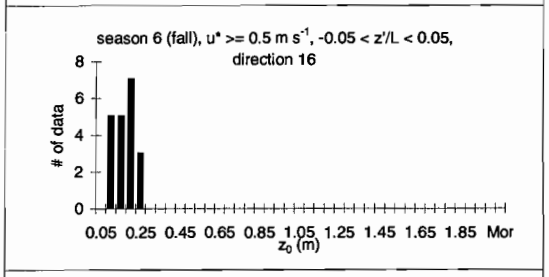

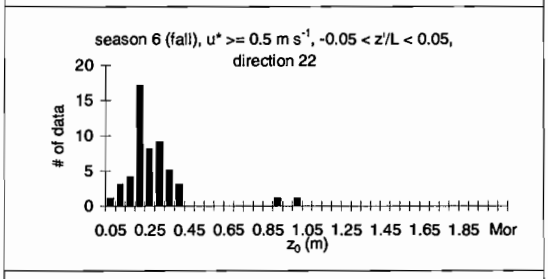

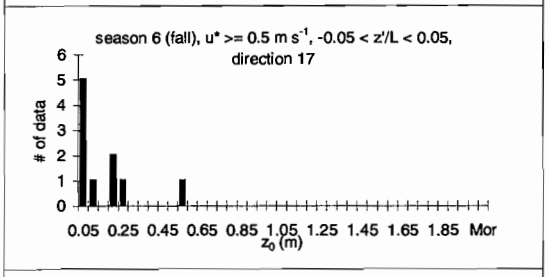

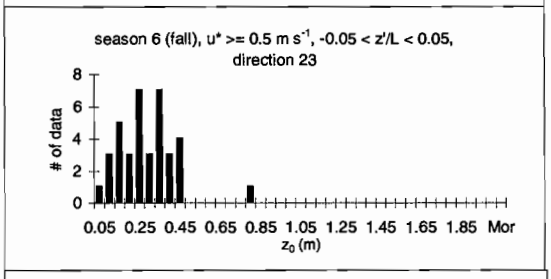

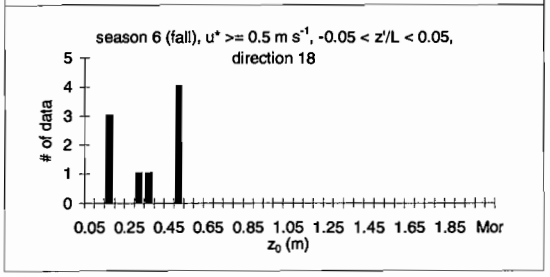

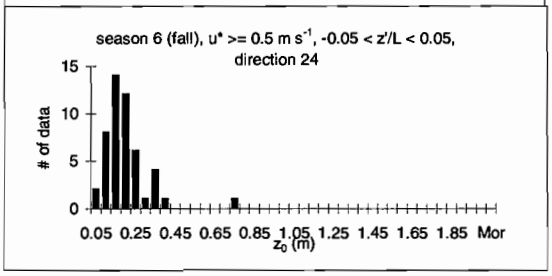

Appendix III: Histograms (z_m = 30 m, z_d = 27 m)

Data are sorted by season and by direction.

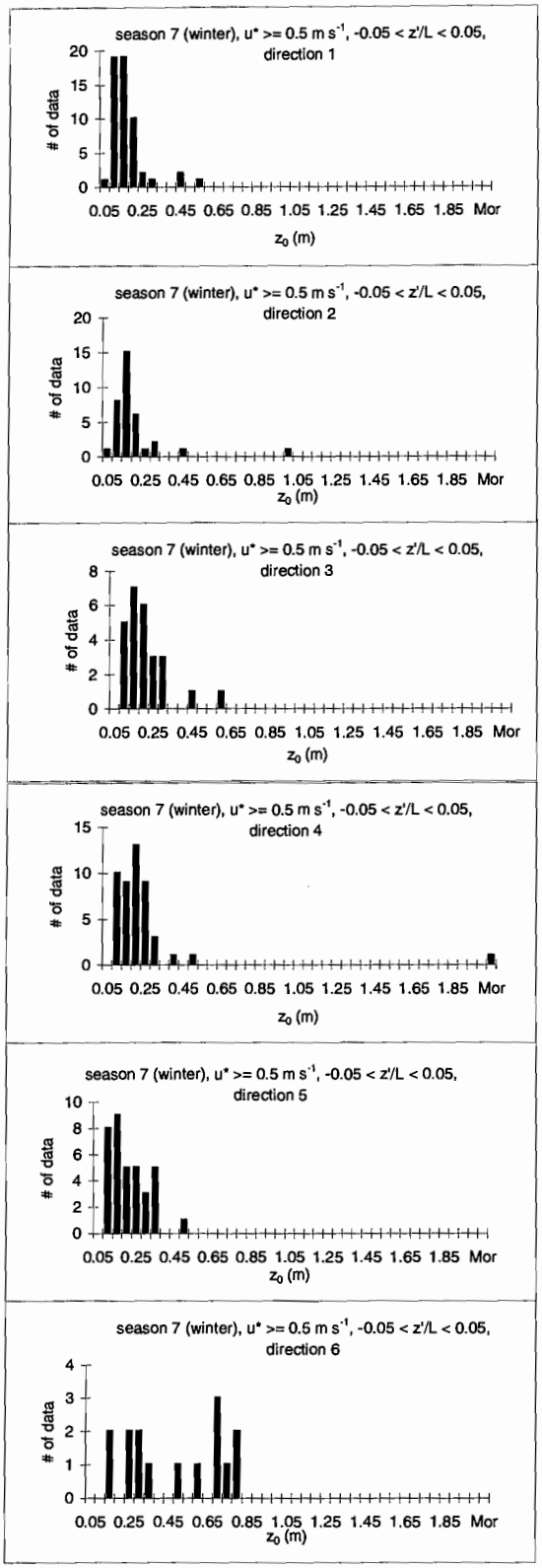

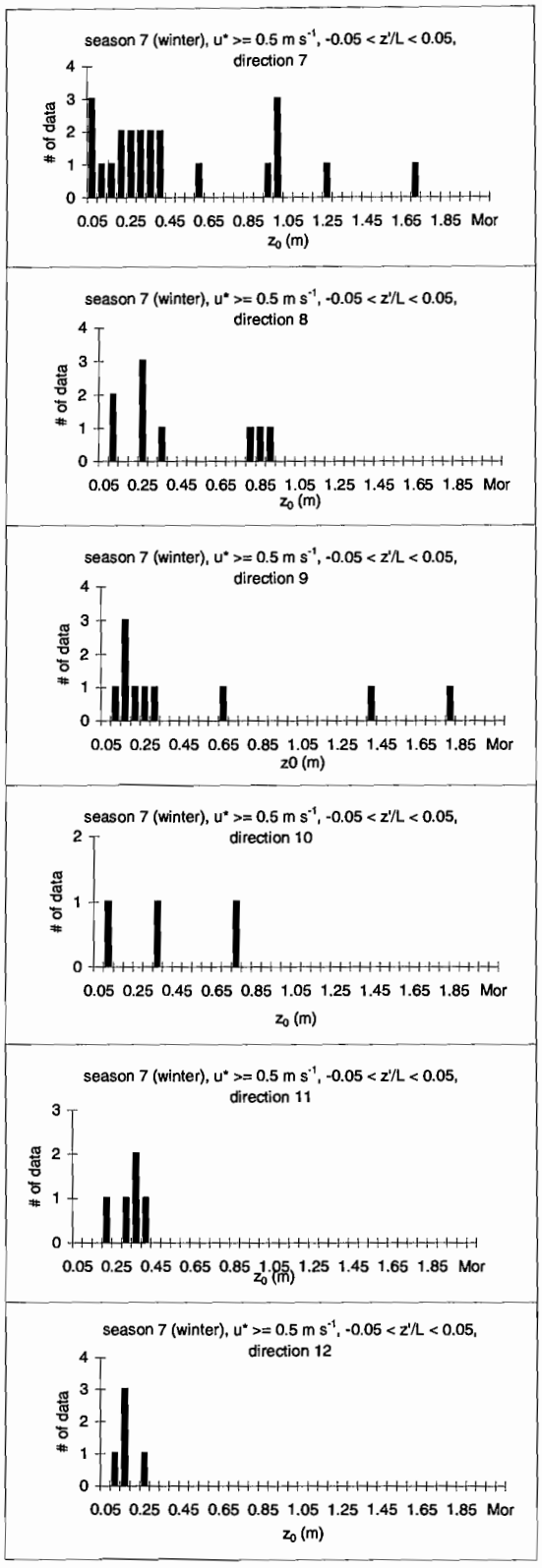

Appendix III: Histograms (z_m = 30 m, z_d = 27 m)

Data are sorted by season and by direction.